Towards Economical Lignin Utilization Through Reductive Catalytic Fractionation

by

Jacob K. Kenny

B.S., University of Nebraska – Lincoln, 2018

A thesis submitted to the Faculty of the Graduate School of the University of Colorado in partial

fulfillment of the requirements for the degree of Doctor of Philosophy

Department of Chemical and Biological Engineering

2023

Committee Members

Dr. J Will Medlin (Chair)

Dr. Jennifer Cha

Dr. Timothy White

Dr. Josef Michl

Dr. Gregg T. Beckham

Kenny, Jacob Kyle (Ph.D., Chemical Engineering)

Towards Economical Lignin Utilization Through Reductive Catalytic Fractionation

Thesis directed by Prof. J. Will Medlin and Dr. Gregg T. Beckham

Abstract

In the last two centuries, humans have relied heavily on the utilization of fossil resources for energy and raw materials, leading to increases in atmospheric CO_2 and other greenhouse gases. Analysis has shown that rapid transition away from GHG emitting processes to environmentally benign processes is necessary to avoid climate disaster. Plant biomass is a promising feedstock for difficult to decarbonize industries such as aviation. The goal of this thesis was to improve the economic outlook in the biorefinery by understanding lignin reactivity and molecular structures. First, the dependence of monomer yield and selectivity on catalyst identity is studied during reductive catalytic fractionation (RCF) without the addition of exogenous hydrogen gas (H_2-free). Evidence is provided for coniferyl/sinapyl alcohol being the reactive intermediate, and the stabilization pathways to various RCF monomers is investigated through the use of model compounds. Next, a new method for the quantification and classification of phenolic hydroxyl groups in lignin and its derivatives, such as RCF oil, is described. Pentafluoropyridine is shown to react fully with phenols in the presence of base, allowing for cheap, safe, and accurate phenolic measurement. Next, a high throughput method for performing RCF is developed and validated, greatly expanding the capabilities of the RCF practitioner while reducing the time and material footprint. Finally, this methodology is then utilized to study the role of substrate, specifically poplar genotype, during RCF through reactions of approximately 600 genotypes. Variance in the extractability of different poplars was discovered with practical implications for the potential poplar RCF biorefinery.

Dedication

To future scientists who might not know it yet. You can do it.

Acknowledgements

The past five years have been an incredible experience both inside the lab and out. My work and life would not be nearly as bright without the amazing people who have helped me along the way, either by showing me a new technique in lab, or just being my friend when I need it. I have looked forward to every day. One of the most enjoyable parts of the research is the first result of a project; a moment that makes you think "this might work." My advisors Gregg and Will have let me pursue many original ideas; some have gone through this stage and turned into papers, and others into deleted excel documents. Nonetheless, developing the ability to approach an idea for the first time, to fail, and try again is perhaps the most valuable skill I have learned in my PhD. I am most appreciative for their trust: even as a young student, they took my results seriously. I have never felt as if I was being tested or doubted. Furthermore, they never dictated to me what experiments I should do. They were never afraid to say they didn't know, which helped me be comfortable with that too. Early on in graduate school, Gregg said he'd always rather do meetings over a beer despite his immense workload, and this helped me realize the world isn't ending tomorrow. Ultimately, I came to graduate school because I wanted to do science, not because I wanted to prove myself to other scientists. I have had many long nights in lab, but as I reflect it was never because I felt like I needed to do it for my advisors. I did it for us, and so that we could push science forward as a team.

To my committee, thank you for showing genuine interest in my research, and asking difficult but necessary questions. Jen and Tim were on my preliminary examination committee and have since accompanied me along my PhD journey. I took Josef Michl's class my first year, which first exposed me to NMR which I have made core part of my thesis. Often the exams along the way are described as somewhat harrowing events, however I have found myself mostly just excited to share what I have done with you all.

Numerous scientists at NREL have taken their time out their days to listen, contemplate, and work with me. David Brandner has been with me every step of the way, from taking me to lunch on my first day at NREL to the long days running the HTP-RCF reactions in the IBRF. I have immensely enjoyed working together on many projects such as RuO_x and solvolysis. You are a great scientist and I have learned a lot from you, and I count you as a true friend. Liz Ware taught me how to perform ^{31}P NMR when I was beginning my work on the PFP project. As a non-chemist, working with dangerous chemicals was scary, but through her guidance I have developed proficiency. In her words, "I don't even shake most of the time." Furthermore, she has been a role model for rigor, and a rare siting of an experienced scientist who still works in the lab skills. Thank you for always being game for an impromptu discussion on plants. Renee Happs showed me how to use the NMRs, and along with Bennett Addison guided me through setting up new ^{19}F and HSQC experiments. You both bring great energy to FTLB-120 and I have greatly enjoyed chatting about whatever the topic of the day may be. Sasha Neefe was an intern at NREL for a year, and her extreme attention to detail was a crucial to executing the HTP-RCF study. It would not have happened without you. The FTLB-140 (Sean, Hannah, Bill, Kelsey and others) and IBRF analytical teams performed analysis for many of my RCF studies, and their expertise is deeply appreciated. Many postdocs at NREL have helped me develop as a scientist; Greg, Jun, Allen, Mike, Lucas, Kevin 1, Kevin 2, Chad, Nina, Ciaran, Caroline, Nick, Ana and others. Thank you all.

To my parents, thank you for not gawking at the idea of me moving away, and taking a somewhat unconventional path to adulthood. They say that if you can't explain it to your mom, you don't understand it yourself. I'll never get tired of trying to explain my research ideas to you both. To the rest of my family: Scott, Grace, and others, thank you for at least pretending to be interested in what I

do. But after explaining what I do, thank you for just letting me just be your same brother, cousin etc again, home for the weekend.

Group meeting presentations are a good way to gauge a student's progress in a PhD. Not through whether they're getting good research results, but whether they've stopped practicing for it. From atrocious prelim practices to hopefully some actually coherent research presentations, the Medlin group has seen me at every stage of PhD student. Although I don't get to do it often, I thoroughly enjoyed just sitting in the office chatting, weighing in on a research question, or helping someone fix a piece of equipment. I felt like a real scientist for the first time in the fall of 2018 when performing CO oxidation experiments with Alex Jenkins. Nothing came of this, except for everything else.

To my roommates over the years, Nick, Ryan, and Taylor. I have truly had some of the happiest moments of my life with you guys. You make it easy to forget that we're supposed to be adults. Even though we won't be living together anymore, I won't forget staying up late for one more episode or enjoying Ryan's cooking. My other friends in Boulder have made my time here so much more than an academic pursuit. From the first day of classes, I knew I had made the right decision coming here.

Mackenzie, my girlfriend, has been with me every step of the way. Moving away to a new place and leaving friends behind is hard. You made it so much easier by coming to see me, and sometimes even bringing some of our friends with you. It's easy to forget about work and focus on the things that matter when I'm with you. I'm excited for the rest of our life together. To my Nebraska friends, when I come home you all make me feel like I've never left. Moving away has made me realize how special and irreplaceable our friendships are. As always, let me know when you're moving to Denver.

Contents

List of Tables

List of Figures

Chapter 1: Introduction

Advances in the conversion of natural resources to fuels and materials has enabled the modern way of life, leading to monumental advances in human health and flourishing.[1] These advances are directly tied to the availability of cheap energy, primarily from fossil fuels, allowing for tremendous growth in human capabilities to transform their surroundings. Growing concern over climate change caused by the emitted CO_2 and other greenhouse gas levels in the atmosphere is motivating the transition to alternative sources of energy and raw materials.[2] Despite many countries, organizations, and businesses pledging to reduce and offset emissions, the current trajectories do not meet proposed 1.5 °C warming scenarios, and thus society will need to dramatically change how we produce and utilize energy.[3,4] Developments in renewable energy have led to dramatic cost reductions for solar and wind energy, making them cost competitive to current generation methods.[5,6] Nonetheless, difficult to decarbonize sectors such as aviation may still require the use of liquid fuels produced from renewable resources.[7,8]

1.1 Lignocellulosic biomass structure and composition

Humans have utilized plants since antiquity for food, shelter, and energy.[9] Plants dominate the terrestrial biosphere, with carbon from living plant biomass measuring over 450 gigatons of globally.[10] Despite sharing many structural and compositional elements, plants vary immensely in terms of appearance and physical properties, and their comprehensive classification is still an actively debated topic.[11,12] In the context of the renewable carbon economy, lignocellulose, comprised of cellulose, hemicellulose, and lignin, is regarded as the most abundant potential biomass feedstock for renewable chemical production.[13] Aside from it taxonomy, lignocellulose can be broadly categorized by its source being a waste stream or dedicated energy crops. First generation biofuels utilized food crops such as corn and soybeans, contrasting with second generation biofuels which attempt to valorize non-food 'waste' sources such as corn stover and wheat residues.[14] Additional waste streams are produced from logging, milling, and forest clearing of woody plants. These two waste sources make up most of the current supply of available lignocellulose, however their future production is limited due to their inherent ties to other activities such as food production. To accommodate decarbonization broadly

across the economy, dedicated energy crops will likely need to be planted for the sole purpose of conversion into fuels and/or chemicals.[15] The proposed substrates span both woody trees such as poplar and herbaceous feedstocks (plants that do not have a woody stem) such as switchgrass that are fast growing, even on land non suited for food production.[8,16,17]

The structural components of lignocellulose are present to provide mechanical support, nutrient transport, and physical and physiological resistance. Minor components in the form of protein, extractives, ash, and any other material produced by living things typically account for less than 10% of the total mass of the plant. In trees, the non-living portion of the plant is referred to as heartwood and accounts for most of the mass of the tree. In contrast, the living portion of the biomass is found only in the outer few layers of cells, referred to as the cambium layer or sapwood.[18]

The most abundant biopolymer in the world, cellulose, is a homopolymer formed from repeating D-glucose units connected through β(1→4) bonds. Polymer chains of cellulose can be up to 10,000 units long, and it can account for up to 50% of the mass of common plants. In the cell wall, cellulose chains aggregate to form microfibrils, giving the cell strength and resistance while allowing for expansion.[19,20] In contrast, hemicellulose refers to less organized polymers formed from other five and six carbon saccharides such as xylose, arabinose, mannose, forming substantially shorter polymers with lengths typically less than 200 repeat units (**Figure 1**).[21]
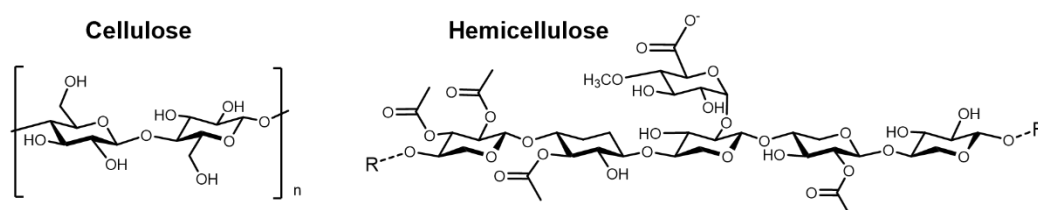
Figure 1. Examples of carbohydrate polymers in plant cell walls. Cellulose is a homopolymer made of repeat glucose units. Hemicellulose come in a variety of forms; shown is an example of xylan with side chain acetylation.

Lignin is an aromatic heteropolymer formed from the polymerization of three primary monolignols: *p*-coumaryl alcohol (H), coniferyl alcohol (G), and sinapyl alcohol (S). The biosynthesis of the various monolignols is well studied and has been reviewed extensively. The pathway originates with the synthesis of the aromatic amino acid phenylalanine from shikimic acid, which then goes on to

be modified by a slate of both specific and general enzymes in the cell cytoplasm. During lignification

(lignin deposition) these undergo kinetically controlled radical coupling reactions to give rise to *p*-
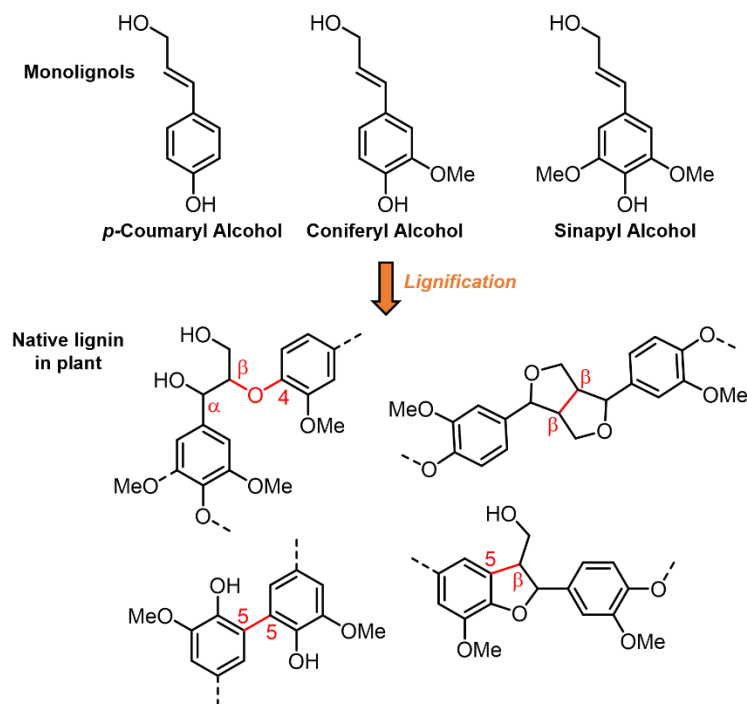
Figure 2. Formation of lignin from monolignols through lignification. Only select examples of lignin linkages shown.

hydroxyphenyl (H), guaiacyl (G), and syringyl (S) moieties in the native lignin.[22–24] In recent years it

has become evident that lignin biosynthesis incorporates many types of aromatic compounds outside of

the three canonical H, G, and S monomers into the native polymer.[25] These can be derived from

"incomplete" lignification where monomers form earlier in the pathway are utilized, sometimes without

apparent detriment to the plant structure and function. Furthermore, a wide variety of flavones can serve

as starting points for lignification, thereby becoming incorporated in the lignin polymer.[25] Once

synthesized, monolignols can be covalently linked by two distinct chemical mechanisms, and the

enzymatically undirected nature of these reactions allows for multiple types of linkages between

aromatic units to be formed. Lignification refers to the growth of the lignin polymer by addition of a

monolignol to the end of a polymer chain by coupling of the β position on the side chain to either a

phenol or 5-position of an aromatic ring. This process leads to linkages such as β-O-4, β-5, 5-5, and 4-

O-5. This is contrasted by the direct dimerization of two monolignols to give linkages such as β-β units

(**Figure 2**).[23]

4

Despite the uncontrolled nature of lignification, lignin is not equally distributed throughout the plant. Confocal Raman measurements has revealed that lignin aggregates in higher concentrations at the cell corners and in the compound middle lamella (CML).[26,27] Still, most of the lignin in the plant (~70% in poplar) resides in the secondary cell wall.[27] Furthermore, the type of lignin shows spatial variability, with higher concentrations of G units residing in the CML. G units also are more concentrated in vessel cell walls, whereas S units shown higher concentrations in the fiber cells.[28]

For the purposes of upgrading, lignin can be simplistically characterized by the relative distributions of 1) the constituent monolignols (i.e. how many S, G, and H units) and 2) the types of linkages between them. Both of these traits vary depending on the type of biomass. Gymnosperms, or softwoods, such as pine or spruce, are devoid of S units, and almost exclusively comprised of G units occasionally accompanied low percentages of H units. Hardwoods such as poplar or birch typically have S/G ratios between 1-5 and contain few if any H units. The can be adorned with pendant units such as *p*-hydroxy benzoic acid.[29] Herbaceous feedstocks contain both S and G units, albeit with S/G ratios between 0.5 to 1, and can contain high amounts of ester conjugates of ferulic and coumaric acid which adorn lignin units.[30]

1.2 Conventional biomass conversion strategies

The polysaccharide portion of plants have long been the primary target of biofuel production, principally in routes to produce ethanol. Even as early as the late early 1900s, companies began investigating ethanol's properties as a fuel.[31] Recent advances in cellulose fermentation by anaerobic bacteria can produce ethanol at high yields and titers directly from biomass.[32] Ethanol can be used as a fuel additive in gasoline, or oligomerized into longer fuel components in the jet fuel range.[33,34] However, for economic conversion of biomass to fuels, lignin must also be valorized.[35]

Pretreatment

Despite the central role of plant biomass to human development throughout human history as nutrition and building materials, the mechanism of cell wall formation through polysaccharide deposition and lignification in growing plant tissue is still an active area of research. Cell walls develop

to be resistant to many types of threats, both physical and physiological. After initial cellulose microfibril formation, hemicelluloses cross link with cellulose.[19,36] Lignification then takes place during cell differentiation and as a response to external stimuli,[37] forming a variety of bonds with hemicellulose which further entangles the biopolymers.[38,39]

The resultant complex network of biopolymers is highly resistant to chemical, enzymatic, or physical breakdown, making eventual biofuel production challenging. Disrupting this network with the goal of making cellulose more accessible for conversion is essential (termed "pretreatment"), and often necessarily involves lignin removal.[40–42] Industrially, the most common lignin removal process is the kraft process which is employs aqueous NaOH and Na_2S to remove lignin for pulp and paper production.[43] A commonly studied alternative strategy for lignin removal is organosolv, where raw biomass is heated organic/aqueous solvent mixtures, often with added acid. Liquid hot water can also be an effective pretreatment option to enable enzymatic sugar release.[44] During pretreatment, the bonds
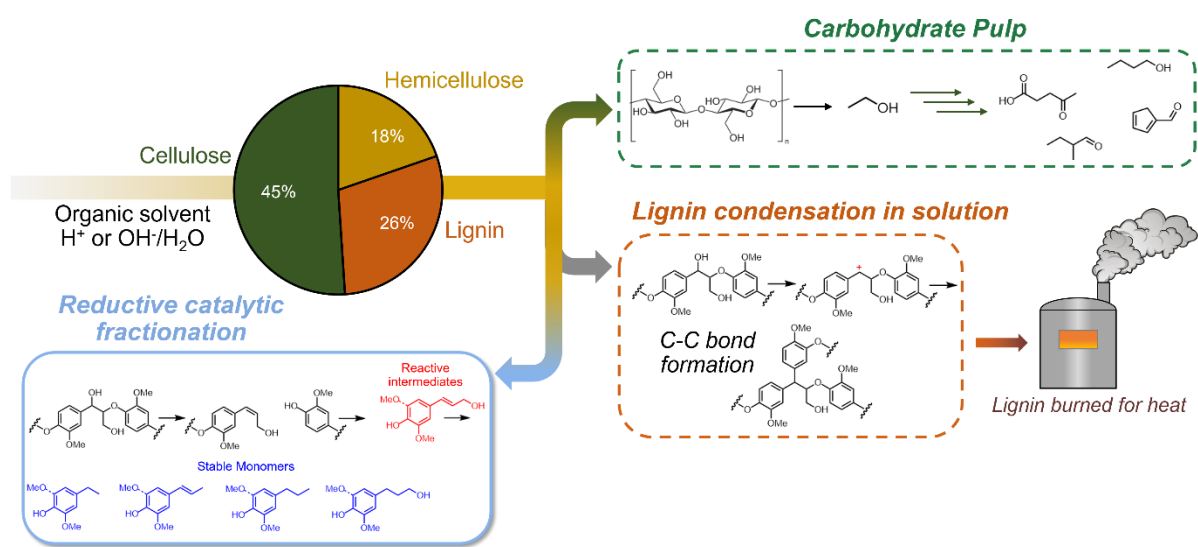
Figure 3. Example of difference between conventional and lignin first biorefining. In conventional lignin extraction, lignin undergoes condensation reactions making it difficult to upgrade. In lignin-First, specifically reductive catalytic fractionation, lignin is converted to aromatic monomers through heterogeneous catalysis.

between hemicellulose and lignin are cleaved, liberating solubilized lignin to then diffuse out the plant structure. Unfortunately, many of the native ether and ester bonds in lignin are also susceptible to alternation. In particular, the β-O-4 linkage, along with other similar aryl-ether linkages, is easily cleaved under moderately severe extraction conditions, and leads to the formation of new carbon-carbon bonds through a process termed condensation. These new linkages are more difficult to cleave

6

catalytically and along with the native C-C bonds in lignin, do not undergo depolymerization during typical lignin extraction. Although these processes can extract a high degree of the lignin, the resultant condensed lignins are much more difficult to valorize, and thus the lignin is merely burned for heat in the kraft process.[43]

Pyrolysis

Fractionation based processes seek to separate the components of biomass into individually processable streams, such as carbohydrates and lignin. This is understandable given the drastically different downstream conversion strategies. In the context of biofuels, carbohydrates typically fermented to glucose/ethanol in a bioreactor, whereas lignin typically needs to be treated under forcing catalytic conditions at high temperatures and pressures. In an alternative to fractionation-based processes, pyrolysis converts whole biomass by heating to high temperatures (up to 700°C) in the absence of oxygen to prevent combustion. This forms a wide variety of light gases, volatile liquids, and heavier species including char. Resultant pyrolysis oil from non-catalytic pyrolysis is acidic and unstable and requires intensive further upgrading to be suitable for fuels. In catalytic fast pyrolysis (CFP), the pyrolysis is quickly followed by catalytic vapor phase upgrading which forms a stabilized oil with a narrower slate of products.[45] CFP has several advantages including simplicity and feedstock diversity, but the resulting oil is still very complex and requiring separation/hydrotreating. Furthermore, catalyst deactivation appears to be a major issue.[46]

1.3 Lignin-first biorefining and reductive catalytic fractionation

Recent technoeconomic analysis has clearly demonstrated that lignin valorization is essential to economic outlook of a biorefinery.[47,48] Given the difficulty associated with valorizing condensed lignin, an alternative approach to conventional lignin removal has emerged which attempts to convert

or stabilize the labile lignin bonds during extraction, so called "lignin-first" strategies. Reductive
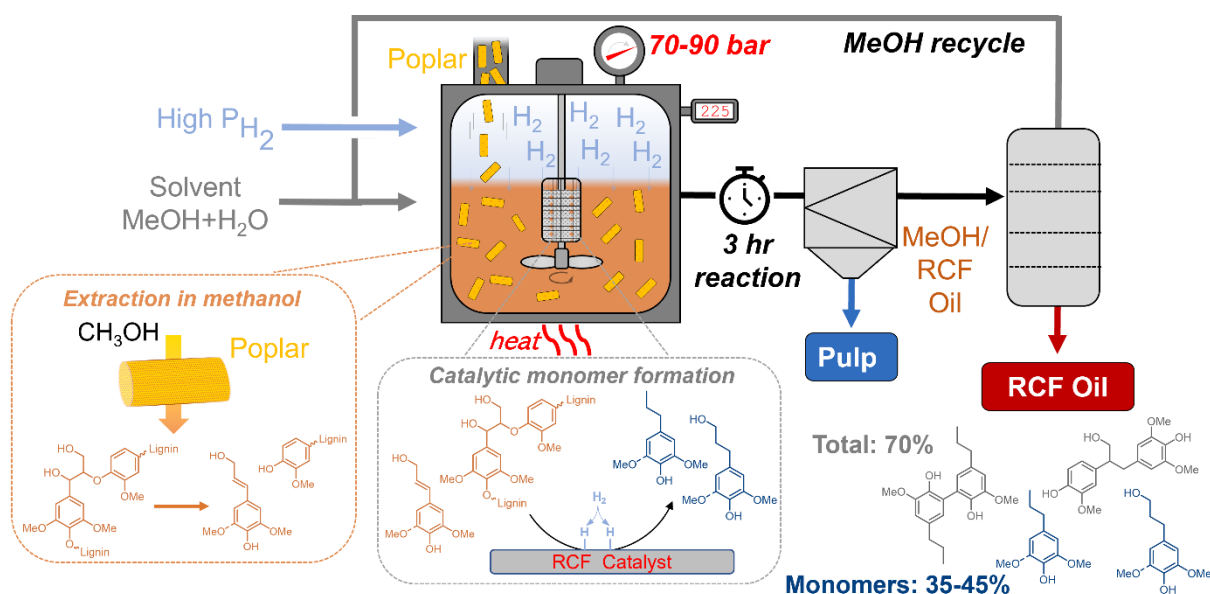
Figure 4. Schematic of RCF reactor where poplar wood undergoes solvolytic lignin extraction in methanol followed by stabilization on a heterogeneous catalyst.

catalytic fractionation (RCF) is one such approach that achieves solvent-mediated extraction of lignin from biomass followed by reductive stabilization of reactive functionalities by a heterogeneous catalyst (e.g. Ni/C, Ru/C, or Pd/C), resulting in a lignin oil that is rich in aromatic monomers with saturated side chains.[49–55]

On the lab scale, RCF processes utilize similar procedures regardless of the practitioner. Typically, the catalyst, biomass, and solvent are combined in a batch reactor. The reactor is then sealed, and hydrogen (H_2) gas is added at a pressure of 10-50 bar. Once heating is initiated, reaction temperature is typically reached within 30 to 60 minutes, and the pressure rises due both to the vapor pressure of the volatile organic solvent and the pressure-temperature dependence of solvent vapor and the H_2 gas. Lignin is extracted from the biomass into the solvent, at which point it is at risk of condensing, similar to uncatalyzed organosolv processes. The success of RCF relies on the reactive lignin fragments interacting with the heterogenous catalyst for stabilization before condensation can occur. The catalyst performs a variety of hydrodeoxygenation (HDO) and hydrogenation reactions to convert the reactive side chain functionalities to stable moieties such as n-propyl and n-propanol monomers. Excess catalyst

loadings are almost always used to ensure near maximal conversion of lignin to aromatic monomers unless the catalyst activity is specifically being studied. Depending on the temperature and solvent used, maximal extraction is obtained in between 2-12 hours after reaching temperature. The reaction is stopped by cooling the reactor. The solvent is then evaporated in a rotary evaporator, yielding the crude lignin oil. A liquid-liquid extraction is performed using water and either ethyl acetate (EtOAc) or dichloromethane (DCM) as the organic phase. The organic fractions are combined and evaporated, yielding the purified lignin oil. The mass of this oil is used to
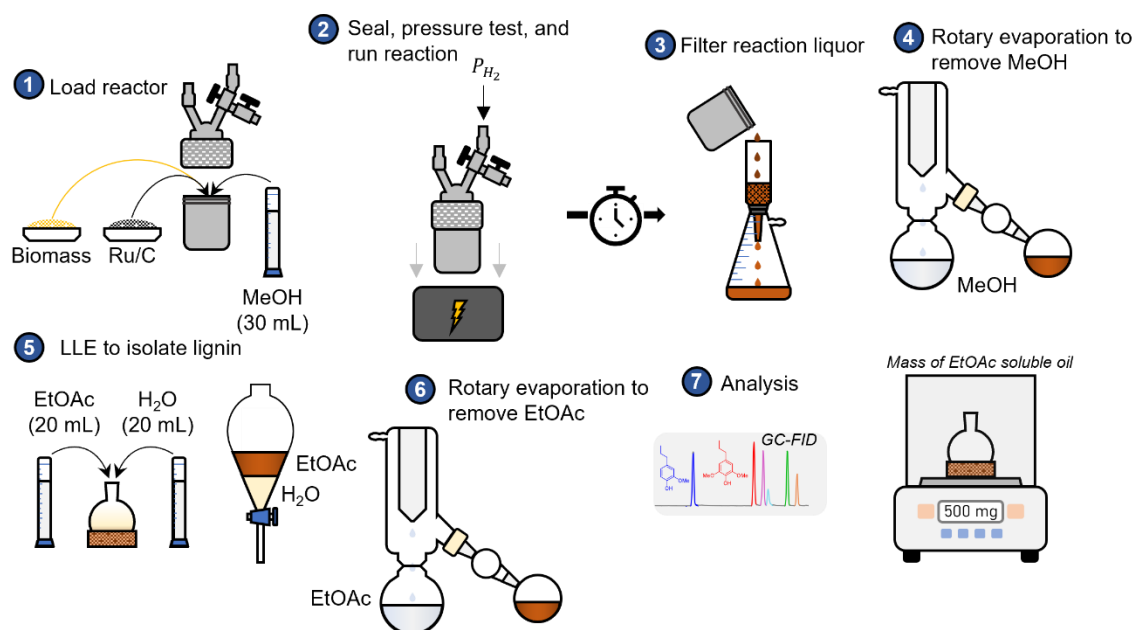
Figure 5. Experimental procedure for conducting RCF on batch scale.

compute the delignification, and the monomers are analysed by gas chromatography.[49,50,56] The typical experimental work-flow for batch RCF reactions is shown in **Figure 5.**

In recent years, studies have revealed many of the crucial factors governing the extraction and stabilization phenomena. In general, RCF reactions on whole biomass are governed both by the extent of lignin extraction and the rate of stabilization of reactive intermediates to monomers.[52,57] If high enough stabilization rates are attained, extracted lignin can be converted to monomers without the build-up of reactive intermediates. In this case, success in RCF comes down to extracting the maximum amount of lignin. Polar-protic solvents such as methanol are usually used at high temperatures (up to 250°C) to obtain high extents of extraction.[49,50] In pure primary alcohols, extraction decreases with

increasing alkyl chain length.[58] At temperatures of 200°C, water actually outperforms methanol in terms of monomer yield and delignification.[50,51] However, mixtures of either methanol/water or ethanol/water were shown to lead to higher extraction than either of the pure solvents alone.[51] RCF is most commonly performed in batch reactors, but multiple accounts of semi-continuous processes of flow-through RCF been demonstrated recently.[57,59,60] The major conclusion resulting from these flow-through studies is that the extraction and stabilization phenomenon can be separated in space and time, giving some indication of the lifetime of the reactive intermediates. Flow-through solvolysis can also be accomplished in pure methanol to extract a near native like lignin, where the short residence time prevents most of the lignin condensation.[61]

A recent report attempted to model the extraction phenomena during lignin-first extraction.[62] Good agreement between the model predictions and measured delignification was obtained, and the authors concluded that reactions using particles larger than 2 mm are likely to be entirely diffusion limited. However, there still were several issues with the modelling approach. First, the reaction-diffusion model assumed that the apparent limitation on extraction (~65% for poplar) was due to the equilibrium reaction for lignin extraction. However, this same delignification limitation is encountered for flow-through extraction where the final stages of extraction occur in virtually pure methanol where no reverse reaction is possible.[61] Furthermore, despite elegant crafting of virtual particles, the finer structure of the cell wall was not considered, and instead lignin was assumed to be equally concentrated in the particle and diffusion in the radial direction was assumed to be 10^3 times slower than in the axial direction. It has been shown that the lignin aggregated in cell corners and in the middle lamella is much more easily extracted compared lignin residing in the secondary cell wall.[26,27]

Once in solution, lignin fragments are solvolytically depolymerized into smaller fragments that can be catalytically reduced to stable monomers.[63] These monomers take on various side chains depending on the catalytic conditions such as propyl, propanol, propenyl, or ethyl. Investigations of the impact of catalyst identity have mainly focused on the selectivity to different product monomers, with comparably less emphasis on the rate of stabilization. Typically, Ru/C, Ni/C, and Rh/C are reported to form propyl substituted monomers through a combination of hydrodeoxygenation and

hydrogenation,[49,52,63,64] whereas Pd/C forms propanol substituted monomers.[51,65,66] Catalyst dependent selectivity has been seen to change based on the other reaction conditions; Ru/C was shown to form mostly propanol products in a 1:1 butanol/water solvent.[54] Similarly, embedding the catalytic Rh in porous hollow carbon spheres switched selectivity to favor propanol products.[63]

Choice of substrate also has major implications for both monomer identity and overall yields, with hardwoods being more amenable to depolymerization and high monomer yields compared to softwoods and grasses.[67–69] This is typically attributed the relative number of β-O-4 linkages between aromatic units.[70] Herbaceous feedstocks fall between hardwoods and softwoods, and owe some portion of the monomer yield to products deriving from the coumarate/ferulate esters which are typically hydrogenated and esterified during RCF.[67,69] Birch is the choice feedstock for many RCF practitioners, and typically gives the highest monomer yields, even compared to other hardwoods. The S/G ratio had historically thought to influence the number of β-O-4 bonds, and this has even been predicted theoretically, but experimental results have led to inconclusive results.[71] Among natural poplar variants, S/G ratio was not found to have any correlation with the monomer yield during flow-through or batch RCF.[72] However, when syringyl units were increased in transgenic poplar, a corresponding increase in β-O-4 units was observed (90%) and RCF monomer yields exceeded 75%.[73] Recently, researchers made an amazing discovery of "C-lignin" in the seed coats of vanilla. The lack of *O*-methyltransferase activity prevents the methylation of the 3-positon hydroxyl group to form guaiacyl units. Instead of conventional S and G units, the sole lignin monomer is caffeyl alcohol which exclusively forms benzodioxane interunit linkages. This ultimately leads to a near homopolymer lignin that when subjected to RCF yield caffeyl analogues of RCF monomers near 90%.[53]

Together, these advances have solidified RCF as an effective extraction and depolymerization method yielding a narrow slate of low molecular weight products. Although high monomer yields (35-50% of initial lignin) are frequently reported, the conventional lignin monomers are not inherently valuable. Therefore, they must undergo further (de)functionalization to become products. Recently, poplar RCF oil was subjected to HDO over molybdenum carbide catalyst in a flow continuous flow-through reactor. The resultant mixture largely consisted of propyl benzene deriving from removing the

methoxy and phenolic hydroxyl groups of conventional propyl RCF monomers, leading to a mixture with properties suitable for jet fuel.[74] In contrast to fuels, methoxy terephthalates, a possible replacement to polyethylene terephthalate, was synthesized from a various wood sources by conversion of both the phenolic group and propyl side chains to carboxylic acids.[75] The success and prevalence of an RCF biorefinery will strongly depend on the further development of efficient conversions of RCF products to valuable products.

1.4 Recent efforts in scale up and modeling of an RCF biorefinery

Given the promising results of bench scale RCF, various groups have attempted to assess the economic potential of an RCF biorefinery. Liao and coworkers evaluated the fractionation of birch with RCF, followed by de-functionalization to produce commodity chemicals such as phenol and propylene. Carbohydrates were converted to ethanol, and lignin oligomers were separated and used as additives in printer ink. The authors highlighted both the hydrogen source as well as sustainable forest management as critical factors to decrease the global warming potential below that of a fossil based refinery.[76] Tschulkow and co-workers demonstrated the impact of feedstock cost and scale (150 kt/y base case) on the breakeven point of an RCF biorefinery. Importantly, waste wood led to the most economically advantaged scenario due to its low cost compared to pine, poplar, and birch.[77]

An extensive analysis of a poplar RCF biorefinery was conducted by Bartling and co-workers which closely modeled four literature described processes: 1) a methanol base case, 2) a complementary process with ethanol/water (85:15 v/v), 3) a hydrogen free case with 1:1 ethanol water, and 4) the use of ethylene glycol. Thorough sensitivity analysis revealed several critical process parameters. First, the capital cost (CAPEX) of the RCF reactor was a major driver of the minimum selling price (MSP). Furthermore, the reaction pressure was a major cost driver of the reactor itself, with higher pressures necessitating more expensive reactors. Reductions in the reactor pressure were realized in the hydrogen-free and ethylene glycol case, leading to lower CAPEX, however both had alternative process shortcomings: a lower monomer yield was assumed in the hydrogen free case, and natural gas costs were much higher due to the need to separate ethylene glycol (boiling point: 197 °C). Reducing solvent

loading was also shown to be important, especially for GWP. Importantly, the application or further processing of lignin oil to saleable products was not considered, leading to a MSP of $1.74 per kg oil.[35]

Most recently, Arts et al. demonstrated the incredible potential of recycling the RCF liquor as a co-solvent to dramatically reduce energy input and subsequent MSP. Recycling of the RCF liquor prior to purification increases the concentration of the oil in the reaction liquor, which correspondingly reduces the external solvent loading and heat demand for separation. Furthermore, mass balances of solvent composition at various recycling ratios showed the build-up of methyl acetate, water, acetic acid produced from endogenous components of the poplar. Experimental validation was achieved by performing reactions with RCF oil making up part of the loaded solvent.[78] This was also previously reported by Jang and co-workers, and surprisingly the inclusion of RCF was even shown to increase delignification compared to pure methanol.[79]

Several conclusions can be drawn from these initial accounts. In academic literature, practitioners have narrowed in on reaction conditions that enable reliable bench scale reactions where process parameters can be conveniently studied. These conventional RCF conditions and workup methodologies do not directly translate to the envisioned biorefinery. This includes the use of 1) filtration rather than centrifugation for separation of solid pulp from the reaction mixture, 2) intermixed powder catalysts rather than physically separated pelleted catalysts, 3) pure solvents rather than realistic recycle streams 4) dry, washed, and extensively size reduced feedstocks. Nonetheless, the field appears to be approaching a potentially viable process to produce aromatics and ethanol sustainably. A recent report demonstrated minimal detrimental impact on monomer yield or delignification when increasing scale from 100 mL to 50 L reactions.[80]

In this thesis, we advance RCF processes through decreasing reactor pressure through H_2-free operation and substrate choice. We also describe a novel method for characterizing the phenol content of lignins, such as RCF oil, with ^{19}F NMR. The results here demonstrate that H_2-free operation of RCF can be pursued without yield penalty if high activity catalysts are chosen. Furthermore, the RCF process appears to be sensitive to poplar genotype, however this may be alleviated through proper condition selection to minimize residence time.

Chapter 2: Catalyst choice impacts aromatic monomer yields and selectivity in hydrogen-free reductive catalytic fractionation

2.1 Summary

Hydrogen-free reductive catalytic fractionation (RCF) is a promising method to extract and depolymerize lignin from native biomass without the use of external hydrogen gas. Here, we show that Pt/C and Pd/C achieve comparable monomer yields regardless of hydrogen pressure, whereas Ru/C and Ni/C show lower yields under H_2-free conditions. Ru/C and Ni/C primarily perform hydrodeoxygenation regardless of the hydrogen pressure, but Pt/C and Pd/C demonstrated the ability to form both ethyl products from dehydrogenation and propanol products through hydrogenation depending on the presence of external H_2. Adding water to the solvent increased HDO selectivity to propyl products for both Pt/C and Pd/C. Monomer yields from poplar RCF showed similar trends in yield and selectivity to reactions with the model compound coniferyl alcohol, suggesting that H_2-free RCF performance is dictated by monomer stabilization rates.

2.2 Introduction

Despite the huge advances described in chapter 1, recent techno-economic analysis highlighted further developments that are needed to make RCF economically viable.[35] One such recommendation was to employ a hydrogen-free (H_2-free) RCF process (i.e. a process run without the addition of H_2 gas), which enabled lower reactor operating pressure, in turn leading to an estimated 32% lower minimum RCF oil selling price, compared to a base case with methanol as a solvent and external H_2 gas.[35] Various H_2-free RCF processes have been pursued to this end, and the pathway for utilizing alternative hydrogen donors appears to be dependent on the catalyst and solvent system. During extraction, multiple species can potentially serve as the source of hydrogen such as the alcohol solvent, hemicellulose, or even the lignin itself. Sels *et al.* reported high monomer yields for both Ru/C and Pd/C-catalyzed hydrogenolysis of birch in methanol at 250°C regardless of whether the reaction was conducted in a N_2 or H_2 atmosphere.[49] Solvent reforming was purported as the hydrogen source. Hensen *et al.* achieved a monomer yield near the theoretical limit with a 2:1 water/methanol solvent during

Pt/Al$_2$O$_3$- catalyzed RCF of birch, similarly citing methanol reforming as the hydrogen source. Interestingly, only a 22% monomer yield was reported when Pd/C was used under the same conditions.[56] Samec *et al*. demonstrated that Pd/C has a perhaps unique ability to utilize formic acid generated from hemicellulose degradation as a hydrogen donor during RCF of birch in an ethanol/water solvent mixture.[70,81,82] Alternatively, Rinaldi *et al*. reported that Raney-Ni stabilizes reactive monomers through transfer hydrogenation using isopropanol as the hydrogen donor.[83,84] Another interesting approach, termed atmospheric-RCF (ARCF), was described by He and co-workers in which ethylene glycol and sulfuric acid were used at comparatively lower temperatures (185-195°C). Acid concentration was optimized to give 25.2% monomer yield after 6 hours using Ru/C as a catalyst. Lower monomer yields (4.8-6.9%) were obtained when using Pd/C regardless of the presence of H$_2$SO$_4$.[85] This process reduced reactor pressure completely, but the separation of RCF products from ethylene glycol is expected to be difficult.[35]

While these H$_2$-free studies have demonstrated high monomer yields, there have been few direct comparisons between catalysts to benchmark the impact of catalyst choice on monomer yields in H$_2$-free conditions. Excess catalyst loadings have often been used to achieve a high conversion of extracted lignin to monomers, making comparison between studies difficult. In situations where catalyst activity has been considered, the goal has be to find the required mass of catalyst for a given substrate loading.[54] Catalyst choice therefore remains an open question for H$_2$-free RCF processes. To that end, here we examine the impact of catalyst choice on monomer yields and selectivity in H$_2$-free RCF.

2.3 Experimental

Batch RCF reactions

2 g of whole poplar sawdust biomass,[61] 100 mg of catalyst, 30 mL of methanol (Sigma-Aldrich) were added to a 75 mL Parr reactor with a magnetic stir bar. The reactor was sealed, purged three times, and pressure tested with He up to reaction pressure (~80 bar). For H$_2$-free reactions, the pressure of He was reduced to ~ 1 bar. For reactions with H$_2$, H$_2$ was loaded at a pressure of 30 bar. The stirring rate was set to 800 rpm, and reactor was heated to 225°C for the desired reaction time (for simplicity "reaction time" is defined to start 30 minutes after heating was initiated. The reactors were quenched at

15

the end of the reactions in an ice bath for 45 minutes. The headspace of H_2-free reactions was sampled with a gas bag. Liquid contents were filtered first through a tared qualitative glass filter and then through a 0.2 µm PES syringe filter, and the methanol solvent was evaporated in a rotary evaporator. Ethyl acetate (Sigma-Aldrich) (20 mL) and DI-water (20 mL) were added to the crude RCF oil and separated in a separatory funnel. The aqueous layer was washed with an additional 20 mL ethyl acetate, and the organic layers were combined in a tared round bottom flask. The ethyl acetate was then removed via rotary evaporation, yielding an oil which was massed, and termed *lignin oil*. The lignin oil was dissolved in 15 mL acetone (Spectrum Chemical). Solid residue, including catalyst, was massed by massing the filter.

Catalyst preparation of 5% Ni/C

A 5 wt% Ni/C catalyst was prepared similar to the preparation performed by Brandner *et al.,* except at a 5 wt% loading.[61] The other catalysts (Ru/C, Pd/C, Pt/C) were purchased from Sigma-Aldrich and used as received.

Model compound reactions

Model compound reactions were performed in a similar manner as RCF reactions. 60 mg of the selected model compound (coniferyl alcohol: Sigma-Aldrich; guaiacyl guaiacylglycerol-beta-guaiacyl ether, TCI America), or 30 mg of coniferyl aldehyde (Sigma- Aldrich) was added to a 75 mL Parr reactor along with 20 mg of catalyst and 30 mL of methanol. The reactor was then sealed, purged, and pressure-tested with He up to reaction pressure. For H_2-free reactions, the pressure of He was reduced to ~ 1 bar. For reactions with H_2, H_2 was loaded at a pressure of 30 bar. The stirring rate was set to 800 rpm, and reactor was heated to 225°C for 1 hour before cooling in an ice bath for 45 minutes. The reaction mixture was filtered through a 0.2 µm filter. Reaction products were analyzed with an Agilent 1290 Infinity II LC equipped with a Phenomenex Luna C18(2)-HST column. Monomer yields for model compound reactions are reported on a molar basis (as opposed to mass basis like poplar RCF yields).

Monomer analysis with GC

The lignin oil was dissolved in 15 mL of acetone. ¼ mL of this oil/acetone solution was added to a vial, along with ¼ mL of pure acetone, and ½ mL of 2 g/L tri-tertbutyl benzene (Sigma-Aldrich) as an internal standard. Samples were injected on an Agilent 8890 gas chromatograph equipped with an FID detector utilizing an HP-5 column. Quantification was performed using calibration curves with authentic standards for all compounds. All commercially available standards were purchased from Sigma Aldrich. 4-propenylsyringol was purchased from AKos GmbH. Ethyl syringol was purchased from AAblocks. Several standards, 4-(3-methoxy)propylguaiacol, 4-propylsyringol, 4-(3-methoxy)propylsyringol, and 4-propanolsyringol, were synthesized in house.[61]

$$monomer\ yield\ \% = \frac{\sum_1^i m_i}{\%\ lignin\ content * m_{poplar}}$$

where m_i is the mass of monomer i, *%lignin content* is the total lignin content measured from compositional analysis, and m_{poplar} is the mass of poplar loaded.

Headspace analysis

Gas from the headspace of H_2-free reactions was captured from the reactor with a gas bag and withdrawn from the gas bag into a syringe. The sample was injected onto an Agilent 7890A gas chromatograph equipped FID and TCD, with two Wasson columns (part numbers 2428, 2378) to measure the mole fraction of each component. Moles of components were calculated using the ideal gas law assuming a headspace volume of 45 mL.

Compositional analysis

Compositional analysis on the solids followed the NREL Laboratory Analytical Procedure (LAP),[41,86] and results are shown in **Table 1.**

Table 1. Composition of biomass substrate used in RCF reactions.

Substrate	Ash	Extractives	Lignin	Glucan	Xylan	Galactan	Arabinan	Mannan	Acetyl	Total
OP-367 (*P. deltoides x P. nigra*)	0.69	3.54	25.95	45.31	13.24	1.34	0.14	2.79	3.84	97.43

2.4 Results

RCF of poplar

We first sought to investigate how the absence of hydrogen impacts extraction and monomer stabilization rates. Time course data allow for direct observation of the impact of H_2-free conditions on the monomer formation rate, as well as whether low monomer yields can be overcome by increasing residence time. Thus, batch reactions were first performed for 1-6 hours (after reactor heat-up) using low catalyst loadings (50 mg 5 wt% Ru/C per g poplar) to prevent the reactions from reaching full conversion of lignin to monomers, allowing for monomer yields to reflect differences in the rate of hydrogenolysis between H_2-free and conventional RCF conditions (see **Figure A1** for temperature and pressure profile, and **Figure A2** for RCF reaction at 200 mg Ru/C loading. As expected, nearly identical lignin oil yields are obtained regardless of the presence or absence of H_2 (**Figure 6**). *p*-Hydroxy benzoic acid (*p*HBA), methyl paraben, and phenol (likely produced via decarboxylation of pHBA) were produced during the RCF reaction as well, the amounts of these products were comparable in all conditions (see **Figure A3** for measurement of *p*HBA and methyl paraben). Notably, the selectivity to *p*HBA was higher in H_2-free reactions ($56 \pm 8\%$) at 1 hour compared to reactions with H_2 ($27 \pm 5\%$). By 3 hours, however, little *p*HBA was measured in either case. H_2, CO, and CO_2 were produced
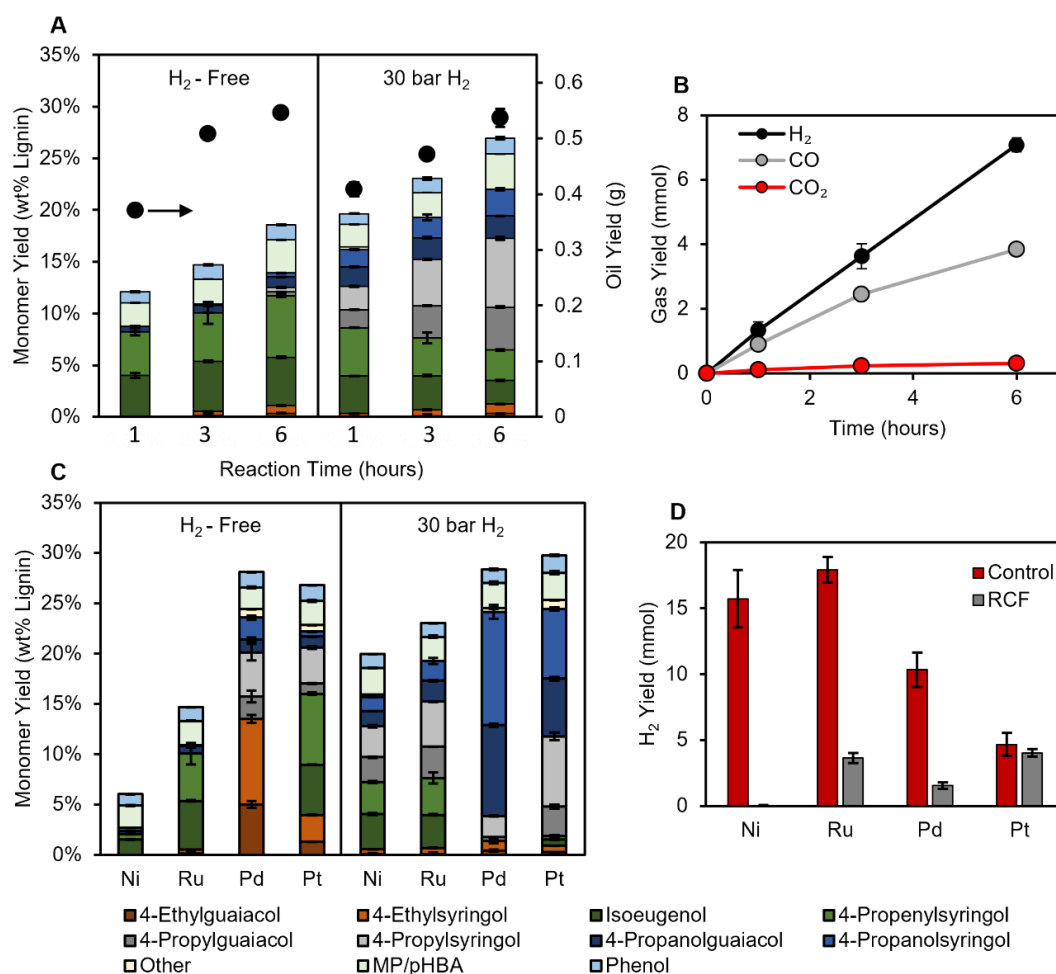
Figure 6. (**A**) Monomer yields (stacked bars, left axis) and oil yields (black circles, right axis) for time course reactions RCF without H_2 (left) and with 30 bar H_2 (right) using a Ru/C catalyst. (**B**) Gas yields during time course reactions with Ru/C. (**C**) Monomer yields for H_2-free reactions (left) and with 30 bar H_2 (right) for each catalyst. (**D**) H_2 gas yields for control reactions (no poplar, red bars) and H_2-free RCF (grey bars). RCF conditions: 2 g poplar, 100 mg catalyst (5 wt% metal), 30 mL MeOH, 225°C, 3 hours. Control reaction conditions: 30 mL methanol, 100 mg catalyst, 3 hours. MP/pHBA is the summed yield of methyl paraben and p-hydroxy benzoic acid. The error bars represent the standard deviation of triplicate measurements.

reaction, reaching a total of 7.1 ± 0.2, 3.86 ± 0.03, and 0.31 ± 0.02 mmol respectively, after 6 hours at reaction temperature (**Figure 6B**); for reference, 30 bar H_2 at room temperature is about 55 mmol. This represents a maximum conversion of approximately 0.6% of the methanol solvent through decomposition, assuming all measured CO and CO_2 are derived from methanol. By the first hour at reaction temperature, > 60% of the delignification (as measured by oil yield) for both H_2-free and 30 bar H_2 reactions had occurred, while only 1.3 ± 0.3 mmol of H_2 was detected in the H_2-free reactor headspace.

Reactions with 30 bar H_2 achieved higher monomer yields than H_2-free reactions at each time point, reaching $27.0 \pm 0.3\%$ after 6 hours compared to $18.6 \pm 0.3\%$ for H_2-free reactions (**Figure 6A**). The lower monomer yield is a result of a lower rate of stabilization relative to condensation, indicating that adequate hydrogen is not available in the H_2-free conditions with this catalyst and solvent system. This is further evidenced by the lower yield of products with saturated propyl and propanol side chains under H_2-free conditions.

Regardless of the hydrogen source, the disparity between reactions with hydrogen present and under H_2-free conditions derives from the process of making hydrogen available on the surface of the catalyst. We hypothesized that other catalytic metals could be differentially active for H_2-free RCF based on their hydrogen generation ability. Thus, batch reactions were performed with Ni/C, Pd/C, and Pt/C (all catalysts are 5 wt% metal loading) with and without 30 bar H_2 for 3 hours (**Figure 6C**).

With H_2 loaded, Pt/C and Pd/C achieved the highest yields of $28 \pm 2\%$ and $30 \pm 1\%$, respectively. Monomer yields for Ru/C and Ni/C were 23.0 ± 0.8 and 19.9 ± 0.5, and still produced unsaturated products at a selectivity of $30 \pm 2\%$ and $33.5 \pm 0.5\%$ respectively, presumably due to the low catalyst loadings. Ru/C and Ni/C formed primarily propenyl and propyl products, while Pd/C formed propanol products, as observed previously.[49] Pt/C formed similar amounts of propyl and propanol products. *p*HBA, methyl paraben, and phenol were measured in similar amounts for all 3-hour reactions regardless of H_2 pressure, suggesting that the pathways from *p*HBA are not substantially dependent on the presence of external hydrogen at high extents of conversion.

Without external H_2 loaded, Pd/C and Pt/C retained high monomer yields, suggesting that monomer yields are limited by the rate of extraction rather than hydrogenolysis under these conditions. When Ni/C was used under H_2-free conditions, monomer yields decreased to $6.0 \pm 0.1\%$, indicating that Ni/C was unable to produce sufficient hydrogen for stabilization (**Figure 6C**).[68]

It was expected that if the hydrogen donor was the methanol solvent, then the respective methanol reforming rates of the catalysts examined here would trend with monomer yield. However, in batch control experiments with methanol and catalyst (without poplar biomass), Ru/C and Ni/C produced the most hydrogen (**Figure 6D**). Hydrogen yields during RCF were lower compared to control

reactions, with only Pt/C achieving a similar H_2 yield (**Figure 6D**). This demonstrates the inhibitory role that the presence of the substrate has on the methanol reforming pathway. The higher monomer yields for Pd compared to Ru, despite the greater H_2 production of Ru, indicates that H_2-free monomer production depends on more than just reforming ability. The availability of routes involving ethyl products on Pd catalysts may be critical, as discussed in more detail below. Given that hemicellulose extraction is low in pure methanol,[51] it is still likely that methanol is the predominant hydrogen donor. However, the mechanism of this activity remains unknown. Considering these results, it seems that complete reforming to H_2 gas may be unnecessary, and it could be advantageous to limit the amount of excess reforming to minimize solvent loss.

Comparing monomer selectivity among the catalysts, Ru/C and Ni/C primarily performed hydrodeoxygenation (HDO) to form propenyl/propyl products, and the presence of external H_2 only increased the rate of formation of these products. Conversely, the absence of external H_2 gas changed the route of stabilization for Pd/C and Pt/C; namely, H_2-free reactions formed ethyl products with selectivities of $48 \pm 3\%$ for Pd/C and $14.8 \pm 0.2\%$ for Pt/C (**Figure A4**). Ethyl products were formed at the expense of propanol products, indicating that the pathway to form ethyl side chains may be inhibited by excess hydrogen. Interestingly, the use of Pd/C exhibited higher selectivity to propyl than propanol products during H_2-free reactions. Running Pd/C reactions with higher catalyst loadings did not change the selectivity to ethyl products, but slightly increased yields of propanol relative to propyl side chains (**Figure A5**). Thus, we conclude that the pathway to form propanol products exhibits a higher sensitivity to hydrogen pressure and potentially hydrogen coverage on the catalyst surface than competing stabilization pathways over Pd/C and Pt/C.

RCF selectivity is thought to be governed mainly by the catalytic metal.[87] However, a recent report demonstrated that other process conditions such as hydrogen pressure or solvent changed selectivity of Ru/C catalyzed RCF from expected propyl monomers to propanol monomers. To test the impact of water content on product selectivity, we ran RCF reactions with 25 and 50 volume percent water for the best performing catalysts, Pd/C and Pt/C (**Figure 7**). When the water content of the reactions with Pt/C was increased to 25%, almost complete hydrogenation of propenyl side chains was

measured (<0.5% propenyl products). A similar effect was reported by Hensen *et al.* in the H_2-free RCF of birch with Pt/Al_2O_3 catalyst, except an even higher water content (approximately 50 vol%) was needed to fully saturate the side chains. When reactions were run at 50 vol% water in our studies, the monomer yield decreased, accompanied by the reappearance of unsaturated products such as propenyl syringol, contrasting with the near theoretical yields reported by Hensen. This is perhaps indicative of the impact of the different feedstock (birch versus poplar). Interestingly, when Pd/C was used in H_2-free reactions with water, selectivity to ethyl products decreased with increasing water content, and propyl products were formed instead. However, the addition of water led to a monotonic decrease in monomer yield, reaching a yield of lignin derived products (omitting phenol and *p*-HBA) of 17.1 ± 0.3% for reactions with 50 vol% H_2O, compared to 24.4 ± 0.3% in pure methanol. Water has been observed in previous studies to significantly affect the rate or selectivity of hydrogenation reactions; for example, water can decrease the magnitude of the enthalpy of adsorption of organic reactants[88] or provide new pathways for hydrogen/proton transfer.[89,90]
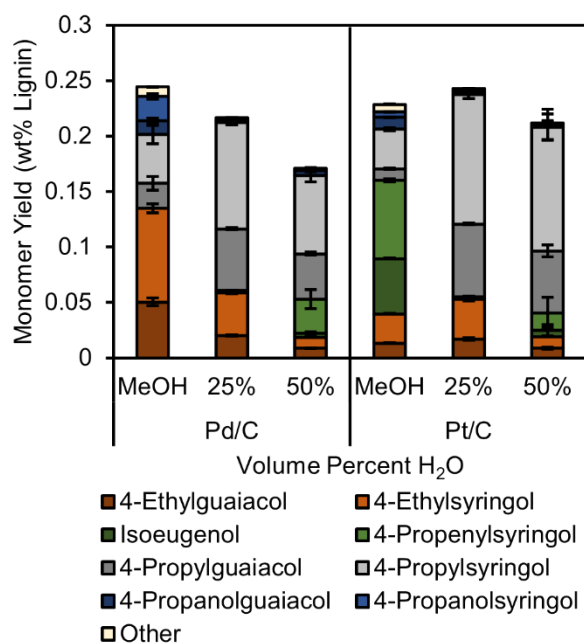
Figure 7. Lignin product monomer yields from H_2-free RCF reactions with water/methanol solvent mixtures. Conditions: 2 g poplar, 100 mg catalyst, 3 hours, 225°C. Percentages are volume percentages of water in the solvent mixture.

Model compound reactions

Previous work has shown that aryl-ether linkages in lignin can be cleaved in solution, followed by stabilization of smaller reactive intermediates.[63] Furthermore, reports have postulated that the role of the catalyst is to stabilize coniferyl alcohol-like intermediates derived from solvolytic β-O-4 cleavage, rather than on dimers or oligomers with the β-O-4 linkage directly.[91,92] Thus, to investigate the role of the metal catalyst further in H_2-free RCF, batch reactions were performed on two common lignin model compounds, coniferyl alcohol (**Figure 8A**) and guaiacylglycerol-beta-guaiacyl ether (GGE) (**Figure 8B**). Both of these model compounds readily undergo degradation reactions at high temperatures,[65,91] allowing for monomer yields to represent the relative rates of stabilization and condensation, similar to RCF reactions on poplar.

Blank reactions of GGE without catalyst achieved $92 \pm 6\%$ conversion and a $29 \pm 3\%$ yield of coniferyl alcohol, confirming that the cleavage of the ether bond occurs readily in solution. Guaiacol yields were consistently lower than GGE conversion, suggesting the presence of alternative routes beyond ether cleavage followed by stabilization/condensation of coniferyl alcohol. Monomer yield trends for reactions with GGE differed from results obtained with poplar. When Pd/C was used under H_2-free conditions, previously unreported products acetovanillone and 1-propanone, 1-(4-hydroxy-3-methoxyphenyl) were formed at 24 ± 3 and $10 \pm 5\%$ yield respectively. Reactions starting from these ketone products under identical conditions showed low conversion (<10%) to other conventional RCF products, ruling them out as intermediates. While GGE is not completely representative of lignin during RCF, the lack of ketone products during poplar RCF supports the mechanism proposed above, where dimers or oligomers with β-O-4 linkages are cleaved in solution to yield reactive intermediates that then undergo reductive stabilization or condensation.
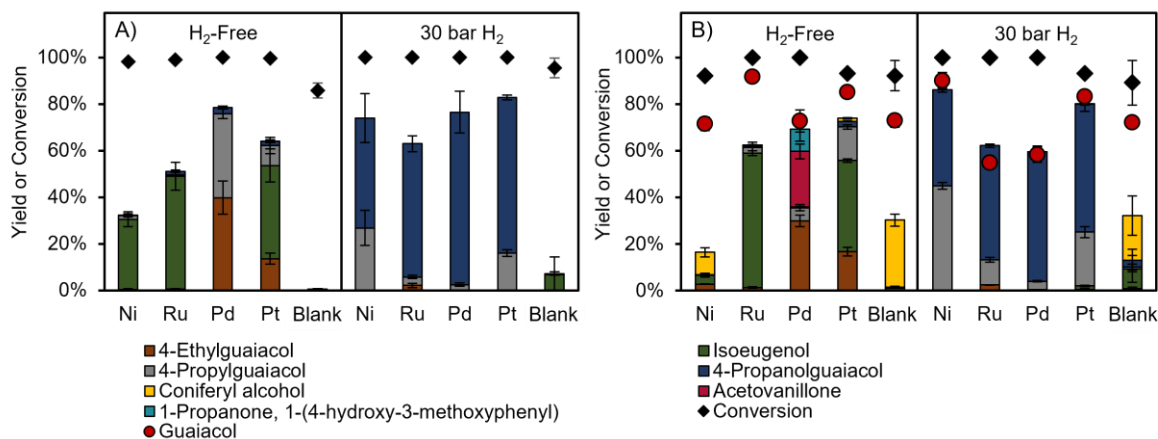
Figure 8. Monomer product yields for model compound reactions with (A) coniferyl alcohol and (B) guaiacylglycerol-beta-guaiacyl ether (GGE) under H_2-free conditions (left) and with 30 bar H_2 (right). Note: for clarity, the bar for coniferyl alcohol is not shown in A. Conditions: 60 mg substrate, 20 mg catalyst, 30 mL methanol, 1 hour at 225°C. Error bars are the standard deviation of three measurements.

Coniferyl alcohol reactions under H_2-free conditions showed good agreement compared to poplar RCF, with Pd/C and Pt/C achieving higher product yields than Ru/C and Ni/C. RCF typically forms propyl or propanol substituted products through hydrodeoxygenation and/or double bond hydrogenation. However, Pd/C, and to a lesser extent Pt/C, can form ethyl products from coniferyl alcohol under H_2-free conditions, in line with this work and earlier reports.[49] Through studies of simpler alcohols, Barteau and co-workers concluded that metals such as Pd, Pt, and Ni induce C-C scission through dehydrogenation to an acyl intermediate.[93,94] To test this proposed mechanistic pathway, we used coniferyl aldehyde as a starting material in model compound experiments that mirror the RCF experimental conditions (**Figure A6**). The use of Pd/C and Pt/C in an H_2-free context resulted in the formation of ethyl guaiacol in $79 \pm 2\%$ and $50 \pm 4\%$ yield, respectively, indicating that dehydrogenation followed by decarbonylation is a possible reaction step to form ethyl products. Conversely, the use of Ru/C and Ni/C in the same conditions exhibited ethyl guaiacol yields of $12 \pm 5\%$ and $4 \pm 2\%$, respectively, which is higher than yields for reactions starting from coniferyl alcohol (<1%). This confirms that Ru/C and Ni/C do not dehydrogenate coniferyl alcohol to a large extent, and instead mainly perform HDO.
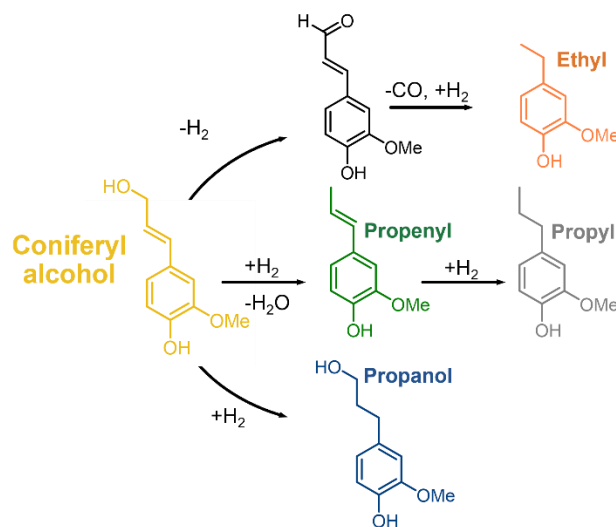
Figure 9. Proposed stabilization pathways from coniferyl alcohol.

2.5 Conclusions

Four common RCF catalysts were compared for their RCF monomer yields with and without external H_2 gas added to the reaction. Clear differences were observed in monomer yield and selectivity under H_2-free conditions. Pd/C and Pt/C retained high monomer yields, while the lack of H_2 decreased monomer yields for Ru/C and Ni/C. Neither the H_2 yields from poplar RCF nor from methanol reforming control reactions correlated with monomer yield. Coniferyl alcohol model compound reactions demonstrated good agreement with poplar RCF monomer yields relative to a β-O-4 model compound, GGE, which supports the previously proposed mechanism where the species reacting on the catalyst is a monomer rather than a dimer or larger. Ultimately, these results show that catalyst choice can impact monomer yields in H_2-free reactions, and that more investigation into the stabilization mechanisms is needed to elucidate the origin of activity differences between catalysts.

Chapter 3: Quantification of phenolic hydroxyl groups in lignin via ^{19}F NMR spectroscopy

3.1 Summary

Phenolic moieties strongly influence lignin reactivity and physical properties, and thus accurate quantification of phenolic groups in lignin is a critical analytical chemistry need. Today, ^{31}P nuclear magnetic resonance (NMR) spectroscopy is widely considered the standard method to this end, but this approach uses a hazardous and expensive derivatization agent, and the NMR spectroscopy experiments are time consuming due to long relaxation times. Here, we report a complementary method that enables accurate identification and quantification of phenolic groups in lignin samples using pentafluoropyridine (PFP) as a derivatizing reagent followed by ^{19}F NMR spectroscopy. Using dimethyl sulfoxide as a solvent in the presence of K_2CO_3, phenolic hydroxyl groups in lignin model compounds were fully converted to the corresponding tetrafluoropyridyl-ether product within 1 minute. PFP exhibits high selectivity for the reaction with phenolic hydroxyl groups relative to aliphatic alcohols, and we show that side reactions with carboxylic acids, if present, can be avoided through the addition of 40% water to the reaction solvent. The PFP ^{19}F method achieved similar results compared to ^{31}P NMR spectroscopy when applied to reductive catalytic fractionation oil from poplar, softwood kraft lignin, and corn stover milled wood lignin, thereby offering a safe and cost-effective method for phenolic measurements in lignin.

3.2 Introduction

To date, many promising approaches to extract and valorize lignin from plants have been investigated, many of which induce chemical changes in the polymer. The resulting distribution of functional groups in lignin-derived products, particularly phenolic hydroxyl groups, governs both reactivity and material properties.[87,95–97] Thus, accurate identification and quantification of these phenolic hydroxyl groups is important for lignin valorization pursuits.

Various methods for characterizing phenolic groups in lignin have been reported, including infrared spectroscopy, UV-visible spectroscopy, and ^{1}H nuclear magnetic resonance (NMR) spectroscopy. However they have not seen widespread use due to insufficient ability to resolve and quantify more detailed structural features, such as the substitution pattern *ortho* to the phenol.[98–101] A ^{19}F NMR method utilizing

fluorobenzylation was reported by Barrelle and others, but isolation of the derivatized lignin was required prior to analysis; moreover, significant overlap between the derivatization agent and phenolic groups in the ^{19}F spectrum was observed.[102–104] Quantitative ^{13}C NMR spectroscopy is rich in structural information, and reports combining analysis of acetylated and underivatized samples can quantify a vast array of structural features which are useful for sample fingerprinting.[105,106] Nevertheless, ^{13}C NMR spectroscopy for lignin suffers drawbacks due to large sample amounts required and/or long NMR experiment acquisition times for spectrometers not equipped with a cryoprobe, complex spectra, and overlap between phenolic OH signals.[98,107]

One of the most widely implemented methods for quantifying phenolic groups in lignin is phosphitylation followed by ^{31}P NMR spectroscopy analysis.[108] Originally used to characterize coal condensates,[109,110] the method was adapted for lignin characterization by Argyropoulos *et al.*, and has since been extensively applied on a variety of lignins.[111–113] Briefly, a derivatizing agent, commonly 2-chloro-4,4,5,5-tetramethyl-1,3,2-dioxaphospholane (TMDP), is combined with the lignin sample dissolved in pyridine/*d*-chloroform. From a 1-D ^{31}P NMR experiment, distinct resonances are obtained for aliphatic alcohols, carboxylic acids, and various phenolics (5-substituted, G, and H) that are integrated relative to an internal standard. The advantages of the ^{31}P NMR method include the organic solvent mixture capable of dissolving a variety of lignins, commercially available reagents, and a straightforward procedure and NMR experiment. However, the method also suffers from several drawbacks. Importantly, the phosphitylation reagent is hazardous, with the potential for serious skin and eye damage (G.H.S. 1B skin corrosion, category 1 serious eye damage) upon exposure. It is also expensive ($217/g from Sigma-Aldrich at the time of writing) and degrades if exposed to moisture. Furthermore, NMR experimental times of ~1 hour per sample are required due to high spin-lattice relaxation values (T_1) of the phosphorus nuclei. When coupled with the limited stability of the derivatized samples, the throughput for ^{31}P NMR measurements is limited.[114]

Recently, pentafluoropyridine (PFP) was shown to be an effective phenol protecting group by selectively reacting at its 4-position to form the corresponding tetrafluoropyridyl (TFP) ether.[115] In the current work, we demonstrate that PFP can fully react with phenolic groups in lignin to form the

corresponding TFP-ethers. These TFP-ethers exhibit distinct chemical shifts in a ^{19}F NMR spectrum based on their *ortho*-substitution. The effects of reaction time, solvent, and ring substitution pattern on the rate of reaction were investigated, and the optimum system was found to be 40% H_2O/DMSO with a reaction time of five minutes. Given these results, the method potentially offers a safer (G.H.S. category 4 acute toxicity for PFP) and cheaper ($6.04/g for PFP on Sigma-Aldrich at the time of writing) alternative to ^{31}P NMR to quantify phenolic content in lignin samples.

3.3 Experimental

Model compound and lignin derivatization

The substrate (either lignin or a model compound, typically between 20-40 mg) was loaded into a 10 mL vial with a stir bar. K_2CO_3 (4 molar equivalents based on the phenol content unless otherwise specified) was added. The internal standard (4,4-difluorobenzophenone) was then added, and the mass was recorded. The solvent was then added via a volumetric pipette. PFP (4 molar equivalents based on the phenol content unless otherwise specified) was then added with a volumetric pipette to each vial. The vials were briefly (~3 seconds) shaken by hand to mix all the components, and put onto a stir plate at 800 rpm, at which point the timer was started. Depolymerized lignins such as organosolv or kraft lignins typically contain higher amounts of phenolic groups compared to native lignins, but vary widely depending on the process and biomass used.[98,116] For lignin samples, a phenol content of 4 mmol/g was assumed for calculation of the required K_2CO_3 and PFP. After the desired reaction time, a sample was taken by filtering the reaction mixture through a 0.2 μm PTFE syringe filter. For reactions in pure solvent, this was done directly from the reaction mixture, and was repeated over the course of the reaction to obtain time course measurements. For reactions in H_2O/DMSO, 2 mL of acetone was added to each vial prior to sampling to resolubilize the lignin and internal standard, and the vials were shaken. For model compounds, poplar RCF oil, and corn stover MWL, re-solubilization was almost instantaneous. However, for kraft lignin, the vials needed to be shaken for approximately 1 minute before the sample fully was dissolved. Subsequently, 0.3

mL of the filtered sample was combined with 0.3 mL of d_6-acetone/Cr(acac)$_3$ (2 mg/mL initial concentration of the d_6-acetone solution, for a final sample Cr(acac)$_3$ concentration of 1 mg/mL).

^{19}F NMR experiments.

A 1D ^{19}F NMR experiment with inverse gating was acquired on a Bruker Avance 300 MHz instrument with a delay of 6 seconds, 64 scans, and a sweep width of 242 ppm. Processing was performed using TopSpin 3.7. The file was apodised with exponential line broadening of 2.0 Hz. The internal standard peak was located and set to -108.4 ppm for reactions in acetone, -106.4 ppm for reactions in DMSO, or -107.4 ppm for reactions in 40% H$_2$O/DMSO. The internal standard peak was made as symmetrical as possible through first order phasing. Then, the PFP peak at -135 ppm was adjusted to be symmetric with first order phasing. The baseline was then corrected using a 6th-order Bernstein polynomial fit in the order of ranges -80 through -110, then -110 through -145, and finally -145 through -165 ppm. The Mestre Nova automatic multipoint baseline correction feature was also found to give satisfactory results. Plots of NMR spectra were produced using Mestre Nova 14.1.

3.4 Results

Method development with phenolic model compounds.

PFP has been shown to undergo S$_N$Ar reactions with a range of phenolic substrates in the presence of base.[115,117] In these reactions, the base deprotonates the phenol to form the phenolate ion, which then adds to PFP, followed by elimination of the fluoride ion to form the TFP-ether product (**Figure 10A**). When a weak base such as K$_2$CO$_3$ is used at room temperature, this reaction occurs exclusively at the 4-position of PFP; however stronger bases and elevated temperatures have been used to enable reactivity at sites *ortho* and *meta* to the nitrogen atom.[118] This reaction produces a stoichiometric amount of HF, but the excess of K$_2$CO$_3$ converts the HF to KF or other potassium fluoride species (See the SI for discussion of chemical safety).[119] By including an internal standard (4,4-difluorobenzophenone) in the reaction setup, we envisioned a method where the reaction mixture can simply be filtered after the desired reaction time to yield a solution that can be analyzed via ^{19}F NMR to quantitatively measure phenolic groups.

To explore the viability of the proposed ^{19}F NMR method for identifying and quantifying phenolic groups in lignin, reactions were first performed on model compounds representative of the chemical motifs found in lignin. In the proposed method, phenols must react completely to form the corresponding TFP-ethers without the formation of side products and in a reasonable amount of time. Furthermore, the ^{19}F NMR resonance must be sensitive to the substitution *ortho* to the ether bond to enable the identification and quantification of different types of phenols. To examine the viability of this approach, experiments were first performed on the series of 4-propyl substituted monomers, namely 4-propylphenol, 4-propylguaiacol, and 4-propylsyringol, which mimic the H, G, and S-type substitution patterns found in lignin, respectively. Reactions were conducted in 10 mL vials at room temperature with magnetic stir bars. The TFP-ether contains two sets of identical fluorine atoms which give rise to resonances in two distinct regions in the ^{19}F NMR spectra: a downfield (DF) region from -89 to -95 ppm (blue fluorine atoms, blue integration region in **Figure 10B**) and an upfield region (UF) from -155 to -162 ppm (red fluorine atoms, red integration region in **Figure 10B**). Conversion of the model compound can be determined by integration of peaks in either region relative to the internal standard.
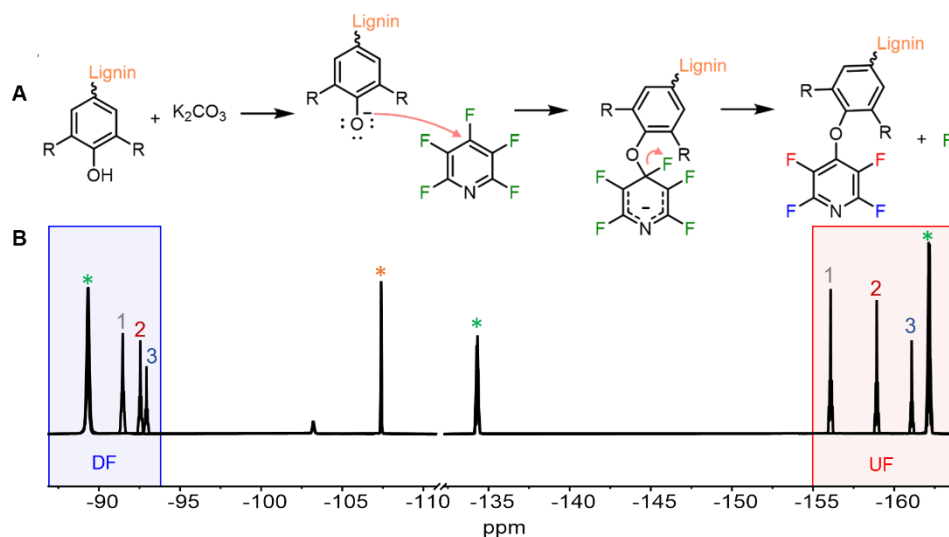
Figure 10. (A) Reaction of pentafluoropyridine (PFP) with a phenolic compound to form a tetrafluoropyridyl (TFP) ether through an S_NAr mechanism. **(B)** The blue and red fluorine atoms in the TFP product correspond to the ^{19}F NMR resonance regions from -89 to -95 (downfield, DF) and -155 to -162 (upfield, UF), respectively. Resonances marked with a green asterisk (*) belong to PFP, and the resonance marked with an orange asterisk (*) is for the internal standard, 4,4-difluorobenzophenone. Numbered resonances correspond to 4-propylphenol (1), 4-propylguaiacol (2), and 4-propylsyringol (3) derivatized in 40% H_2O/DMSO.

When reactions were performed in acetone with 4 equivalents of PFP and K_2CO_3, full conversion of each of the three 4-propyl substituted compounds to the desired TFP ether product was measured within two hours (**Figure 11A**), and no side products were observed in the ^{19}F spectra. The rate of reaction followed the order of 4-propylphenol (H) ~ 4-propylguaiacol (G) > 4-propylsyringol (S), presumably due to steric hinderance by the *ortho* methoxy groups in the case of 4-propylsyringol. The ^{19}F NMR resonances of the TFP-ether products were also impacted by the substitution pattern *ortho* to the phenol. In both UF and DF regions, 4-propylphenol exhibited the furthest downfield shift, followed by 4-propylguaiacol, and then 4-propylsyringol. However, the separation between the resonances was larger in the UF region (**Figure 10B**). Similar dependencies of substitution on reaction rate and ^{19}F NMR shift were observed for both unsubstituted (phenol, guaiacol, syringol) and aldehyde substituted (*p*-hydroxybenzaldehyde, vanillin, syringaldehyde) model compounds (**Figure 11B**). Aldehyde reactions were conducted in DMSO due to solubility limitations in acetone, as discussed in further detail below. The stir bar size was also observed to affect the rate of reaction. When a medium stir bar (15 x 6 mm, which is the size used for model compound reactions) was used for the derivatization of syringol, full conversion was observed within 2 hours, similar to 4-propylsyringol. However, using a smaller stir bar (13 x 3 mm) extended the time necessary for complete derivatization to approximately 12 hours. Further increasing the stir bar size (30 x 8 mm) showed no increase in reaction rate (**Figure B1A-B**).

To further investigate factors impacting the reaction rate, the slate of model compounds used was expanded. The G-type model compounds guaiacol, 4-propylguaiacol, and vanillyl alcohol all showed similar yields of the TFP-ether after 5 minutes of reaction time in acetone (**Figure 11C**). However, when vanillin and acetophenone were used under the same conditions, the reactions exhibited higher conversions at 5 minutes, with the vanillin reaction being complete. These differences correlate with the relative acidities of the aromatic compounds (guaiacol pK_a = 9.93; 4-propylguaiacol pK_a = 9.85; vanillyl alcohol pK_a = 9.78, vanillin pK_a = 7.36; acetovanillone pK_a = 7.81)[120] and indicate that the population of the phenolate may be governing the observed reaction rates. In general, the phenolic hydroxyl groups on compounds where the α-position is a ketone, ester, or aldehyde are more acidic than those where the α-hydroxyl is still present
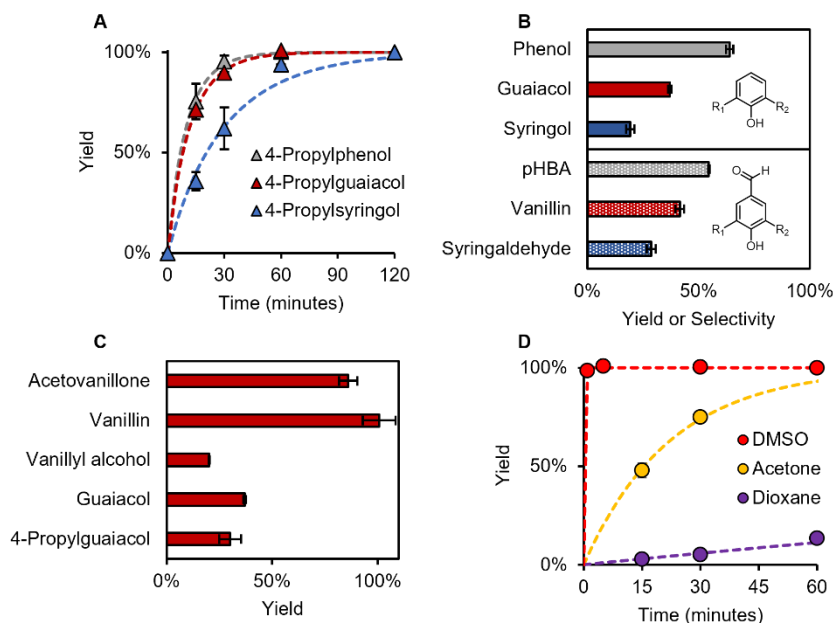
Figure 11. (A) Time course measurement of TFP ether formation for 4-propylphenol (H), 4-propylguaiacol (G), and 4-propylsyringol (S) in acetone. Conditions: 4 mL acetone, 4 eq. K_2CO_3 and PFP, room temperature. **(B)** Yield of TFP-ether for phenol, guaiacol, and syringol (conditions: 1 mL acetone, 4 eq. K_2CO_3 and PFP, room temperature, 5 minutes reaction time) compared to the selectivity observed for combined reaction of *p*-hydroxybenzaldehyde, vanillin, and syringaldehyde reaction. To accommodate for the high expected rate of reaction of the aldehydes in DMSO, the relative rates were measured by derivatizing the three substrates in the same vial with only 0.2 equivalents of PFP based off the total phenols loaded, allowing for the selectivities of the TFP-ethers to indicate the relative rates of reaction. Conditions: 1 mL DMSO, 4 equivalents K_2CO_3, 5 minutes, conversion is limited by adding 0.2 equivalents of PFP. **(C)** Yield of TFP-ether for guaiacyl type model compounds. Conditions: 5 minutes reaction time, 1 mL acetone, 4 equivalents PFP & K_2CO_3. **(D)** Reaction of syringol in DMSO (red), acetone (yellow) and dioxane (purple). Conditions: 4 mL solvent, 4 eq. K_2CO_3 and PFP, room temperature. Error bars indicate duplicate measurements.

or has been removed or etherified.[120] A single lignin sample can contain multiple functionalities at the α positions, and this is expected to impact the observed rate of reaction of different lignin samples accordingly.[24,107,121]

When attempting to derivatize a wider array of model compounds in acetone, solubility issues were encountered. For example, when the derivatization of syringaldehyde was attempted in acetone, no product was observed in the ^{19}F NMR spectrum, and instead a white precipitate was formed. While acetone is a common laboratory solvent and allowed for the convenient measurement of reaction rate, other solvents such as DMSO offer improved ability to dissolve a wide range of lignins.[122–124] Repeating the derivatization of syringaldehyde in DMSO showed full conversion to the TFP-ether within 1 hour. Aside from affecting the solubility of substrate, solvent choice can also modulate reaction kinetics, especially for S_NAr

33

reactions.[125,126] Given the fast reaction of vanillin, reactions were instead performed with syringol to measure the effect of solvent on reaction rate. When DMSO was used as the solvent, full conversion of syringol to the desired TFP ether was observed within 1 minute, much shorter than the 2 hours required for the same reaction in acetone (**Figure 11D**). Reactions in dioxane, another common solvent for lignin, displayed the lowest reaction rate, achieving less than 15% conversion in 1 hour. The observed solvent effect may be a result of the higher solubility of K_2CO_3 in DMSO compared to the other solvents,[127,128] and reinforces the conclusion that reactivity of alcohols with PFP is dependent on deprotonation of the alcohol. In the scope of the prescribed method, the drastic increase of reaction rate can reduce time needed for derivatization, and ultimately leads to higher throughput if desired. We thus selected DMSO as the preferred solvent for further investigation due to the faster reaction rate and improved dissolution ability.

Given the promising results showing complete and selective conversion of model compounds to their corresponding TFP-ethers, we further expanded the scope of model compounds tested to 29 total (**Table B1**). While quantitative yields of the desired TFP-ether were observed for most model compounds using DMSO as a solvent, issues were encountered when carboxylic acid containing models were used. For example, when syringic acid was derivatized in DMSO, only a ~62% yield of the TFP-ether product(s) was measured across multiple resonances in the ^{19}F NMR spectrum (**Figure 12A-B**). Furthermore, 64% of the initial PFP loaded was converted to tetrafluorohydroxypyridine (TFHP), identified by previously reported ^{19}F NMR shifts;[129] the ^{19}F NMR resonances for TFHP do not overlap with the TFP-ether products (**Figure 12B**). Brittain and Cobb showed that carboxylic acids react with PFP to form acyl fluorides and TFHP. These acyl fluorides could then react further with phenols to yield esters (**Figure 12C**).[129] These side reactions consume the K_2CO_3 and PFP reagents and also prevent phenols from being measured, potentially precluding the method from use on substrates that contain carboxylic acids.

The acyl fluoride-forming reaction relies on the nucleophilic attack of the fluoride ion on a TFP-ester intermediate. Halides such as F$^-$ are particularly reactive in polar aprotic solvents such as DMSO, but reactivity is reduced in protic solvents such as water.[130] Thus, we examined the impact of water content in the derivatization solvent. As water content in the derivatization solvent was increased to 20% and 40%,

the yield and selectivity to a single TFP-ether resonance increased (**Figure 12A-B**). When the solvent

contained 40% water, nearly full recovery of the desired TFP-ether was observed from a single resonance,

showing that the addition of water can prevent this side reaction (**Figure 12**). TFHP could form from the

reaction of water and PFP; however, only 4% of the PFP was converted to TFHP for reactions in 40%

H_2O/DMSO, indicating that TFHP is formed mainly from the acyl fluoride-forming reaction, rather than

from direct reaction of PFP and water. The presence of water in the reaction solvent is expected to increase

the rate of phenolic derivatization due to increased solubility of K_2CO_3, but the reaction occurs too quickly

to confidently measure the change in rate directly.
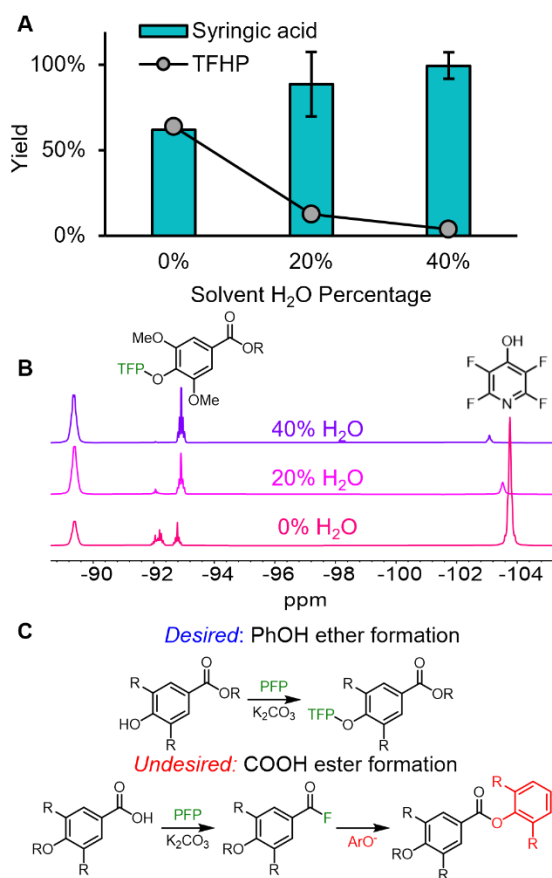
Figure 12. (A) Yield of the syringic acid-TFP ether (teal bars) and TFHP (gray circles) as a function of water content in the derivatization solvent. (**B**) ^{19}F NMR spectra of reactions from **A.** (**C**) Desired TFP-ether formation reaction from carboxylic acid-containing substrates and undesired ester production through acyl fluoride formation followed by esterification with an additional phenolic molecule. Conditions: 1 mL reaction solvent (0%, 20%, or 40% H_2O/DMSO), 4 equivalents PFP & K_2CO_3, 5 minutes reaction time, room temperature, 2 mL acetone added to the reaction vial to resolubilize products and internal standard, error bars represent the range of duplicate measurements.

Utilizing 40% H_2O/DMSO solvent, full conversion of the starting material was observed in 5 minutes for almost all phenolic monomer model compounds tested, and the average and range of observed resonances are shown in **Figure 13** for each substitution pattern. The one exception is that when the model compound 5-5 GG, (3,3′-dimethoxy-5,5′-dipropyl[1,1′-biphenyl]-2,2′-diol) which contains two phenolic groups, was derivatized for the standard reaction time of 5 minutes, two resonances were observed in the ^{19}F NMR spectrum at -94.12 ppm and -92.78 ppm (**Figure B2A**). As the reaction time increased, the upfield resonance decreased and the downfield resonance increased, indicating that the downfield peak is likely due to the partially derivatized product (mono-TFP ether). For a reaction time of 5 minutes, the mono- and di-TFP ether accounted for 59% and 25% yield of the starting material, respectively. Allowing the reaction to proceed to 3 hours showed full conversion to the fully derivatized product (**Figure B2B**). When *ortho*-eugenol, another 5-substitued model compound, was tested, full conversion to the desired TFP-ether was measured in the desired time of 5 minutes. These results suggest that the low quantification for 5-5 GG derives at least in part from steric blocking of the first derivatized phenol. Importantly, the partially derivatized 5-5 compound can be detected by its resonance at -94.12 ppm, which is outside of the phenolic integration range, allowing for monitoring of this issue in lignin substrates. Catechol and protocatechuic acid were both fully converted to the desired di-TFP ethers, indicating that the 1,2-dihydroxy substitution does not inhibit full derivatization. However, the derivatization of gallic acid and 3,4,5-trihydroxybenzaldehyde was unsuccessful, leading to precipitate formation and under quantification (gallic acid: 78 ± 6%; 3,4,5-trihydroxybenzaldehyde: 58 ± 2%, duplicate measurements) across multiple resonances in the ^{19}F spectrum, presumably arising from the incomplete derivatization products (**Figure B3**). The tri-hydroxy substitution pattern is known to prompt degradation reactions in the presence of oxygen, especially under alkaline conditions.[131]

Distinction between syringyl (S), guaiacyl (G), *p*-hydroxy phenyl (H), and condensed-G (G$_c$, G-type compounds with substitutions at the 5-position other than a methoxy group) phenolics could be achieved in both regions for most model compounds tested (**Figure 13**). One exception was that aldehydes such as vanillin and syringaldehyde displayed resonances that were substantially downfield of similarly

substituted phenols, causing overlap with other integrations in the DF region (**Figure B4**). For G_c compounds such as *ortho*-eugenol and 5-5 GG, resonances were mostly downfield of S phenolics in the UF region, indicating that G_c and S phenolics can be distinguished in this region. In the DF region, however, G_c phenols completely overlapped with the syringyl peak, indicating that this region may be a mixed measure of total 5-substituted phenols, rather than purely S-type (**Figure 13**, dark blue; **Figure B4**). Catechol and protocatechuic acid displayed DF resonances which overlapped with the H region (-91.0 ppm), but the UF resonances (-156.99, -156.87 ppm) did not overlap with any other studied model compounds (**Figure B3**). Although this may indicate the possibility of using this region to quantify catechols, this region is currently included in the G region. Overall, these results indicate that PFP derivatization in 40% H_2O/DMSO followed by ^{19}F NMR allows for reasonably accurate identification of H, G, G_c, and S phenolics. The full list of shifts of all model compounds tested can be found in **Table B1**, and comparison of select spectra can be seen in **Figures B2-B3**. Recommended integration ranges for quantifying different phenolics are given in **Table B2**.
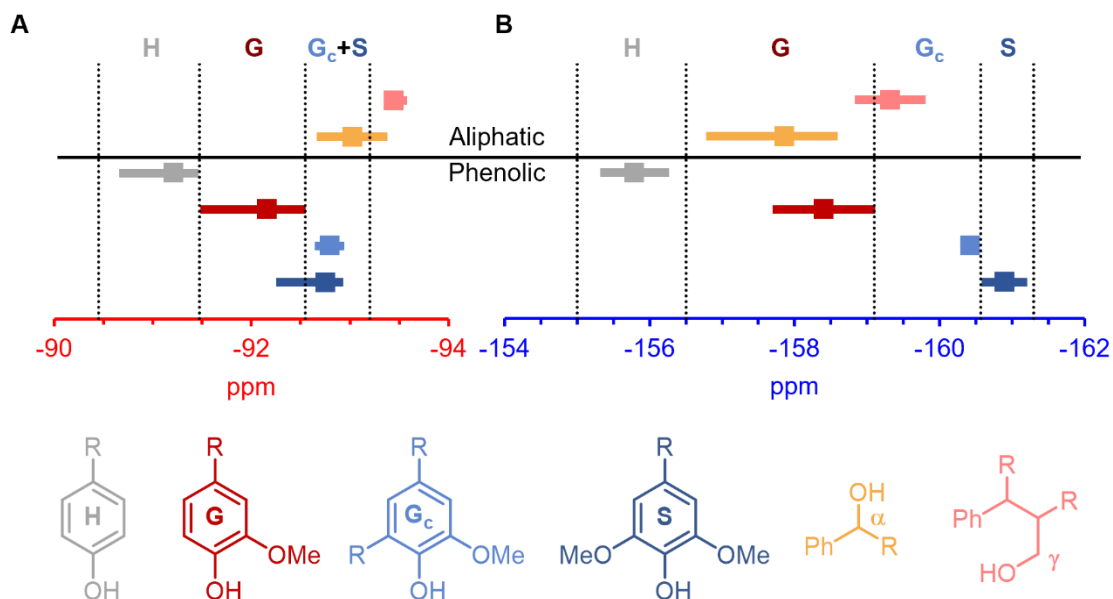
Figure 13. ^{19}F Resonances of model compounds for **(A)** downfield (-90 to -94 ppm, red axis) and **(B)** upfield (-155 to -162 ppm, blue axis) regions for derivatizations conducted in 40% H_2O/DMSO. The square marker indicates the average shift of the models tested, and the colored lines indicates the total range observed. Vertical dotted lines show the used integrations ranges. R groups tested include H, propyl, aldehydes, and carboxylic acids, among others. The number of compounds reported for each group is: G_c = 2; S = 5; G = 6; H = 5; α = 7; γ = 4. Conditions: 1 mL 40% H_2O/DMSO, 4 equivalents PFP & K_2CO_3, 5 minutes reaction time, room temperature, 2 mL acetone added to the reaction vial to resolubilize products and internal standard.

Derivatization selectivity to phenolic hydroxyl groups.

In addition to phenols, native and derivatized lignins contain additional hydroxyl groups at the α and γ positions on linkages between aromatic rings. For the PFP-based method to be effective, reactions with these alcohols must not interfere with phenolic regions in the NMR spectra. If their resonances do not overlap, their reaction can be ignored. However, if aliphatic hydroxyl resonances fall within the phenolic integration region, their reaction rate must be sufficiently slow compared to the phenolic derivatization rate to ensure high selectivity to phenolic hydroxyl groups. Aliphatic alcohols, especially those which lack heteroatoms such as halides, are considerably less acidic than phenolic alcohols, with aliphatic alcohols exhibiting pK_a values in the range of 15-16.[132,133] Given the evidence above that suggests the link between the pK_a value of a phenol and its TFP-ether formation rate, reactions with aliphatic alcohols were expected to be much slower than phenolic reactions. Nonetheless, acidity does not constitute the full picture of S_NAr reactivity, which also depends on the nucleophilicity of the conjugate alkoxide.

To measure the potential impact of aliphatic hydroxyl groups on the quantification of phenols, model compounds containing aliphatic hydroxyl groups were derivatized to determine their resonance and reaction rate (**Table B1**). Aliphatic hydroxyl groups behaved similarly to phenols, exhibiting a single resonance due to TFP-ether formation. All tested aliphatic alcohols showed resonances in the UF guaiacyl or condensed-G phenolic integration region, indicating that these alcohols would cause interference in measurements of lignins if converted to TFP-ethers during derivatization. However, in the DF region, most aliphatic shifts were upfield of the phenolic resonances (**Figure 13,** gold markers represent α-hydroxyl groups; pink markers represent γ-hydroxyl groups). The exceptions were some benzylic alcohols such as vanillyl alcohol, in which the derivatized aliphatic overlapped with the region for S phenolic hydroxyls in the DF region. For example, 3,4-dimethoxybenzyl alcohol exhibited resonances of -93.38 ppm and -158.59 ppm, which are outside of the phenolic DF region (-90.5 to -93.2 ppm) but overlap with the UF phenolic region (-155 ppm to -161.35). However, vanillyl alcohol displayed resonances of -93.0 ppm and 158.44 ppm, which overlap with the DF and UF integration regions respectively (**Figure B5**).

The fact that aliphatic alcohol resonances overlap with phenols to a lesser degree in the DF region compared to the UF region can give insight into the extent of aliphatic reaction during a derivatization. In the event of aliphatic reaction, additional resonances will the present in the ^{19}F NMR spectrum. In the DF region, most of these are expected to be upfield of the phenolic integration region, although some will lie in the S region, which will inflate the value obtained for the phenolic content. In the UF region, all reacted aliphatics will be quantified as phenols, increasing the value obtained for the phenolic content, such that the UF measurement will be greater than the DF measurement. This difference can indicate the extent to which aliphatic alcohols have reacted, serving as an internal reference as to whether aliphatic alcohol groups are interfering in the measurement. If similar values are obtained for both regions, the interference from aliphatic hydroxyls is expected to be low, and the UF integration region should be used as the preferred region, given the greater separation between resonances. However, if the UF region quantifies a higher phenolic value than the DF region, we recommend that the DF region be used for quantification. The syringyl integral from the UF region may still be integrated since no aliphatic alcohols displayed resonances there (**Figure 13**).

Overall, the yields from reactions with other aliphatic alcohols show that the reaction rate, and therefore the expected potential interference with phenolic measurements, was highly dependent on substrate (**Figure 14A**). Nonphenolic model compounds such as 2-(3,4-dimethoxy phenyl)-ethanol showed the highest reaction rates, achieving 51% yield to the corresponding TFP-ether in 5 minutes in 40% H$_2$O/DMSO (**Figure 14A**). Conversely, the phenolic analogue, homovanillyl alcohol, exhibited only 5% conversion of the aliphatic alcohol. For phenolic substrates vanillyl alcohol, homo-vanillyl alcohol, and 4-propanolguaiacol, the aliphatic yield decreased with longer chain length. The difference in reactivity of phenolic/non-phenolic models could be due to inherent differences in the reactivity of the respective aliphatic alcohols, such as the aliphatic alcohol of the non-phenolic models being systematically more acidic or nucleophilic than phenolic analogues, although this is not expected. Alternatively, this could indicate an effect where the presence of the phenol impacts the rate of derivatization through another mechanism, such as consumption of limited reactants. To elucidate the role of phenols on the rate of aliphatic reaction, 2-

(3,4-dimethoxy phenyl)-ethanol was derivatized again, this time with a 1:1 mole ratio of 4-propylguaiacol. Only a 16% yield of the derivatized aliphatic alcohol was measured, indicating that the presence of phenols reduces the rate of aliphatic derivatization (**Figure B6**). Substrates containing the β-O-4 linkage such as guaiacylglycerol-β-guaiacyl ether (GGE) and 1-(3,4-dimethoxyphenyl)-2-(2-methoxyphenoxy)propane-1,3-diol (VGE) exhibited high reactivity compared to similarly substituted compounds (**Figures 14A, B7-B8**). For instance, the secondary benzylic hydroxyl group on 4-hydroxy-3-methoxy-α-methylbenzyl alcohol showed only 2.3% conversion to the corresponding TFP-ether in 40% H_2O/DMSO after 5 minutes, whereas VGE showed almost 58% yield under the same conditions. The low yields of aliphatic derivatization for model compounds containing phenolic hydroxyl groups demonstrates that aliphatic interference should be low for most lignin samples that contain free phenolic groups. However, native-like lignins that contain abundant β-O-4 linkages may be especially prone to aliphatic interference.

To further investigate whether derivatization conditions could impact selectivity, reactions were conducted with vanillyl alcohol, which contains both a phenolic and an aliphatic alcohol group. Time course reactions in acetone showed that the benzylic alcohol was derivatized concurrently with the phenolic group, and the initial rate of phenolic derivatization was about 100x faster than the corresponding reaction with the benzylic alcohol. When the aliphatic hydroxyl group was derivatized, the corresponding phenol resonance on the same molecule was shifted slightly downfield (**Figure B9B**). Complete conversion of vanillyl alcohol to the phenol-TFP derivative was observed in approximately 2 hours, at which point the yield of the aliphatic TFP ether was 4% (**Figure 14B**, blue circles; **Figure B9A**). Decreasing the amount of PFP and K_2CO_3 used to 1 equivalent decreased the reaction rate but did not alter the selectivity of phenol reaction over aliphatic reaction (**Figure 14B**, blue diamonds). Similar experiments were conducted in DMSO and 40% H_2O/DMSO, except the conversion of the phenol was controlled by reducing the equivalents of PFP, due to the much faster rate of reaction. Changing the base from K_2CO_3 to NaOH resulted in multiple resonances, potentially from reactions at positions other than the 4 position of PFP. Using $Ca(OH)_2$, which is much less soluble in water, resulted in only 1 resonance, but had a slightly lower selectivity to the phenol (**Figure 14B**, purple square). Regardless of the solvent and the varying overall

40

rates of reaction, the extent of aliphatic reaction at a given phenol conversion was similar, although reactions in 40% H_2O/DMSO showed a slightly lower selectivity to phenolics. This suggests that that selectivity cannot not be appreciably modulated through solvent or base selection, and that aliphatic interference can mainly be controlled by selecting the proper reaction time for the given solvent.
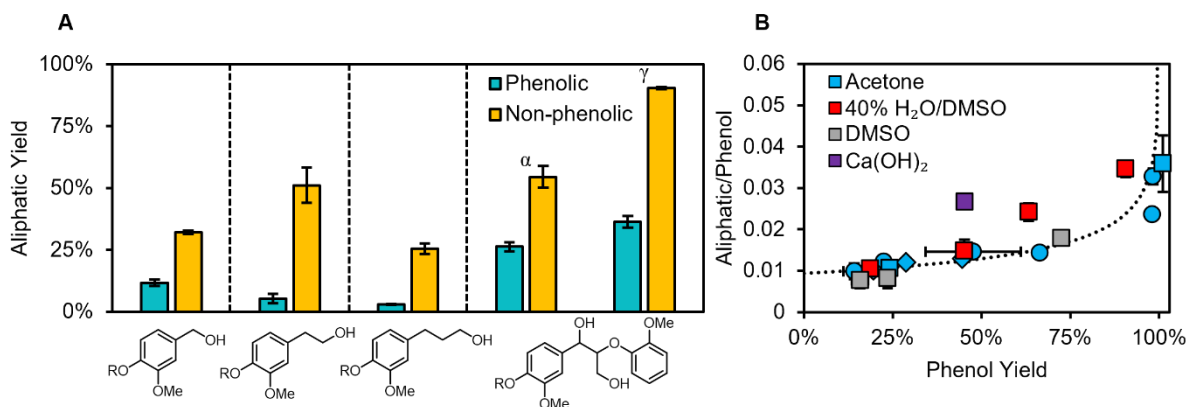
Figure 14. (A) Yield of TFP-ether products from aliphatic alcohols for phenolic (teal) and non-phenolic model compounds (yellow). Conditions: 20 mg substrate, 4 equivalents K_2CO_3 and PFP, 1 mL 40% H_2O/DMSO, room temperature, 5 minutes reaction time, 2 mL acetone added post reaction for re-solubilization. **(B)** Impact of different solvent systems on the selectivity of aliphatic derivatization as a function of phenolic conversion using vanillyl alcohol as a substrate. Squares represent partial conversion experiments, wherein conversion was controlled by limiting the PFP used. Circles correspond to time course reactions where samples were taken consecutively from the same reaction over time with 4 equivalents of PFP & K_2CO_3, whereas diamonds represent reactions with only 1 equivalent PFP and K_2CO_3. Conditions: 20 mg vanillyl alcohol, 4 equivalents K_2CO_3 & PFP unless otherwise stated, 1 mL solvent, 2 mL acetone added post reaction for re-solubilization for reactions in 40% H_2O/DMSO. Error bars represent the range of two replicate experiments.

Application and benchmarking of the ^{19}F NMR method on lignin substrates.

Given promising results of the model compound studies, we next sought to validate the ^{19}F method by comparing phenolic measurements of diverse lignin substrates to measurements obtained using ^{31}P NMR, and validating the trends observed in model compound reactions.[108,134] From model compound experiments, none of the tested solvent systems showed a substantial advantage in selectivity to phenolics as a function of conversion. For the method to be useful for lignin substrates, a set reaction time should be implemented that ensures the complete derivatization of phenolic hydroxyls while minimizing the interference from aliphatic hydroxyls. The real selectivity will then depend on the absolute rates of reaction and the total time the substrate is in contact with the reagents, including the time during reaction preparation and post-reaction sampling, which is about 1 minute for each sample. For reactions in acetone which occur

on the order of hours, small deviations in the total reaction time for different samples is inconsequential. However, for reactions in 40% H_2O/DMSO where the TFP-ether formation is much faster, the time required for preparation and sampling is comparable to the total reaction time. Allowing reactions to proceed for slightly longer could be expected to give lower selectivity to phenols given the drastically different absolute rates of reactions. Thus, it is important to confirm the insensitivity of phenolic selectivity on the derivatization solvent.

We first investigated PFP derivatization of reductive catalytic fractionation oil (RCF oil) from poplar in acetone. While acetone showed a lower reaction rate and dissolution ability compared to DMSO for experiments with model compounds, its use also allowed for the measurement of spectral characteristics and quantifications as a function of time, providing confirmation of trends seen in model compound experiments. The RCF process cleaves β-O-4 ether bonds in lignin, leading to a highly depolymerized oil with phenolic monomers, as well as dimers and oligomers containing carbon-carbon linkages.[41,135] While RCF oil is still a complex mixture, a high percentage of its constituent molecules are aromatic monomers that are routinely quantified, making it comparatively simpler than native lignin.[57,136] Approximately 200 mg of RCF oil was derivatized in a 10 mL vial with 10 mL of acetone with 2 equivalents of PFP and K_2CO_3 using a small stir bar (see SI for the impact of the stir bar size), and samples were time obtained by filtering an aliquot of each vial at the desired reaction time. Within 1 hour of reaction time, well-resolved peaks for S and G moieties expected of a hardwood began to appear (**Figure B10A**). Poplar also contains *p*-hydroxybenzoate (PHBA) pendent units that are ester-linked to lignin and cell wall components.[137,138] PHBA is converted to methyl paraben and phenol during RCF in methanol,[139] and these can be individually resolved in both the ^{19}F and ^{31}P methods (**Figures 15B, B10A**). As expected from model compound studies, these H units reacted the fastest, followed by G and then S species (**Figure B10B,C**).

Comparison of the DF and UF regions showed that the quantifications of H and total phenol were indistinguishable at each time point. However, there was disagreement between the S and G-type quantifications (**Figure B10D**). Notably, the quantity of total 5-substitued phenolics quantified from the DF region was lower than that obtained from the UF region (DF: 1.55 ± 0.01, UF: 1.84 ± 0.07, [31]P: 1.85 ±

0.09 mmol/g), and more closely reflected the measure of purely S-type phenols measured from the UF region (UF: 1.47 ± 0.03, [31]P: 1.63 ± 0.07 mmol/g). This was compensated by the DF region quantifying a higher number of G-type phenols than the UF region (DF: 1.36 ± 0.02, UF: 1.09 ± 0.05, [31]P: 1.11 ± 0.05 mmol/g). This discrepancy may derive from species that are quantified as 5-substitued in the UF region but as G in the DF region. Model compound studies showed that aldehyde-substituted compounds, such as syringaldehyde, were substantially downfield of other S model compounds tested, however the presence of oxidized substituents is unlikely given the reducing reaction conditions of RCF. Alternatively, RCF oil could contain additional G_c compounds whose resonances fall downfield of the tested G_c model compounds, 5-5 GG and o-eugenol, and the DF resonances may overlap with G phenolics in the DF regions. Nonetheless, the identical total quantifications between the UF and DF regions show that aliphatic hydroxyl groups were not interfering to a large extent, and thus the UF region can be confidently used for quantification. After 24 hours of reaction, the quantification of total phenolics in the UF region showed no statistically significant differences to the values obtained using the ^{31}P NMR-based method (**Figure 15A**, [19]F: 3.52 ± 0.1, [31]P: 3.40 ± 0.2, $\alpha = 0.05$). Allowing the reaction to proceed for 48 hours led to little change in integration values or spectral characteristics, confirming that the reaction with the aliphatic hydroxyl groups is slow. Further leaving the reaction for 6 days eventually led to the appearance of additional resonances and increased integration values, presumably from the eventual reaction of aliphatic hydroxyl groups.

To confirm the solvent effects observed during model compound experiments, derivatization of RCF oil was repeated in pure DMSO (1 hour reaction time) and 40% H_2O/DMSO (5 minutes reaction time) using large stir bars. As expected, the reaction proceeded much faster in the more polar solvents. When the 40% H_2O/DMSO system was used, the lignin began to precipitate shortly after the addition of PFP, necessitating addition of solvent for re-solubilization after 5 minutes of reaction time. By using the ratio of 1 mL reaction volume to 2 mL of acetone, we observed full re-solubilization of the lignin sample and internal standard. Identical quantifications were obtained for all measurements compared regardless of the solvent ($\alpha = 0.05$), indicating that phenol selectivity remained the same at the time of measurement despite

the differences in absolute reaction rate (DMSO UF: 3.59 ± 0.1 mmol/g, 40% H_2O/DMSO UF: 3.52 ± 0.1, **Figure 15A, B11**). The similar quantifications obtained when using pure DMSO and 40% H_2O/DMSO as solvents can be attributed to the lack of carboxylic acids in the RCF oil as measured by the ^{31}P method. Similar to reactions in acetone, allowing reactions in DMSO and 40% H_2O/DMSO to proceed for additional time led to the quantification increasing above the value measured from the ^{31}P method, presumably from the formation of aliphatic-TFP ethers. This increase with continued reaction time was more pronounced in the UF region than the DF region, in line with the observation that most aliphatic hydroxyl group shifts do not overlap the DF region.

We next tested the derivatization of softwood kraft lignin (SWKL) with DMSO and 40% H_2O/DMSO solvents, since SWKL is not soluble in acetone. The kraft process consists of hydrothermal treatment of wood in the presence of NaOH and Na_2S, inducing extensive structural changes to the lignin.[140,141] These conditions prompt the formation of recalcitrant C–C bonds at the expense of aryl-ether linkages. Much work has gone into elucidating the resultant structure but it is still largely uncertain.[140,141] When SWKL was derivatized in DMSO, a slightly lower than expected phenolic quantification (^{19}F UF: 3.52 ± 0.08 mmol/g, [31]P: 3.77 ± 0.07 mmol/g) was obtained (**Figure15A**). This is possibly due to the presence of carboxylic acids (0.61 mmol/g as measured by ^{31}P method), leading to esterification and depletion of phenols. Repeating this derivatization in 40% H_2O/DMSO for five minutes led to a higher quantification of 3.92 ± 0.05 mmol/g (**Figure 15A**). DF quantification was only slightly lower at 3.71 ± 0.07 mmol/g total phenols. Extending the derivatization time to 10 minutes did not alter the quantification, indicating that phenols are fully derivatized within the 5-minute reaction time (**Figure B12**). Identification of structural motifs between the ^{19}F methods and ^{31}P was significantly different: ^{31}P NMR measured 0.67 ± 0.01 mmol/g of syringyl phenolics; however, lignin derived from softwoods should only contain guaiacyl and *p*-hydroxy phenyl moieties.[22] This is a known problem with ^{31}P NMR spectroscopy deriving from the significant overlap between G_c and S phenolics, regardless of the ^{31}P derivatization agent used.[98] The ^{19}F method measures 0.15 ± 0.01 mmol/g of syringyl units in the UF region, potentially showing this method has less overlap between S and condensed-G phenolics. Total 5-substituted content from the ^{19}F method

was still under-quantified relative to ^{31}P NMR (UF ^{19}F: 1.05 ± 0.01, ^{31}P: 1.59 ± 0.02), and the corresponding measurements of G and H units were higher. This may be due to the presence of non-conventional lignin phenols such as substituted catechols, but it is uncertain which method gives a better description of the functional groups given the lesser-known structure of the lignin.
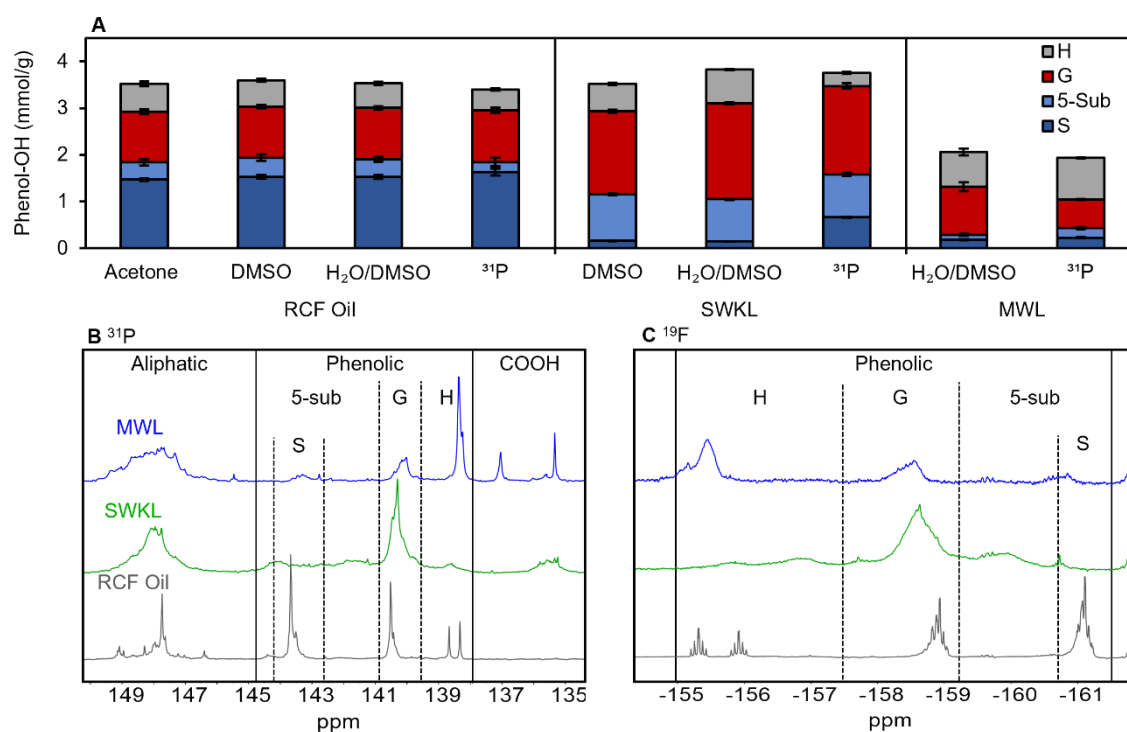
Figure 15. (A) Comparison of various ^{19}F derivatizations with ^{31}P NMR results. **(B)** ^{31}P spectra of tested lignins. **(C)** ^{19}F spectra of tested lignins. Reactions conducted in 10 mL glass vials at room temperature using 20-40 mg of lignin substrate, 4 equivalents of PFP and K_2CO_3 for DMSO and 40% H_2O/DMSO reactions and 2 eq. for acetone reactions, reaction time of 24 hours for acetone, 1 hour for DMSO, and 5 minutes for 40% H_2O/DMSO. For reactions in 40% H_2O/DMSO, 2 mL of acetone were added to resolubilize the precipitated lignin. Error bars show the standard deviation of 3 replicate measurements. See **Figure 7** for statistical comparison of the ^{31}P NMR method with the ^{19}F NMR using 40% H_2O/DMSO.

The method was applied to corn stover milled wood lignin (MWL). MWL is intended to represent native lignin,[142] and ^{31}P NMR shows that there are a greater number of aliphatic alcohols (2.90 ± 0.03 mmol/g) than phenolics (1.94 ± 0.05 mmol/g) as expected from a lignin that has not been extensively depolymerized. When the ^{19}F method was applied, the UF integration region measurement was 20% higher (2.48 ± 0.07 mmol/g) than the DF region (2.06 ± 0.2 mmol/g) (**Figure B13**). This is likely due to aliphatic reaction during derivatization, and thus only the DF region was used for integration. From model compound

experiments with GGE and VGE, it is expected that β-O-4 structures in the MWL caused the increased aliphatic reaction compared to the RCF oil and SWKL. Reasonable assignment of phenol type was achieved, with ^{19}F measuring a higher amount of G type phenols (DF ^{19}F: 1.02 ± 0.09, ^{31}P: 0.61 ± 0.01) at the expense of 5-substituted (DF ^{19}F: 0.29 ± 0.02, ^{31}P: 0.43 ± 0.02) and H type (DF ^{19}F: 0.75 ± 0.07, ^{31}P: 0.890 ± 0.009) phenolics.

We thought that mixing could be especially important for reactions in 40% H_2O/DMSO due to the precipitation of the derivatized lignin during the reaction. Interestingly, using a medium stir bar led to a slightly lower quantification than values obtained using the large stir bar for all three substrates, although results were only significantly different for SWKL (**Figure B14**). We thus recommend the use of a large stir bar.

For any quantitative measurement, sample stability is an important consideration. Sample degradation may prevent accurate quantification, and limits analytical throughput and flexibility. Sample stability was measured for each solvent system where applicable by leaving the samples in the NMR tubes at room temperature. In the DMSO based systems, performing ^{19}F NMR experiments up to 14 days after derivatization resulted in identical integrations for the compared to the samples analyzed immediately after derivatization, implying that they are stable (**Figure B11C**). However, measured phenolic content of samples derivatized in 40% H_2O/DMSO increased by 3-6% over the course of 24 hours (**Figure B14A**), indicating that these samples should be analyzed immediately for best results. It is worth noting that ^{31}P samples are known to begin degrading immediately depending on the sample and internal standard, and it is also recommended that samples are analyzed immediately.[98,114] Experiments with SWKL conducted with two internal standards (4,4-difluorobenzophenone and 1,4-difluoro-2,5-dimethoxybenzene) showed no deviation in their expected ratio, nor did their relative integrations change over the course of 48 hours (**Figure B14B**). The increase in measured phenolic content therefore appears to be caused by the continued reaction with aliphatic alcohols enabled perhaps by the increased solubility of K_2CO_3 with the addition of water, rather than degradation of the internal standard as is common with the ^{31}P method.

Overall, the ^{19}F-based method appears to agree well with results obtained from ^{31}P NMR spectroscopy, with all R^2 values greater than 0.9. (**Figure 16A**). To assess the agreement of the ^{19}F method compared the ^{31}P method more thoroughly, t-tests were performed on quantifications of total phenolics and individual species (**Figure 16B**). Total phenolics are very closely recovered; however, SWKL is significantly different ($p \leq 0.05$). RCF oil is quantified most closely, with only the value of H phenolics qualifying as statistically significantly different (DF [19]F: 0.52 ± 0.03, [31]P: 0.44 ± 0.03). However, almost all individual quantifications for SWKL and MWL are significantly different, which indicates that the two methods are not equivalent for these more structurally complex lignins. While minimal deviations in the resonance classifications were observed for model compounds, these differences may point to unexamined species in the SWKL and MWL which violate the classifications, and more in-depth structural characterization is needed to determine the origin of these differences.
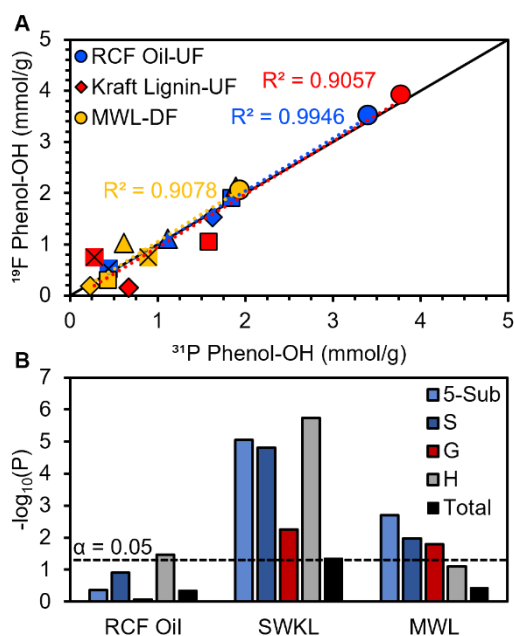
Figure 16. (**A**) Parity plot of quantifications of total phenol (circle), total 5-subsituted (square), S (diamond), G (triangle), and H (square with cross) obtained from the ^{31}P NMR method and the ^{19}F NMR method using 40% H_2O/DMSO as the solvent. (**B**) The negative logarithm of the p-value obtained from comparing ^{31}P and ^{19}F NMR measurements.

3.5 Conclusions

In summary, we developed a phenolic measurement method using pentafluoropyridine as a derivatizing agent followed by ^{19}F NMR spectroscopy. Reactions with aliphatic alcohol groups can be limited by tuning the reaction time. If carboxylic acids are not expected to be present, such as in lignins without ester-linked units, pure DMSO can be used as a solvent (1 hour reaction time), and samples can be assumed stable. In such cases, the ^{19}F method could be amenable to high-throughput analysis. The presence of carboxylic acids necessitates the use of 40% water as a co-solvent with a shorter derivatization reaction time of 5 minutes, and samples should be analyzed immediately. The method achieved comparable results to ^{31}P NMR spectroscopy in terms of total phenolic measurement for the three diverse lignins studied. Similar distributions of functional groups were obtained for corn stover MWL and poplar RCF oil, but softwood kraft lignin showed significantly different results, most notably 5-substituted groups were under-quantified using the PFP-based method. The ^{19}F method exhibits advantages in both the low cost of the derivatization reagent and its low toxicity, but it does not overcome the issue of sample stability that is present in the ^{31}P NMR method. Furthermore, the ^{19}F method is hindered by both aliphatic alcohols and carboxylic acids, whereas the ^{31}P method efficiently measures all hydroxyl groups. Further developments of this approach could focus on evaluating derivatization conditions to minimize the interference of aliphatic alcohols, but nonetheless the method can find immediate application to supplement the analytical toolbox available to lignin chemists.

Chapter 4: Reducing the footprint of RCF through design and validation of a high-throughput methodology

4.1 Summary

Reductive catalytic fractionation (RCF) is a promising method to extract and depolymerize lignin from biomass, and bench-scale studies have enabled considerable progress in the understanding of the RCF process in the last decade. Conventional bench-scale RCF experiments are typically conducted in individual pressurized batch reactors of volumes typically between 50-1000 mL which limits the typical throughput of these experiments to ~ 1-6 reactions per day for an individual researcher. In this study, we report a high-throughput RCF (HTP-RCF) method capable of performing 240 reactions per day, where each reaction is conducted in 1 mL reactor wells. We first designed and fabricated 24-well Hastelloy reactor plates which could seal high pressures generated from organic solvents by a stacked pin and seat mechanism. We screened various solvent combinations and catalyst loadings for the hydrogen-free RCF of 50 mg poplar at the 0.5 mL reaction scale. The system of 1:1 isopropanol/methanol showed optimal monomer yields and selectivity to 4-propyl substituted monomers, and validation reactions using 75 mL batch reactors were shown to yield identical monomer yields compared to reactions on a 30 mL scale. To accommodate for the low material loadings, we modified the workup procedure to allow for the parallel filtration, washing, and drying of samples to further increase sample throughput. A 1H NMR spectroscopy method was developed to quantify the extracted lignin RCF oil without needing to perform liquid-liquid extraction. Finally, 50 switchgrass samples were screened for their RCF performance in the HTP plate reactors, revealing a high degree of variability for monomer yield (21-36%), S/G ratio (0.41-0.93), and oil yield (40-75%). These results were validated by repeating RCF reactions in 75 mL batch reactors for six switchgrass samples, and near identical yields of total monomers and hydroxycinnamates were obtained. We anticipate that this approach can be utilized for rapid screening of substrates, catalysts, and reaction conditions with at least 10x higher throughput compared to larger scale batch reactors.

4.2 Introduction

RCF appears to be a convenient and robust technique for extraction of lignin and conversion to monomers. Still RCF reactions consume high amounts of materials including biomass, catalyst, solvent, and most importantly, a researcher's time. Much progress has been made in maximizing lignin conversion and characterizing the resulting lignin oil and carbohydrate pulp. The impact of solvent composition,[50,51] flow conditions,[57,60,61] exogenous H_2 gas pressure,[56,70] and catalyst[49,54] have been explored. However, the interdependence of reaction parameters has recently come to light,[68,143] and thus only a small space of these variables has been examined due to the low throughput. Bench scale studies of RCF are often conducted in pressurized batch reactors where biomass and catalyst are intermixed. Typical reaction conditions require up to two grams of biomass, 5-20 wt% (mass catalyst/mass substrate) of supported metal catalysts, 20-40 mL of an alcohol solvent such as methanol, pressurized with 20-50 bar hydrogen as a reducing agent, and heated to 190-250°C for 1-12 hours. Furthermore, the reaction workup procedure is time intensive, involving filtration, multiple steps of rotary evaporation, and liquid-liquid extraction which is inefficient for characterization of a large volume of substrates or reaction parameters. Combined, these factors limit the throughput of screening conditions for RCF.

High-throughput (HT) reactor systems are advantageous for rapidly testing variables in complex systems. In heterogeneous catalysis, development of high-throughput catalyst synthesis and characterization infrastructure, along with parallelized reactor systems and techniques for rapid assessment of catalyst activity have enabled the discovery of new and improved catalysts. For example, combinatorial HT studies have discovered optimal binary or ternary metal or metal oxide systems for applications such as aqueous phase reforming of biomass-derived oxygenates,[144] amination of benzene to aniline,[145] paraffin isomerization,[146] ethane dehydrogenation,[147] and the hydrogen evolution reaction.[148] These experiments are run on a wide variety of reactor systems, depending on the demands of the reaction being studied (i.e. temperature, pressure, corrosion resistance) and the desired capabilities for throughput, reaction scale, product characterization, and catalyst preparation.

Liquid-phase HT reactor systems for thermochemical lignocellulose upgrading have also been designed to analyze how pretreatment conditions and feedstock composition impact the digestibility of sugars by enzymes.[149–153] These reactors were developed with fewer capabilities for stirring or dosing gasses, but achieved much higher throughput to enable the screening of entire populations of naturally variant poplar genotypes, and were machined from Hastelloy capable of operating at temperatures as high as 200°C with acidic aqueous solutions. In one notable design, the 96-well plates were sealed by stacking together, making a simple modular system that is easy to assemble and achieved 960 individual biomass pretreatment experiments in parallel with a stack of ten plates. Biomass research has also benefitted greatly from increased throughput for characterization using a variety of techniques including ^{1}H-NMR,[154] pyrolysis-molecular beam mass spectrometry,[155] and others.

Here we report a method for conducting high-throughput RCF (HTP-RCF) reactions with a 0.5 mL reaction volume amenable to the screening of various biomasses, catalysts, or solvent systems. A stackable plate reactor capable of performing 240 parallel batch reactions was designed. The wash/transfer solvent that maximized product recovery and reproducibility was found to be 3:1 v/v ethyl acetate/hexane. Given the low substrate loadings, a ^{1}H NMR method was developed to measure extracted lignin in place of gravimetric measurement of organic soluble oil. The impact of catalyst/biomass ratio on aromatic monomer yield was investigated to determine catalyst limited and extraction limited regimes. Method validation was pursued by performing RCF reactions of various substrates using both the HTP-RCF method and conventional 75 mL batch reactions. Overall, the HT method recovers similar trends to the larger scale conventional methodology, showing potential for significantly faster reaction optimization and condition screening.

4.3 Experimental

75mL scale RCF Reactions in Parr reactors

RCF reactions were conducted in 75 mL Parr® reactors. To the reactor bottom with magnetic stir bar was added 2 grams of substrate and 400 mg of Ru/C (the catalyst is 5 wt% metal loading). The catalyst

was then wetted with 400 mg of deionized water to prevent ignition of the solvent. Methanol was then added to bring the total volume to 30 mL, and the reactor was sealed and pressure tested at 90 bar. The reactor was purged three times with He, and then filled with H_2. The reactor was heated to 225°C in approximately 30 minutes and held for three hours. After reaction, the reactors were cooled in ice water to room temperature. Then, approximately 10 mL was filtered through a 0.22 micron syringe filter. To measure the oil yield, a 0.5 mL aliquot was taken and dried under flowing air, and resuspended in 0.5 mL of 1 g/L 1,3,5-tri-tert-butylbenzene (TTB) in acetone-d_6. A ^{1}H NMR experiment was performed on a Bruker 400 or 600 MHz instrument with 32 scans and a delay of 3 seconds. A sample was prepared for GC-FID analysis by combining 0.5 mL of the RCF liquor with 0.5 mL of a 2 g/L solution of TTB in methanol.

Liquid-liquid extraction for isolation of lignin oil

Approximately 5 mL of original RCF solution from parr reactions was added to a 100 mL round bottom. The methanol was evaporated in a rotary evaporator, and the resulting oil was subjected to liquid-liquid extraction with ethyl acetate and water to isolate the lignin oil. The organic phases were combined and evaporated in a rotary evaporator, yielding the lignin oil. The lignin oil was then redissolved at a known concentration in acetone-d_6 with TTB as an internal standard. Aliquots of this stock solution were combined with additional acetone-d_6 with TTB (1 g/L) to give solutions of various concentrations. A ^{1}H NMR experiment was performed using 32 scans and a 3 second delay (d1) on a Bruker 400 MHz instrument equipped with Prodigy cryoprobe. The S (6.2-6.6 ppm) and G (6.6-7.2 ppm) regions were integrated relative to the TTB peak (~7.3 ppm), giving the moles of the respective units after adjusting for the number of hydrogen atoms.

HTP-RCF Procedure

To accommodate the multi-step HTP-RCF procedure, setup, operation, and workup were conducted over multiple days. On the first day, O-rings are placed on the bottom of ten 24-well reactor plate which serve to seal the plate below. A solids loading robot is utilized for the loading of biomass and

catalyst into the wells. Solids dispensing hoppers were loaded with approximately 250 mg of whole biomass. A solution of 2 g/L octadecane (surrogate standard) in the desired reaction solvent (1:1 v/v IPA:MeOH for reactions other than where reaction solvent is noted) is prepared through massing each component. The following day after solids are loaded into the wells, 0.5 mL of the reaction solvent is added to each well using a 1000 µL positive displacement pipet. Plates are labeled with rows A (furthest from user) to D (closest to user) and columns 1 to 6 (left to right), stacked, and numbered from 1 (bottom) to 10 (top). An 11th empty plate is prepared with O-rings and stacked to seal plate 10. Plates are then mounted onto the bottom holder plate, and the top holder plate is installed. Twelve all threads cut to 14 inches are prepared by adding ten spring discs/Belville washers to each along with three nuts. All threads are then routed through the top plate and screwed into the bottom plate. The nuts were then tightened in a star pattern to compress the spring discs and seal the O-rings. Under the high temperature and correspondingly high vapor pressure in the wells, an imperfect seal will likely lead to the reaction solvent evaporating. Furthermore, cooling the plates via flooding the hot reactor with cooling water leads to large shifts in temperature in a short amount of time. To ensure proper sealing, unrestricted travel of the nuts through the tightening length of all thread is necessary to allow for perceived rotation difficulty to be an indication of tightness of the compression discs. The reactor is then inserted into a steam parr reactor, and the parr reactor is sealed. Saturated steam at 200 psi is added to the steam parr used to heat the plates to between 196-198 °C (temperature is monitored using a thermocouple in contact with the outside of the plates), marking the start of the reaction. At the desired reaction time (6.5 hours in all results presented in this work) the steam is shut off and cooling water is added to the steam parr. Cooling water is drained and then added again five times or until the thermocouple reads 35 °C, at which the reactor is opened, and plates are lifted out. Plates are left to continue cooling and drying overnight.

A 3:1 v/v Ethyl Acetate to Hexane solution ("workup solvent") is prepared using graduated cylinders. A vacuum manifold is loaded with 24, 4-mL vials labeled A1-D6 and a 24-well 0.2µm Thomson Rapid Clear filter plates from Thomson Instrument Company is placed on top of the manifold. The plates are unsealed, and one plate is revealed at a time by removing the above adjacent plate. Using a 6-channel

1000 µL Rainin Pipet and clean Rainin wide-orifice 1000 µL Rainin pipet tips for each well, RCF product liquid (about 0.1 mL) is transferred to the corresponding wells in the filter plate system. Using clean, regular 1000 µL Rainin pipet tips, 0.5 mL of the ethyl acetate-hexane solution is added to row A. Using wide orifice pipet tips, liquid and some solids from row A are transferred to the corresponding filter plate wells. This solvent addition and transfer is repeated two more times for a total of three solvent rinses for row A, and subsequently this procedure is repeated for each of the three rows remaining in the plate. After row D has been completed, vacuum is pulled until no liquid is present in the filter plate. 1 mL of the ethyl acetate-hexane solution is added to each well in the filter plate and vacuum is pulled again until the wells dry. The filter plate and remaining solids in the reactor plate is disposed of into reactive catalyst waste, and the 4-mL vials are transferred from the manifold to the three middle rows (8 vials per row, excluding the two edge spaces) of a custom printed vial rack within a 10-nozzle Turbovap LV drying system. Air at 9 psi is blown over the samples for 22 minutes or until all solvent has evaporated from the vials, minimizing extra drying time to prevent RCF monomer evaporation. After drying, 1 mL of 1 g/L tri-tertbutylbenzene in acetone-d6 is added to each of the 24 samples using a 1000 µL positive displacement pipet and the samples are all capped and vortexed. Samples are then uncapped one row at a time and, using a 6-channel 1000 µL Rainin Pipet and clean 1000 µL Rainin pipet tips, 150 µL of sample is transferred into 2 mL Agilent GC vials with 300 µL inserts. GC vials are capped with 2 mL Agilent vial crimp caps. Using the same 6-channel pipet and tips, 500 µL of sample is transferred into high throughput NMR tubes and capped.

GC-FID analysis of monomers

Monomer quantification of 16 analytes were performed similarly to conventional scale RCF by injection on an Agilent 7890 GC equipped with a flame ionization detector (FID) using an injection volume of 1 µL. A method time of six minutes was enabled by utilizing a low thermal mass (LTM) column, significantly shortening the time required to inject the full run of 240 samples. All desired products are calibrated for using authentic standards.

Monomer yields from were calculated with the following equation:

54

$$y_i = \frac{C_{GC-FID}*V}{\frac{C18_{GC-FID}}{0.5*C18_i}*m_{biomass}*X_{lignin}} \quad (1)$$

where C_{GC-FID} is the concentration of the monomer measured by GC-FID, V is the volume of the sample (1 mL total sample), $C18_{GC-FID}$ is the concentration of octadecane measured from GC-FID, $C18_i$ is the initial concentration of octadecane in the reaction (target was 2 g/L in 0.5 mL reaction solvent, leading to a total of approximately 1 mg of octadecane in each well), $m_{biomass}$ is the mass of biomass dispensed into the well, and X_{lignin} is the lignin content (mass percent) of the biomass as measured by pyrolysis-molecular beam mass spectrometry. *p*HBA is measured from proton NMR and included in the total monomer yields reported.

¹H-NMR for delignification

The inclusion of NMR as an analytical technique requires the sample to be dissolved in deuterated solvent. After the transfer and filtration of the product, samples are dried down using an air drier (Turbovap LV). The optimal drying time for the lignin products dissolved in 3:1 v/v ethyl acetate:hexane was 22 minutes at 9 psi utilizing three of the five Turbovap channels. The dried oil is then brought up in a known volume of deuterated acetone which includes 1 g/L of TTB. For HTP-RCF reactions, NMR samples were analyzed on a Bruker Avance 600 MHz instrument using 32 scans, 3 second delay, 4 dummy scans, spectral width of 12 ppm. Integrals are normalized to the internal standard TTB. Oil yield is calculated using the region 6.2-6.6 is used as the measure of syringyl protons, and the region 6.6-7.2 is used as a measure of guaiacyl protons. When present, the singlet arising from 4-propenylsyringol at approximately 6.67 ppm is omitted from the guaiacyl region and added to the syringyl region. *para*-Hydroxy benzoate and methyl paraben are measured by integrating the protons at 7.9 ppm, and the masses are included in the oil yield. Where observed for high-throughput reactions, primarily *para*-hydroxybenzoic acid is measured.

Substrates such as switchgrass and corn stover contain ester-linked coumarate and ferulate units. During RCF, these ester bonds can be cleaved to yield coumaric acid and ferulic acid, which can further

react by being hydrogenated and/or converted to the ester of the alcohol solvent. Furthermore, they can undergo decarboxylation to yield 4-ethylphenol and 4-ethylguaiacol. This leads to ten total products that must be quantified. 4-Ethylguaiacol and 4-ethylphenol were measured on GC-FID. The eight remaining products were quantified using ^{1}H NMR. For reactions on the 75 mL scale with H_2 pressure, only the hydrogenated methyl esters were observed. However, for the high-throughput reactions, some of the unsaturated products were also observed. No carboxylic acid products were observed, indicating full conversion to the methyl esters. For calculation of the oil yield, the known compounds (coumarates, ferulates, ethyl phenol) were subtracted out of their respective syringyl and guaiacyl regions, and the oil yield was calculated as usual with 200 mg/mmol average mass of a syringyl aromatic unit. Only the beta protons of unsaturated coumarates and ferulates overlaps with the S region, and these were accounted for integrating the alpha protons on the same linkages at 7.57-7.56 ppm. The G region is overlapped by the 3,5 protons of coumaric acid/methyl coumarate, the 5,6 protons of ferulic acid/methylferulate, and all aromatic protons from dihydrocoumaric acid/methylhydrocoumarate, 4-ethylphenol, dihydroferulic acid/methylhydroferulate. The yield of the known compounds was calculated and added to the lignin oil yield obtained from the addition of the S and G peaks to give a total oil yield (equations 2-5. The regions used are in the **Table C1**.

$$\mathbf{S} = 1.5 * M_S * n_{TTB} * \frac{I_S + I_{P=S} - I_{HC_\beta}}{I_{TTB} * R_{C18}} \qquad (2)$$

$$\mathbf{G} = M_G * n_{TTB} * \frac{I_G - I_{P=S} - I_{MC} - 2I_{MHC} - 2I_{MF} - 3I_{MHF} - 2I_{EP}}{I_{TTB} * R_{C18}} \qquad (3)$$

$$\mathbf{HC_i} = N * MW_{HC_i} * n_{TTB} * \frac{I_{HC_i}}{I_{TTB} * R_{C18}} \qquad (4)$$

$$\mathbf{Oil\ Yield} = \frac{S + G + \sum_i HC}{m_{biomass} * X_{lignin}} \qquad (5)$$

Where **S** is the mass of syringyl oil, **G** is the mass of guaiacyl oil, **HC** is a hydroxycinnamate product, I is the integral of the indicated region, P=S is 4-propenylsyringol, MC is methyl coumarate, MHC is methylhydrocoumarate, MF is methyl ferulate, MHF is methylhydroferulate, EP is 4-ethylphenol, M_s is the calibrated mass of the syringyl unit (200 g/mol), M_G is the calibrated mass of the guaiacyl unit (170 g/mol), n_{TTB} is the moles of TTB in the sample, HC_β is the beta proton of unsaturated hydroxycinnamates, R_{C18} is the recovery of octadecane measured by GC-FID, MW is the molecular weight of the desired hydroxycinnamate product, and N is an integer to adjust for the number of protons giving rise to the resonance relative to TTB (N = 1.5 for coumarate derived products; N = 3 for ferulate derived products).

4.4 Results

Increasing throughput of RCF is a multifaceted problem with interrelated design constraints. To enable HTP-RCF, significant modifications to the typical RCF procedure were needed. Low substrate loadings are desired to limit material use, and this must be accompanied by low solvent loadings (and therefore reactor volumes) to maintain relevant solvent/biomass ratios. Furthermore, the operation of RCF in separate reactors requires individual intervention for sealing, heating setup, and reactor quenching for each reactor. We begin this study by demonstrating the feasibility and utility of small scale RCF (0.5 mL solvent) using a custom plate reactor. Aside from the issue of scale, direct application of the above protocol to small scale reactions does not necessarily increase in throughput since a significant amount of researcher time is dedicated to the post-reaction workup procedure. In the following sections we present adaptations to the pre and post reaction procedure to increase throughput, and the resultant optimized procedure is shown in **Figure 17.**

Development of a HTP-RCF reactor

To enable a higher throughput with lower material and time requirements, we sought to modify the typical RCF procedure (Chapter 1, **Figure 5**) to accommodate a smaller reaction volume. Inspired by previous work on a 96-well plate design, a 24-well plate (4 rows x 6 columns) stackable reactor was designed and fabricated. To contain the pressure generated by high-temperature organic solvents, a pin-

and-seat mechanism with a PTFE O-ring was used to seal each individual 1 mL well. By machining the

pins into the bottom of the plates, the wells are sealed by the plate stacked directly above. The stacked

plates are then compressed between endplates using threaded rods and disc spring washers (**Figure C1**).

To verify that each well was capable of maintaining reaction pressure, solvent recovery experiments were

conducted by loading 0.5 mL of 1:1 MeOH/IPA into the wells and adding a colored dye to alternating wells.

After heating to 200°C for six hours, minimal solvent loss was measured, and no contamination of undyed

wells was observed, indicating that each well was capable of containing the reaction pressure (**Figure C1E**).
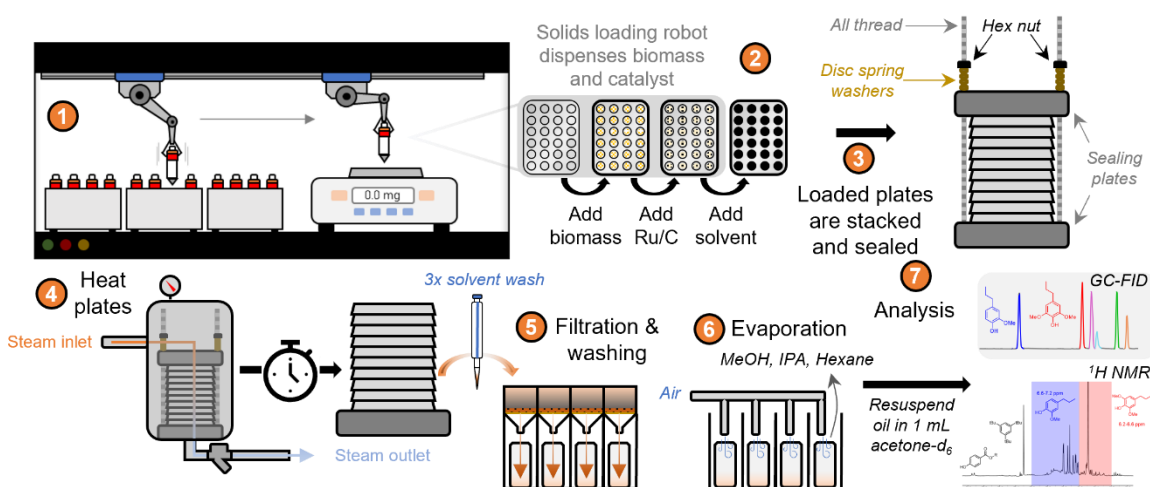
Figure 17. High-throughput RCF procedure. 1) Solids loading robot dispensed biomass and catalyst and records masses 2) Solvent is added to the wells 3) Loaded plates are stacked, all threads are inserted and fastened between end plates, and tightened to compress O-rings 4) Plates are heated in a steam reactor, initiating the reaction 5) After stopping the reaction by introducing cooling water, product recovery is performed by filtering the reaction mixture and washing the wells and filter 6) Reaction solvent and transfer solvent is evaporated and the lignin mixture is resuspended in acetone-d_6 7) Products are analyzed by ^{1}H NMR for oil yield and GC-FID for monomer yield.

Reaction engineering at 0.5 mL scale.

With a viable reactor in hand, we next turned to the operation and analysis of RCF reactions on the 0.5

mL scale. When designing a high-throughput reaction system, ideally all aspects from larger scale reactions

would be translated to the small-scale reaction. However, several aspects of conventional RCF are not

feasible in the stacked plate design. First, reactor wells are not stirred, and thus mixing occurs only through

convection with heating of the solvent. While the lack of stirring may increase local extracted lignin

concentrations,[62] stirring rate was previously shown to only weakly affected total monomer yield.[91] The

second limitation is the lack of high-pressure hydrogen gas dosing. While hydrogen pressure does increase the stabilization rate under catalyst limited conditions,[52] many schemes for hydrogen-free (H_2-free) RCF have been reported to date.[49,56,70,83] Our group demonstrated that Ru/C and Ni/C were less active for H_2-free RCF in methanol (MeOH) compared to Pd/C and Pt/C, and thus catalyst choice is an important parameter in developing H_2-free processes that can achieve comparable monomer yields to those employing exogenous hydrogen.[139] Furthermore, previous work has repeatedly shown the interdependence of catalyst and hydrogen donor for H_2-free RCF.[81,143,156] Notably, Rinaldi and co-workers showed that higher monomer yields were be obtained by using isopropanol (IPA) instead of MeOH in the Ni/C catalyzed RCF of birch,[156] in contrast to results from Sels using Pd/C and exogenous hydrogen.[50] In the context of the HTP method, H_2-free RCF serves as an important model experiment both for its relevance to realizing an economically viable RCF process,[35] but also due to the necessity for achieving a sufficiently high rate of stabilization so that extraction limited/substrate dependent behavior can be elucidated.

To begin our studies of HTP-RCF, we hypothesized that the addition of IPA to the MeOH solvent could increase the rate of H_2-free stabilization while retaining a high degree of lignin extraction. Furthermore, IPA has the added benefit of a lower vapor pressure compared to MeOH (IPA: 26 bar,[157] MeOH 38 bar,[158] at 200 °C) reducing the pressure load on the HTP reactor. We elected to use Ru/C as the catalyst due to its widespread use in RCF literature, commercial availability, and relatively cheaper cost compared to Pd/C and Pt/C but acknowledge that the results obtained are likely dependent on this choice. RCF reactions were performed on 50 mg of poplar using 10 mg Ru/C by placing the plate reactors in an oven set to 180 °C for 15 hours. Varying ratios of IPA/MeOH were used while keeping solvent volume constant at 0.5 mL (**Figure 18A**). The aromatic monomer yield was measured via GC-FID with only minor adaptations. We note that this workup for these reactions was not yet optimized for maximal throughput as the focus was on analyzing the reactivity in the plate reactors. An optimized workup procedure is described below (*vide infra*). The total yield of aromatic monomers was consistent at approximately 17% for reactions in MeOH (17.9 ± 1%), 3:7 IPA/MeOH (16.8 ± 2%) and 1:1 IPA/MeOH (17.3 ± 2%) indicating that similar yields can be obtained

with 1:1 IPA/MeOH compared to MeOH while reducing reactor pressure. Over this range, the selectivity of 4-propyl substituted monomers increased with IPA content from $44 \pm 3\%$ for MeOH to $57 \pm 3\%$ for 1:1 IPA/MeOH while selectivity to 4-propenyl monomers, indicating a higher hydrogenation rate. Increasing the IPA content further to 7:3 IPA/MeOH and ultimately pure IPA resulted in a decreased total monomer yield, likely due to the poorer ability of isopropanol to extract lignin which has been correlated to its polarity.[50] Interestingly, reactions in isopropanol produced high yields of ethyl substituted monomers. Previous work on H_2-free RCF had shown that this pathway may proceed through dehydrogenation of coniferyl/sinapyl alcohol intermediates followed by C-C scission, but this primarily occurred on Pd/C with Ru/C showing almost no activity for this route.[49,139]

RCF conditions are typically chosen to maximize lignin extraction, which typically requires high temperatures, long reaction times, and/or the addition of water to the reaction solvent.[51,159] To increase extraction, the reaction temperature was increased to 200 °C using 1:1 IPA/MeOH.
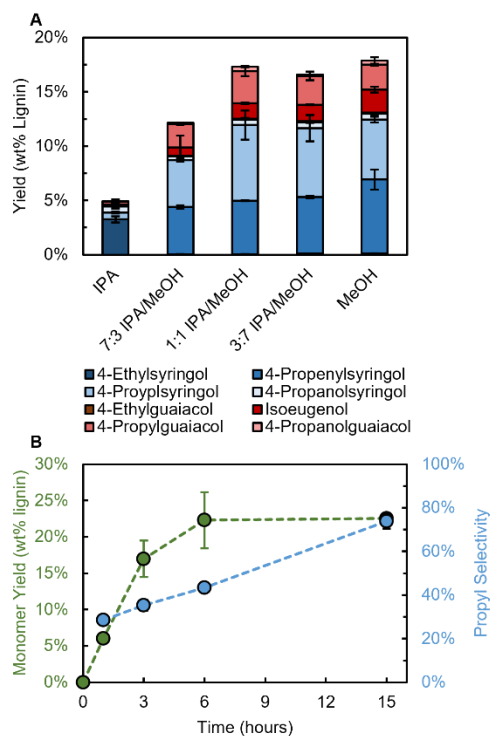
Figure 18. HTP-RCF reactions run in 0.5 mL wells in the plate reactor. **A)** Comparison of solvents showing that 1:1 (vol/vol) IPA/MeOH can achieve similar monomer yields compared to MeOH while retaining

higher selectivity to monomers with propyl side chains. Conditions: 50 mg poplar, 10 mg 5 wt. % Ru/C, 0.5 mL solvent, 15 h at 180 °C. **B**) Time course reaction showing similar yields are obtained for 6 hour and 15 hour reactions. Conditions: same as above, except 0.5 mL 1:1 IPA/MeOH, 200 °C. Analyzed with Method I workup procedure.

Both total monomer yield and the selectivity to 4-propyl products increased to $22.5 \pm 0.7\%$ and $74 \pm 3\%$ respectively for reactions run for 15 hours. Reactions were then run using the same loadings for shorter reaction times with the goal of increasing throughput. Total monomer yield increased from 1-6 hours, but remained constant from 6 hours to 15 hours, indicating that 6-hour reactions can provide similar information as the 15-hour reactions. Selectivity to 4-propyl products did continue to increase during this time however, from 43.3 ± 7 at 6 hours to $74 \pm 3\%$ at 15 hours (**Figure 18B**).

Previous work has identified two major regimes of RCF: at low catalyst loadings or hydrogen pressures, monomer yields are limited by the rate of stabilization. Conversely, at more forcing catalytic conditions, yields are instead governed by the rate of lignin extraction.[52] The proper selection of operating conditions is thus important to ensure that reaction results (monomer and oil yield) reflect the desired information such as catalyst activity or biomass variability. Batch reactions are typically conducted with sufficient catalyst (10-20 wt.% relative to the biomass substrate) so that reactions are limited by extraction and therefore monomer yields near the theoretical limit governed by linkage abundance can be achieved. Given the significantly different scales and the lack of stirring, it is important to examine the operating regimes of using the plate reactors. We performed reactions with catalyst weight loadings varying from 0 to 60 wt.% Ru/C (**Figure 19A**). As expected, reactions without catalyst yielded only $1.0 \pm 0.2\%$ monomers. With the addition of just 10 wt.%, catalyst yield jumped to $19.4 \pm 0.6\%$. As catalyst loading increased up to 60 wt.%, the monomer yield asymptotically increases to $26.6 \pm 2\%$. Above 20 wt.%, total monomer yield is only a weak function of catalyst loading and extraction limited conditions can be obtained. However, selectivity to 4-propyl over 4-propenyl substituted products does still increase with increasing catalyst loading throughout the studied range. Conversely, catalytic stabilization activity can be analyzed where total monomer yield is a function of the catalyst loading (around 10 wt.%). The higher weight percent of catalyst

needed to reach extraction limited conditions may derive from the lack of stirring leading to insufficient mixing.

To validate the results above, we performed an analogous reaction in a 75 mL batch reactor (20 mL 1:1 IPA/MeOH) with identical solvent/biomass (0.1 g/mL) and catalyst/biomass (30 wt.%) loadings. This reaction gave nearly identical results compared to the plate reactors in terms of total monomer yield (75 mL: $24 \pm 1\%$, plates: 24.1 ± 0.4) and S/G ratio (75 mL: $2.23 \pm 0.04\%$, plates: 2.09 ± 0.03) demonstrating that the HTP reactor accurately recovers results from the larger scale (**Figure 19B**).
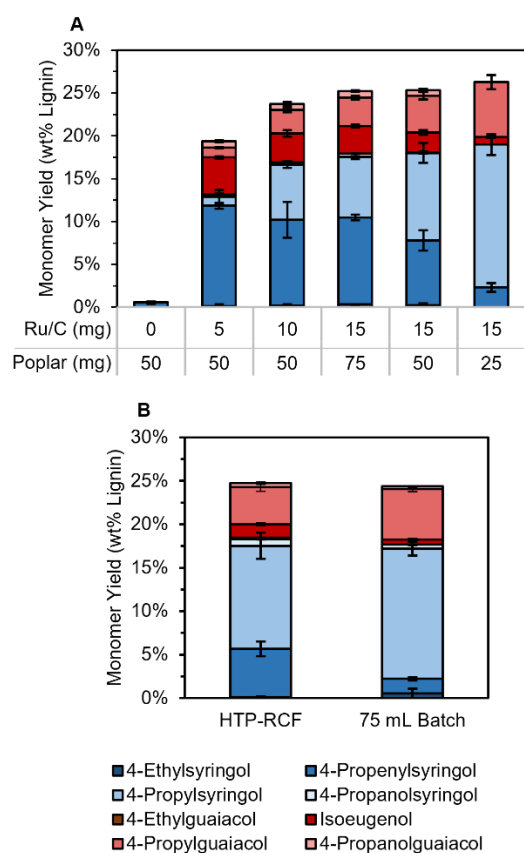
Figure 19. Optimization and validation of the plate reactors. **A**) Impact of catalyst weight percent loading during HTP-RCF (catalyst mass/poplar mass) on monomer yield using the HT method. Conditions: 25-75 mg poplar, 5-30 mg Ru/C, 200 °C, 0.5 mL 1:1 IPA/MeOH, 6 hours reaction time, workup procedure II (*vide infra*). **B**) Comparison of HTP-RCF reactions to analogous reaction in a 75 mL batch reactor. HTP conditions: 50 mg poplar, 15 mg 5 wt% Ru/C, 0.5 mL 1:1 IPA/MeOH, 6 hours, 200 °C. 75 mL batch conditions: 2 grams poplar, 600 mg 5 wt% Ru/C, 20 mL 1:1 IPA/MeOH, 6 hours, 200 °C. Error bars represent the standard deviation of triplicate measurements.

Measurement of delignification

In addition to the aromatic monomer yield, RCF practitioners often measure the total amount of extracted lignin, referred to as delignification or oil yield. Since GC-FID is routinely utilized to analyze small quantities of material, minimal adaptations were required for application to the HTP procedure. However, given the low mass of substrate, direct gravimetric measurement of the extracted oil as typically done for larger scale RCF experiments was found to be infeasible. The oil mass (5-10 mg oil from 50 mg total biomass) was overestimated and highly variable at this small scale. Identical wells were combined and processed together in an attempt to increase the measured mass, but this did not alleviate the variation.

To overcome the difficulty encountered in gravimetric measurements, we sought an alternative method to quantify extracted lignin that was suitable for high-throughput analysis of small quantities of RCF oil. Proton NMR is a ubiquitous tool in chemistry laboratories, and quantitative information can be obtained from small sample quantities within minutes. Typically, more intricate (and therefore time-consuming and/or non-quantitative) NMR schemes are usually preferred for lignin analysis due to its structural complexity.[41,107] For softwoods such as pine, which contain almost exclusively G units accompanied by a low percentage of H units, the aromatic region could be reasonably assumed to closely reflect the number of aromatic units. However, for hardwoods such as poplar that contain both S and G units, this overlap would prevent accurate determination, and this issue would be further complicated for substrates that contain all three moieties, such as switchgrass. Interestingly HSQC of RCF oils reveals that aromatic resonances overlap substantially less than in the corresponding native biomass.[56,107] In the HSQC spectrum of RCF oil from poplar (**Figure 20A**), the $S_{2/6}$ resonances are centered at 6.45 ppm, while the three guaiacyl resonances are centered at 6.63, 6.74, and 6.80 ppm. Previously, Samec and co-workers utilized these characteristic shifts to determine the yield of S and G type aromatics in birch RCF oil using a ^{1}H NMR method.[60] We sought to expand on this methodology and hypothesized that aromatic resonances in RCF may be sufficiently resolved to enable their integration from a simple ^{1}H NMR experiment for a variety of substrates.

To probe the viability of the method, the ^{1}H NMR spectra of poplar, pine, and switchgrass RCF oil were compared to model compounds representative of lignin structures (**Figure 20B, C2**). Clear resonances corresponding to 4-propyl and 4-propanol substituted monomers were observed for all oils, in line with their high abundance measured from GC-FID. In poplar and switchgrass, which contain both S and G lignin, aromatic resonances spanned from approximately 6.2-7.0 ppm, whereas resonances in the pine spectrum are mostly confined downfield of 6.6 ppm. In accordance with the model compound spectra, these data indicate that S and G type functionality can potentially be distinguished by their resonance positions upfield and downfield of 6.6 ppm, respectively. Exceptions to this rule were encountered, including the $S_{2/6}$ resonance of 4-propenylsyringol (6.67 ppm, downfield of the G_6 resonance of 4-propylguaiaicol) and the alpha proton of unsaturated side chains (6.32 ppm) (**Figure C2**).

In addition to the S, G, and H monolignols, lignins can also be adorned with aromatic ester-linked units such as *p*-hydroxybenzoic acid (*p*-HBA), which esterifies S units in some hardwoods, and *p*-coumaric and ferulic acid, which are found in nonwoody biomasses such as switchgrass and corn stover.[30] During the RCF process, species containing carboxylic acid and alkene functionalities of these pendent units can undergo further reactions such as esterification with the alcohol solvent, double bond hydrogenation, and decarboxylation to C_2 side chains. *p*-HBA and its ester analogue, methyl paraben, exhibit distinct ^{1}H NMR resonances located at 7.9 ppm, allowing for their direct measurement. From *p*-coumaric and ferulic acid, a total of 10 possible products must be considered (including *p*-coumaric and ferulic acid). Conveniently, most of these products exhibited unique resonances in the ^{1}H NMR spectrum (**Figure C3**), and these can be observed in the switchgrass spectrum mostly dispersed around other G aromatic units. Products deriving from *p*-coumaric acid show characteristic doublets that are easily distinguished from the lignin oil. The most problematic product is dihydroferulic acid (3-(3-methoxy-4-hydroxyphenyl)-propionic acid), whose resonances overlap with lignin-derived G-type compounds. However, these carboxylic acid groups are typically esterified in the presence of alcohol solvent with long enough residence time.[139,160] The methyl ester analogue, methylhydroferulate (methyl-3-(3-methoxy-4-hydroxyphenyl)-propanoate), shows a

distinguishable resonance at approximately 6.88 ppm.

The ^{1}H NMR spectra of RCF oil contain clearly defined resonances and appeared to be delineated broadly by S and G type functionality. Nonetheless, use of aromatic resonances in the ^{1}H NMR for quantification of delignification requires careful consideration. Namely, lignin extraction yields are typically reported on a mass basis (mass of lignin extracted relative to mass of lignin loaded), but integration of the NMR spectrum gives a mole-based measure of the corresponding protons. For translation to mass, the molar measurements need to be multiplied by a molecular weight, which further requires identification of individual resonances corresponding to known compounds. Although many components of RCF oil are known, quantification of each species in RCF oil from a ^{1}H NMR spectrum is infeasible due to low abundance.

To overcome this complexity, we hypothesized that the aromatic signals could be converted to the oil mass using a calibration factor. We note this is not the average molecular weight of species in the lignin oil, which includes dimers and oligomers, but rather the average mass of the aromatic unit with the accompanying side chain. RCF reactions were performed in 75 mL batch reactors with 2 grams of either poplar, pine, or switchgrass, 400 mg Ru/C, 30 mL MeOH for 3 hours, and an ethyl acetate/water liquid-liquid extraction was performed to isolate the lignin oil. ^{1}H NMR spectra were recorded for samples with varying concentrations of RCF oil, and the obtained integrals were compared to the known gravimetric masses. Given the apparent distribution of S and G signals in poplar, pine, and switchgrass spectra, this calibration value can be further informed via differentiation between these units since they give rise to a different number of protons per aromatic unit, although we note that this is not essential (*vide infra*). The optimal calibration values were found by manipulating the S unit mass (from which the G unit mass can be obtained by subtracting the mass of one CH_2O group, assuming the same side chain chemistry occurs for S and G units). An average S unit mass of 200 mg/mmol was obtained for poplar measurements (mean absolute error (MAE): 0.97 mg, average percent error: 6.8%), which is close to the molecular weight of 4-propylsyringol (196 mg/mmol) (**Figure 20C, Figure C4**). The poplar calibrated values were also

satisfactory for calculation of oil mass from pine (MAE 1.0 mg, average percent error: 17.2%). Integration of the S region quantifies a small number of aromatic units leading to a calculated S/G ratio of 0.19, indicating the presence of non-syringyl type species that exhibit resonances in the S region.

Compared to poplar and pine samples, NMR measurements on switchgrass oils showed significant deviations from gravimetric values. The gravimetric oil mass was much greater than the calculated value using the poplar calibrated average aromatic unit mass (MAE: 8.8 mg, average percent error: 39.5%). Solving for a switchgrass specific value of the average aromatic unit mass gave a value of 320 mg/mmol, which is much greater than the mass of possible side chains. The inflation of the mass for switchgrass must therefore derive from measurement of non-aromatic species in the ethyl acetate-soluble oil mass, possibly due to the presence of extractives. While oil mass is a commonly employed metric and is important for process design, it does not guarantee the exclusive measurement of lignin. Non-lignin species derived from extractives, carbohydrates or inorganic ions may also be dissolved in the organic fraction, and thus inflate the measured mass.[161] Alternatively, decomposition of lignin products may also act to reduce the measured oil mass. Previous work from our group has also shown a large mismatch between the oil yield and real delignification measured by compositional analysis, especially for non-woody substrates.[69] In this case, the ^{1}H NMR method is expected to reflect the lignin content in the oil more accurately that the mass of organic soluble oil.

Aside from the calibration of the S unit mass, an additional source of error can be traced to assigned S and G regions in the ^{1}H NMR spectrum. The S/G ratios obtained from the ^{1}H NMR method for poplar were systematically lower than those obtained from ^{1}H-^{13}C HSQC and from monomer products quantified via GC-FID (**Figure C5**). This incorrect measurement of S/G ratio causes underestimation in the delignification; however, the sensitivity of the oil mass to the S/G ratio is still low. The error in NMR oil masses did not show a dependence on S/G ratio of the oil (**Figure C6**). Utilizing the monomer S/G ratio for calculation of oil yield for poplar only increased the calculated oil mass by 6.5% on average. The low sensitivity results from the relatively low difference between S and G unit mass combined with the narrow

range of S/G ratios encountered in naturally occurring biomasses. This indicates that even total aromatic protons (integral of 6.2-7.2 ppm) would also be an appropriate metric for delignification.
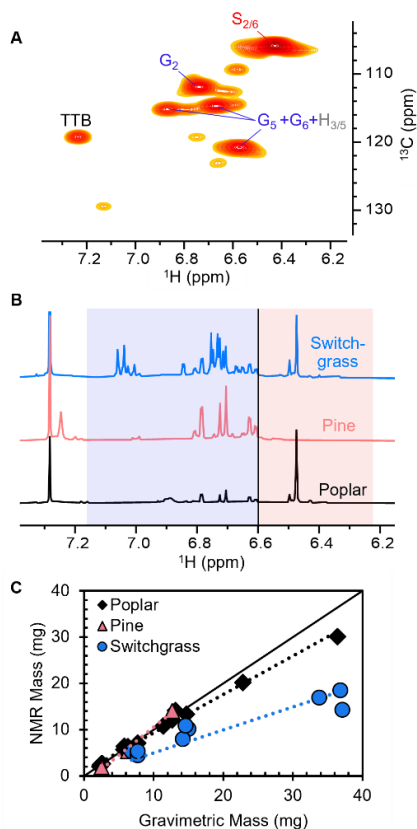
Figure 20. A) HSQC NMR of RCF oil showing separation between syringyl and guaiacyl resonances. **B**) ^{1}H NMR spectra of RCF oil from various substrates with the syringyl region highlighted in red and the guaiacyl region highlighted in blue. **C**) Agreement between the oil mass measured gravimetrically relative to the ^{1}H NMR method for poplar (5 samples), pine (1 sample), and switchgrass (3 samples). RCF oil from 75 mL batch reaction using 2 g biomass, 400 mg Ru/C, 30 mL MeOH, 3 hours, 225 °C, ethyl acetate/water liquid-liquid extraction.

Development of a HTP-RCF procedure.

The results from exploratory HTP experiments showed that RCF reactions run at 0.5 mL scale in the plate reactors are representative of results obtained at larger scales. Although this alone can provide an increase in throughput, the major time requirements of RCF come from loading the reactions and preparing the samples for analysis. To expedite the throughput, we sought to make further improvements to the procedure to minimize the per sample researcher time. First, we focused on the loading of solid biomass and catalyst in the reactor. For larger scale experiments, quantitatively adding biomass and catalyst to the

67

reactor is straightforward. However, loading small masses (5-75 mg) of solids into the reactor wells was tedious and potentially imprecise due to transfer losses. To overcome this, the plate reactors were designed to be compatible with a solids-handling robot (Symyx Powdernium) which allowed for autonomous loading of catalyst and biomass with online mass measurements to verify proper loadings (**Figure C7**). Dispensing containers (hoppers) are loaded with biomass and catalyst, and O-rings were affixed to the pins on the plate bottoms. Precise dispensing from up to 200 hoppers (20-75 ± 1 mg biomass; 5-30 ± 1 mg Ru/C catalyst in this work) into ten 24-well plates was accomplished in less than 24 hours without supervision or human intervention (**Figure C8** for dispensing accuracy). To complete the reaction preparation, 0.5 mL of reaction solvent was added by hand with a volumetric pipette to the solids-containing wells, and the plates were stacked and sealed. Although liquid dispensing robots could be used for this, quick application of solvents was preferred to prevent evaporation.

With a viable approach to load and operate RCF reactions at high temperatures, we next investigated the preparation of the reaction product for analysis. Post-reaction, the products from each well need to be recovered for analysis. Similar to the 75 mL reaction procedure, the catalyst and pulp must first be separated from the RCF liquor. To do this, wide pipette tips were used to transfer the reaction product to a 24 well filter installed on a vacuum manifold. To increase total material recovery, the wells, solid residual biomass, and filters were washed three times with 0.5 mL of a transfer solvent (*vide infra*) to ensure maximal transfer of the reaction mixture, followed by a final 1 mL wash of the filter. The total recovery of RCF oil was found to be variable, and complete recovery was not possible despite numerous washings. To correct for this in the initial exploratory reactions above (**Figure 18, 19B)** an internal standard was added to each well post reaction to account for transfer losses. While this was sufficient and led to good agreement to reactions on a larger scale, we thought that further time reductions could be realized by including the internal standard in the initial reaction solvent (termed surrogate in this work), and thus preventing the need to add a known amount of transfer standard to each well individually after the reaction. A surrogate is necessarily inert, non-volatile, and can be measured by the analytical methods used such as GC-FID here. Due to the

conditions in RCF, molecules containing aromatic rings or hydroxyl groups were thought to be too reactive for use as a surrogate. Octadecane was chosen as a surrogate in the reaction because it is inert and stable under RCF conditions, nonvolatile, and soluble in the solvent mixtures used in this work.

Given the differing polarities of octadecane and the lignin oil, it was necessary to investigate the relationship between transfer solvent and material recovery. Five recovery solvents and their mixtures with hexane were screened for the effectiveness at solubilizing and transferring products from a HTP-RCF reaction with poplar. The recovery of RCF products and the surrogate were both impacted by the transfer solvent. In the case of polar protic solvent such as methanol, an inverse relationship between C_{18} recovery and monomer/oil yields was observed, indicating that the surrogate and lignin products are not co-recovered. For less polar solvents such as ethyl acetate, C_{18} recovery and lignin product yields were positively correlated, indicating their co-recovery. Solvent mixtures were evaluated both on the total recovery of the reaction mixture calculated as the sum of lignin yields and C_{18}, and the variability as measured by the standard deviation. Many solvent compositions offered sufficient recoveries and the chosen solvent was 3:1 ethyl acetate/hexane (**Figure C9**).

To quantify the delignification and monomer yield, the combined reaction mixture and wash solvent needed to be brought to a known volume in deuterated solvent. The collected reaction mixture and washes were then evaporated under flowing air for approximately 20 minutes until dry. The dried oil was then redissolved in 1 mL acetone-d_6 containing 1 g/L 1,3,5-tri-*tert*-butylbenzene (TTB) as in internal standard for both GC-FID and ^{1}H NMR. Half of this solution (0.5 mL) was added to an NMR tube and capped, while the remaining solution was analyzed via GC-FID for aromatic monomers. For confirmation, reactions were performed using these developments. Identical results were obtained as presented in **Figure 19,** highlighting the robustness of the workup procedure (**Figure C10**).

Application to switchgrass population.

Recent techno-economic analysis (TEA) of an RCF biorefinery demonstrated the critical importance of achieving high delignification and monomer yield.[35] Given the substantial influence that substrate choice

has on monomer and oil yield,[30,69,160] an RCF biorefinery is expected to be sensitive to the feedstock. However, RCF variability up to this point has mainly focused on biomass type (hardwood versus softwood) or genus (i.e. poplar versus birch), rather than intra-genus variability. Previous work revealed variation in both composition[162] and sugar release[44] within populations of undomesticated poplar, and this variability was further shown to be key in determining the minimum selling price of ethanol produced from the carbohydrate fraction.[154] A key aspect of these studies was the use of high-throughput analysis to ascertain the degree of variability at the population level. Lignin extraction and monomer yield may also show similar variation within a species with potentially large economic consequences; however the low throughput of conventional RCF reactions has proved to be a barrier to exploring this variance.[163]

To demonstrate the utility of the method, we screened the RCF behavior of 50 switchgrass genotypes in the HTP system in triplicate (**Figure 21**). To allow for yields to be substrate dependent (extraction limited), a catalyst loading of 30 wt% was selected (15 mg Ru/C, 50 mg switchgrass). Conventional lignin monomers such as 4-propyl, propenyl, ethyl, and propanol substituted monomers were quantified via GC-FID, and hydroxycinnamate products were identified and quantified using the ^{1}H NMR method. To calculate the oil yield, the contributions of the hydroxycinnamate products were subtracted out of their respective S and G regions and their yields were added to the total oil yield using the known molecular weight, rather than the calibration mass described above.

Lignin-derived (non-hydroxycinnamate) aromatic monomer yields ranged from 12-25% ($\bar{x} = 17.7\%$, $\sigma = 2.6\%$) with high selectivity to propyl and propenyl side chains as observed for the exploratory reactions on poplar. Aromatic monomers deriving from *p*-coumarate and ferulate esters contributed an additional 7-12% to the total monomer yield ($\bar{x} = 9.9\%$, $\sigma = 1.4\%$), leading to total
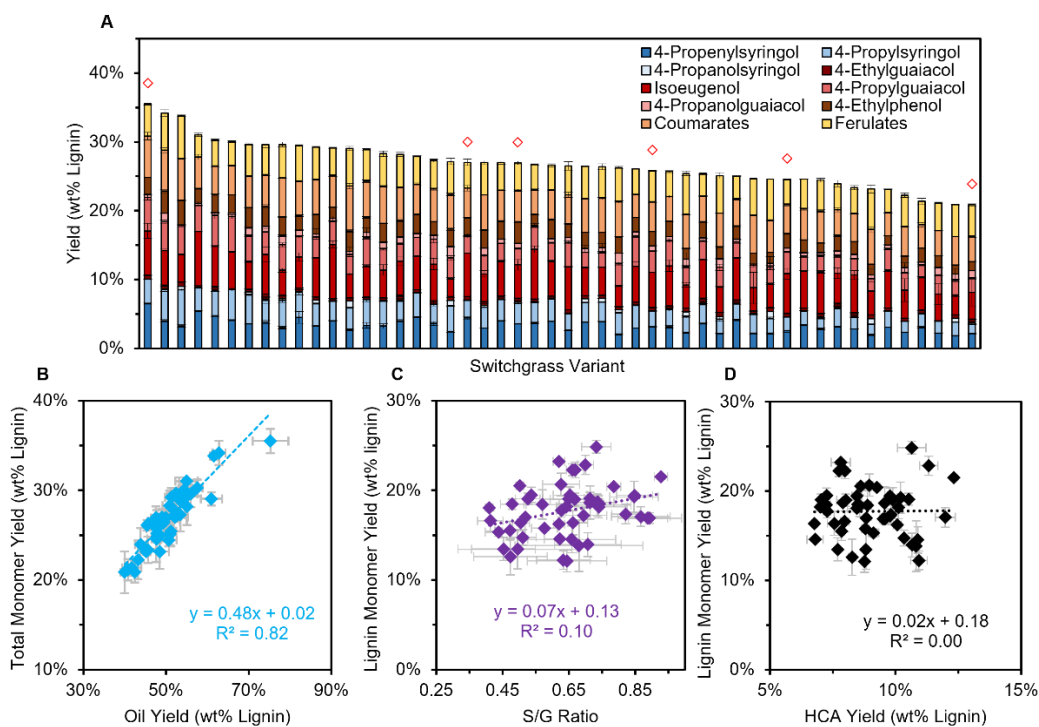
Figure 21. Results from screening 50 switchgrass samples using the HTP-RCF method. **A**) Monomer yields with multiple products deriving from hydroxycinnamate units grouped into ferulates and coumarates **B**) Relation between oil yield and total monomer yield. **C**) Lack of impact of S/G ratio on the yield of lignin monomers (non-hydroxycinnamate derived products). **D**) No correlation between total hydroxycinnamate yield (ferulates + coumarates) and the lignin monomer yield. Conditions: 50 mg switchgrass, 15 mg Ru/C, 0.5 mL 1:1 IPA/MeOH, 6 hours, workup Method II. Error bars are the standard deviation of triplicate measurements.

monomer yields in the range of 21-36% ($\bar{x}$ = 26.7%, σ = 3.2%). The average coefficient of variation (C.V. = $s/\bar{x}$) of triplicate measurements for total monomer yield was 4.6% (average standard deviation 1.2%), indicating high reproducibility across reaction wells. No free carboxylic acids were observed in the ^{1}H NMR spectrum for coumarate and ferulate derived products, indicating complete esterification.[160] The side chain double bonds were partially hydrogenated, leading to a mixture of saturated and unsaturated products similar to lignin derived products. Additionally, 4-ethylphenol and 4-ethylguaiacol were observed, indicating partial decarboxylation (4-ethylsyringol was not measured). A positive relationship between oil yield and total monomer yield was observed (R^2 = 0.82), indicating that the ratio of monomers to total oil was consistent at approximately 0.48 (**Figure 21C**). Lignin monomer yield and total hydroxycinnamate yield showed no correlation, but *p*-coumarate and ferulate-derived products exhibited a positive correlation. Only weak correlations between the S/G ratio and hydroxycinnamate (R^2 = 0.26) and lignin monomer yields (R^2 = 0.10) was measured, indicating that the ratio of syringyl and guaiacyl units does not exert control over the RCF monomer yield, in-line with previous results on naturally variant poplar.[72] In the context of a switchgrass biorefinery, the sensitivity of RCF results on genotype would be expected to strongly modulate the corresponding economic outlook, with higher yielding variants leading to more favorable economics.

Given the significant differences between conventional and HTP-RCF scales and procedures, we sought to validate the HTP method by comparing HTP reaction results to RCF conducted in 75-mL batch reactors. Although the conditions chosen for HTP reactions were replicable at the 75 mL reactor scale, conventional batch reactions are typically run at higher temperatures (225-250 °C) to achieve higher extents of lignin extraction. We sought to demonstrate that the substrate variability measured with the HTP system was not due to the choice of solvent or reaction conditions, and that the less severe HTP conditions chosen can be representative of substrate behavior at more standard conditions. We selected six switchgrass samples, including the variants which gave maximum and minimum monomer yield, for validation in the 75 mL reactors. Reactions were conducted in 75 mL reactors at 225°C for 3 hours with 30 bar external H_2 using 20 wt. % loading of 5 wt. % Ru/C as the catalyst to ensure full conversion of the extracted lignin to

monomers. Nearly identical values of both lignin monomer yield and yields of hydroxycinnamate derived products were observed in 75 mL and HTP-RCF (**Figure 22**). This indicates that the lower temperature (200 °C) in the HTP-RCF was sufficient to extract lignin to a similar extent as the 75 mL scale reactions conducted at 225 °C.
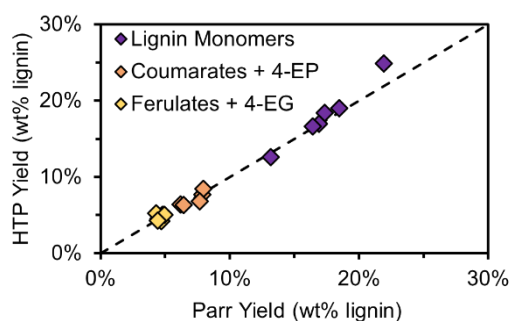
Figure 22. Comparison of HTP reaction results with 75 mL reactors for select switchgrass variants. HTP conditions: 50 mg switchgrass, 15 mg Ru/C, 0.5 mL 1:1 IPA/MeOH, 6 hours, workup Method II. 75 mL conditions: 2 g switchgrass, 400 mg Ru/C, 30 mL MeOH, 3 hours.

4.5 Discussion and conclusions

We developed a small scale RCF reactor capable of running 240 RCF reactions using 50 mg of biomass and 0.5 mL solvent. Reaction parameters such as catalyst loading and reaction solvent were investigated, and the reaction results closely mimicked results from larger scale reactions. Several aspects of the pre/post reaction protocol were adapted to increase throughput, including the development of a ^{1}H NMR to quantify extracted lignin in lieu or gravimetric oil mass. The NMR method has several advantages which make it both convenient for use in the HTP setup, but also a viable alternative to gravimetric measurement in other contexts. It requires only a small amount of oil and avoids the need for tedious evaporation and liquid-liquid extraction. Furthermore, by relying on the presence of aromatic signals, the measurement is unaffected by the presence of extractives or other non-lignin organic soluble components. It can also be leveraged for quantification of the aromatic monomer content for reactions that are expected to give selectivity to known aromatic monomers. Finally, RCF was performed on fifty switchgrass variants using the HTP method, revealing a high degree of variability in monomer yields which could have important consequences for the

biorefinery. Interestingly, monomer yields showed no correlation with the S/G ratio. Instead, a positive correlation between extracted lignin and monomer yield was observed, indicating that improving RCF yields may rely on increasing lignin extractability. The method was validated by repeating reactions in 75 mL reactors for a subset of switchgrass variants at more standard conditions, and nearly identical yields were obtained.

If the switchgrass reactions shown in this work had been performed solely in 75 mL reactors, the process would have required 150 separate reactions consuming 300 grams of biomass (2 g per reactor), 4.5 liters of methanol (30 mL per reactor), and 60 grams of Ru/C (400 mg per reactor). Assuming that six reactors could be successfully run per day, this amounts to 25 days of reactor use. In contrast, the HT system only consumed 7.5 grams of biomass, 75 mL of solvent, and 2.25 grams of Ru/C. Low material loadings preserve potentially valuable biomass substrates, and limit excess use of reaction solvent and catalyst, the latter potentially being critical for investigations where catalysts need to be synthesized prior to use rather than purchased commercially. All reactions could be performed in a single experiment using 10 plates, and the of a full experiment of 240 reactions can be completed and analyzed within 7 days, clearly demonstrating the time and material advantage of the HT system. In total, we estimate a minimum of a 10x increase in throughput per unit of researcher time (**Table 2**).

Table 2. Comparison of material and time requirements for conventional and batch RCF.

	75 mL batch	HTP
Samples	50	
Replicates	3	
Total reactions	150	
Ru/C per reaction (g)	0.4	0.015
total Ru/C (g)	60	2.25
Solvent per reaction (mL)	30	0.5
total solvent (mL)	4500	75
Biomass per reaction (g)	2	0.05
total biomass (g)	300	7.5
Reactions per set	6	240
Sets required	25	0.625

Time: solids loading, solvent addition, sealing (hour)	1	6
Time: filtration, evaporation (hour)	6	6
Time: sample preparation (hour)	1	6
Time: sample analysis (hour)	0.5	4
Sum (hour)	8.5	22
Time per reaction (hour/reaction)	1.42	0.092
Ratio: 75 mL batch/HTP		15.45

Still, the described reaction system is limited by key factors which inhibit its ability to fully represent conventional RCF reactions. While HTP-RCF results closely recover results from larger scale experiments, we stress that the reaction results here should serve as an example of the utility of the system, and to guide future experimentation. We do not wish to convey that the catalyst and solvent choices presented as optimal here should serve as a definitive recommendation for representing all instantiations of RCF. The number of interrelated variables is too great to guarantee that all phenomena at larger scales are adequately represented by the parameter set chosen in this work. Although H_2-free RCF schemes are becoming increasingly popular, the majority of RCF reactions still utilize external H_2 gas, and catalyst performance appears to be sensitive to this.[56,85,139] As RCF schemes evolve to utilize different process configurations, the lack of stirring may not capture relevant mass transfer effects. Reactions using the 1:1 IPA/MeOH system did not reach full extraction of lignin, and thus potentially represent the mixed effects from of both extractability and linkage abundance variation across substrates. The inclusion or NMR as an analytical method requires volatilization of the solvent, and therefore direct application of the protocol would be unfeasible for higher boiling solvents such as ethylene glycol without additional method development such as a liquid-liquid extraction with an immiscible solvent.[143]

Chapter 5: Application of HTP-RCF to explore poplar population

5.1 Summary

The choice of feedstock in a biorefinery affects all aspects of production. Outside of growth and harvesting characteristics, the substrate choice can further impact upgrading behavior. The comparison of different feedstocks for RCF typically centers on the substantially different monomer yield and composition between hardwood, softwood, and herbaceous feedstocks, but has no reports of variation within a genus has been previously reported. Motivated by this idea, we investigated the genetic variation in RCF performance within a population of approximately 600 natural variant poplar trees grown in Corvallis, Oregon using the HTP-RCF methodology. We measure that extractability, rather than linkage abundance, seems to be governing RCF performance, and that a large distribution of this phenotype exists. Follow up studies revealed the reaction factors affecting these measured differences to elucidate the origin and permanence of these differences.

5.2 Introduction

Various proposed feedstocks for biofuels such as switchgrass and poplar vary greatly in growth behavior, composition, and harvesting demands, and settling on a single feedstock must balance resource demand and productivity. Furthermore, considerable genetic variability exists even within a genus such as *Populus* which can affect conversion efficiency.[164] The yield of biomass (size of the tree) dictates the maximum production rate of all products, and was estimated to be the most impactful economic driver for ethanol production.[154] Differences in the relative amounts of cellulose, hemicellulose, and lignin also impact material flows, where total fermentable carbohydrates determine the maximum ethanol production rate. Aside from mass balances, lignin content also impacts conversion efficiency, with increasing lignin contents decreasing fermentation yields. Decreasing lignin content through genetic engineering is suspected to enable improved ethanol economics. [44] However, the past focus on ethanol production has mostly ignored the impact of substrate characteristics on lignin valorization to valuable products. As product streams for lignin valorization become clearer, ideal substrate composition will also depend on the relative profits of

the final products. For example, even though lignin may decrease fermentation yields in a carbohydrate-first biorefinery, residual pulp from RCF is highly amenable to ethanol production.[91] The desired composition will then depend on which product, deriving from carbohydrates or lignin, can be sold for a higher margin, among other factors.

Genetic variation in lignin characteristics is considerable in poplar. Harman-Ware et al. measured significant variability for both total lignin and S/G ratio in poplar trichocarpa variants, ranging from 22-28% and 1.5-2.5 for lignin content and S/G ratio respectively. Although microspatial environment showed some impact on phenotypes, broad sense heritability (H^2) was high, indicating strong potential for capitalizing on substrate varaition.[162] Recently, an in-depth analysis of lignin interunit linkages was conducted by Bryant et al, and showed large variation in the β-O-4 bond abundance.[165] Both of these traits are expected to impact lignin-first upgrading, but this has yet to be studied. The impact of substrate choice for RCF studies is typically described by group behavior, such as hardwoods outperforming or softwoods in terms of monomer yield. Here, we apply the HTP-RCF method to a population of approximately 600 poplar trees.

5.3 Experimental

HTP-RCF Reactions

HTP-RCF experiments were conducted using the conditions and protocols described in chapter 4. Briefly, 50 mg of poplar and 15 mg of Ru/C were dispensed into the wells of 24 well plates. Solvent (0.5 mL 1:1 MeOH/IPA) was dispensed using a 1 mL positive displacement pipette, and the plates were stacked and sealed. The plate reactor was heated for 6.5 hours (including heat-up) using steam delivered at 200 psi (approximately 198°C). After reaction, reactions were sampled by filtering and washing the wells with ethyl acetate and hexane (3:1 v/v) and the solvent was dried under flowing air. Samples were redissolved in acetone-d_6 and analyzed via GC-FID and ^{1}H NMR for monomer and oil yield, respectively.

To operate the system on a continual schedule, two sets of reactor plates were used. While the previous run was being analyzed, the next set of plates were loaded for the following week's reaction. The

morning of the reaction, solvent was added to the wells and the reaction was run. After cooling the reactor, it was left in a fume hood overnight. The following day, the wells were collected and washed, and the pooled samples were dried. On the third day, the dried samples were redissolved in acetone-d_6, and GC-FID samples and NMR samples were prepared. Using autosamplers on both instruments, measurement took 2-3 days. Data is presented normalized for octadecane recovery, but without further normalization.

Poplar samples for the HTP-RCF studied were obtained from Corvallis, OR, and harvested in 2013. Further details can be found in the report by Happs et al.[154] To calculate yields of lignin derived products on a weight percent lignin basis, we used lignin contents from the report by Harman-Ware.[162]

Batch Parr Reactions

Poplar (2 g), catalyst (400 mg Ru/C), and solvent (30 mL) were massed into a 75 mL reactor. For reactions in methanol, 400 mg of water was added also to wet the Ru/C to prevent ignition. Reactors were sealed, pressure tested with helium, and charged with 30 bar H_2 (room temperature pressure). Heating was started, and heat-up to the temperature set point took 30 minutes. Reactions were stopped by cooling the reactors in ice water. Post reaction, the reaction mixture was filtered, and solvent was evaporated in a rotary evaporator. A liquid-liquid extraction was performed using 20 mL of both ethyl acetate and water. The water layer was washed twice more with 20 mL ethyl acetate, and the organic layers were combined, dried over sodium sulfate, and evaporated in the rotary evaporator yielding the lignin oil. The lignin oil was redissolved in methanol. The sample was diluted 10x and 40x for GC-FID or LC analysis, and 0.5 mL was dried under N_2 for ^1H NMR analysis.

Follow-up reactions in 75 mL Parr reactors used poplars from the same field site in Corvallis, OR, harvested in 2022. The poplar trees had been subjected to two coppice cycles between 2013 and 2022 in 2016 and 2019. Compositional analysis was performed at NRE according to the NREL LAP for measuring lignin and carbohydrates.[86]

5.4 Results

Control reactions with GW-9947

HTP-RCF experiments consisting of 240 separate reactions were run weekly for 10 weeks resulting in 1854 successfully run samples, 572 trees, and 521 unique genotypes (51 biological replicates). During each week, 30 reactions were devoted to standard poplar control reactions using the GW-9947 genotype (CBI standard poplar) to measure method variation, and 210 reactions were allocated to variants/alternative substrates. Averaging over each plate position across the 10 weeks shows no low variability, and the effect of plate position therefore seems to be small (**Figure 22A**). Weekly averages of total monomer yield and
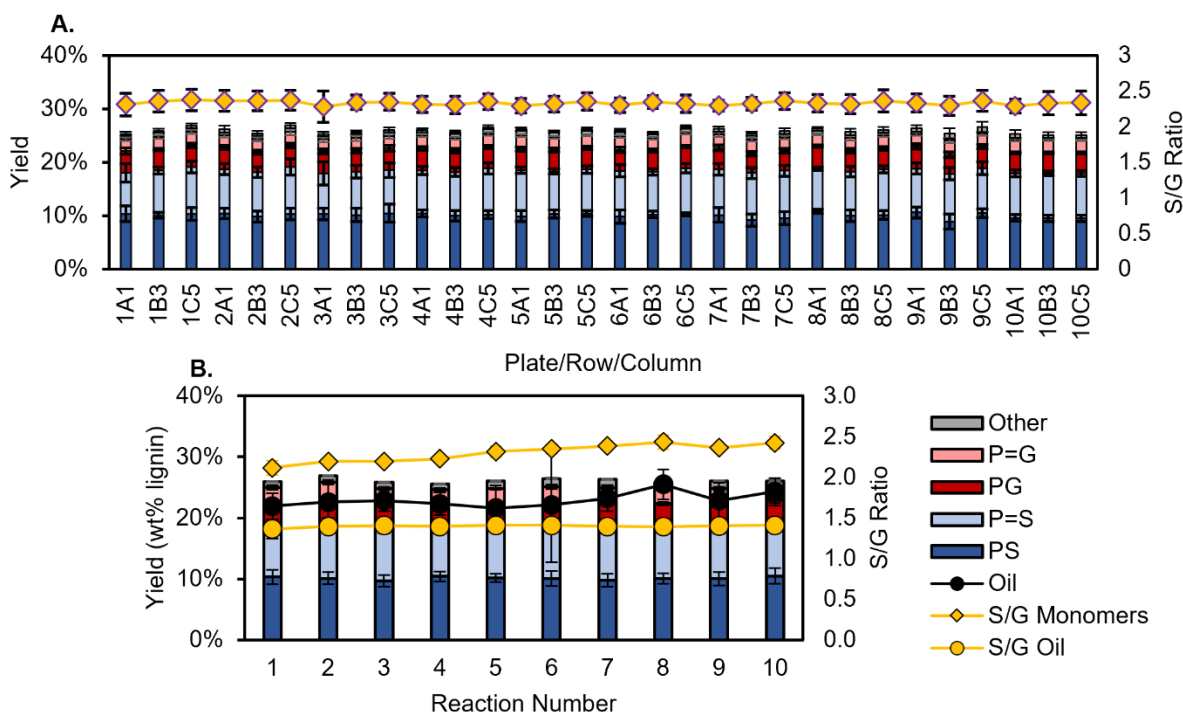
Figure 23. Variation in control reactions of a single poplar variant (GW-9947). A) Average monomer yields for each plate position across 10 reactions. B) Average of all controls for grouped by the reaction number, showing a slight increase in monomer S/G ratio over the campaign.

oil yield showed little variation from week to week, however the S/G ratio of the monomers increased slightly over the campaign (**Figure 22B**). The S/G ratio calculated from NMR does not show this same increase, indicating the variance is likely coming from the GC-FID quantification. Average GC-FID

79

quantifications of 4-propylsyringol and 4-propenylsyringol increase by 1.7% and 6.8% respectively, whereas 4-propylguaiacol and isoeugenol decrease by 6.4% and 12.1% respectively from reaction 1 to reaction 10 (only the guaiacyl monomers are significantly different at $\alpha = 0.05$). Total monomer yields from reactions 1 and 10 are not significantly different (Reaction 1: $26.0 \pm 1.6\%$; Reaction 10: $26.1 \pm 0.7\%$; $\alpha = 0.05$) indicating that these effects are cancelled out in the pooled metric.

Poplar natural variant population

Results from the poplar population show greater variability than the CBI standard for monomer yield, oil yield, and S/G ratio indicating that these are valid targets for gene association studies (**Figure 23**). Monomer yields ranged from 24%-37% with an average value of $30 \pm 2\%$. Assuming a normal distribution, 95% of monomer yield measurements lie within the range of 26.4% to 33.2% (width 6.7%), compared to
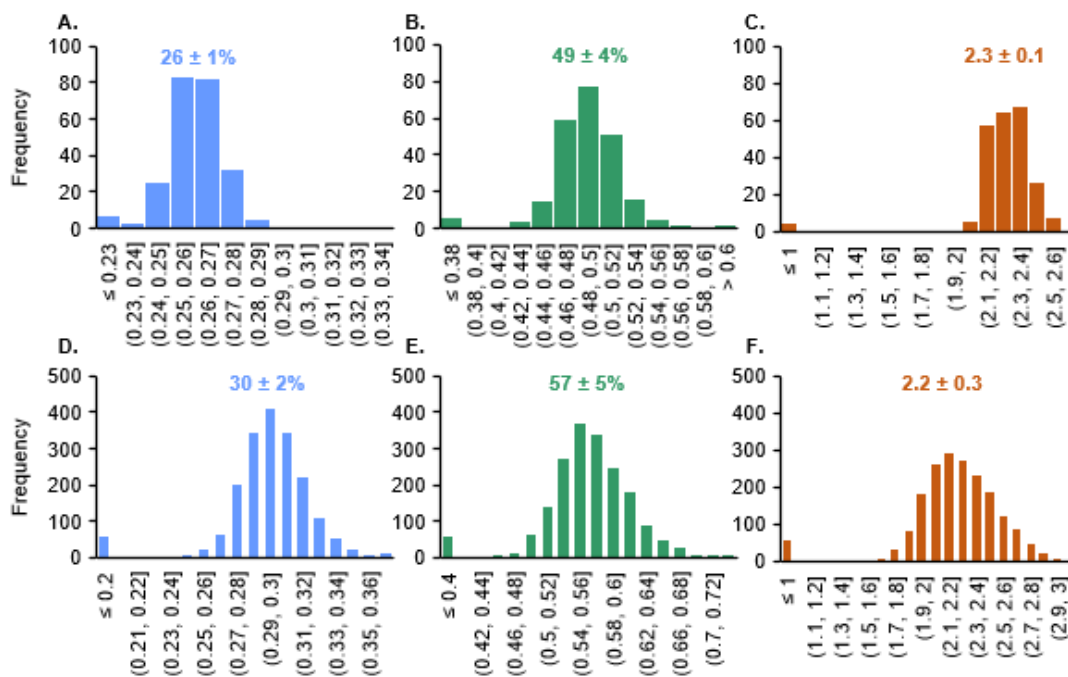
Figure 24. Histograms of monomer yield (**A, D**), oil yield (**B, E**), and S/G ratio (**C, F**) for the control reactions (**A, B, C**) and reactions of poplar variant population (**D, E, F**).

the range of 23.8% to 28.4% (width 4.6%). The measured method variability impacts the power of the method to resolve differences in the greater poplar population. For instance, if method variability is too

high, the method is unable to discern if variance in the population data is due to the genotype. This depends on the average and standard deviation of the metric, as well as the spread in the population. To gauge the method variability, we can calculate the percentage of samples that are significantly different from the mean. The average total monomer yield across all standard samples is 26.1 ± 1%, and 95% of monomer yield measurements lie within the range of 23.8% to 28.4% (width 4.6%). Assuming a random sample has

this same standard deviation of the standard poplar, we can calculate the necessary monomer yield difference from the average of the population to be deemed significantly different (α = 0.05). For total monomer yield, approximately 18% of extreme samples are significantly different from the mean, meaning that there is a high likelihood that observed variance is at least partially due to the different genotypes (**Figure 2**). Similar conclusions can be drawn for the monomer S/G ratio (STD: 2.3 ± 0.1; Variants: 2.2 ± 0.3) and oil yield (STD: 49 ± 4%; Variants: 57 ± 5%).

The results above indicate that there is significant variability in the population of natural poplar variants. For monomer yield, this variation between substrates would canonically be attributed to β-O-4 abundance. Mechanistically, if β-O-4 bonds are randomly distributed in the polymer, a poplar with higher β-O-4 abundance would give a higher monomer yield than a correspondingly low β-O-4 poplar assuming equal levels of extraction and full conversion to monomers. This could be quantified in the ratio of monomer yield to oil yield (M/O). Interestingly, M/O is fairly consistent across the both the standard reactions and the greater poplar population with similar degrees of variation at a value 0.53 ± 0.02 (**Figure 3**). This indicates that there is no effect of genotype on the M/O ratio. Mechanistically, this could mean that RCF monomer yield under these reaction conditions is limited by extractability, rather than linkage abundance. Alternatively, this data could indicate that β-O-4 abundance is related to extractability, but these two hypotheses are not distinguishable at this point.

Improving extraction of poplar can impact the RCF biorefinery can have important implications for reducing the minimum selling price the RCF oil. First, faster extraction can reduce required residence time to achieve a certain extraction, leading to smaller reactor batch sizes for a given annual throughput. Furthermore, if oil yield differences are maintained at higher extractions, the same process can produce

more lignin oil for virtually zero added cost, and potentially aid in carbohydrate valorization due to the lower lignin content of the pulp. In HTP-RCF reactions using the 1:1 MeOH/IPA solvent system at 200°C, it is suspected that the reaction is not at maximal extraction.
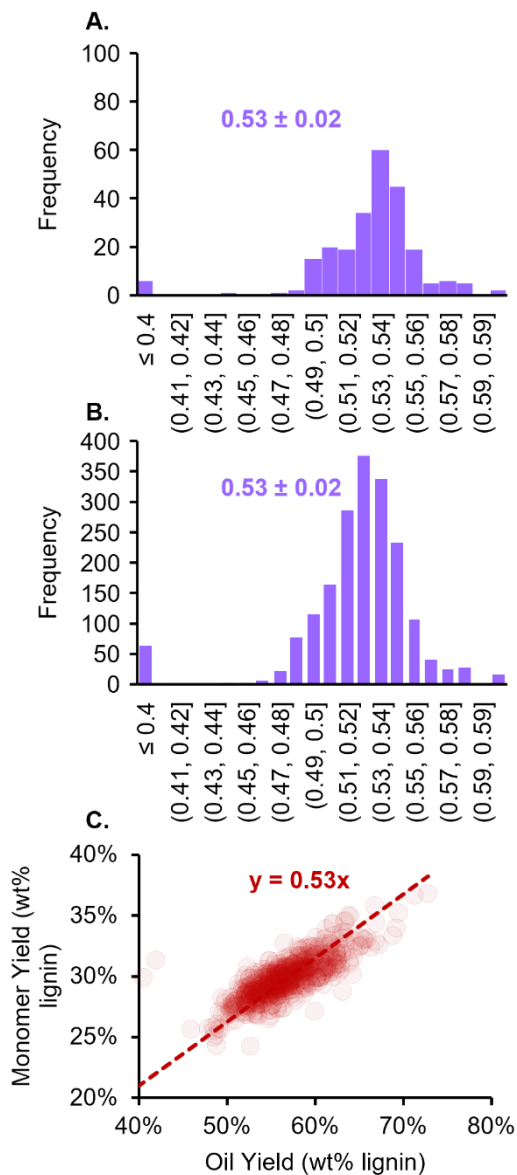

Figure 25. Relationship between monomer yield and oil yield. **A**) Histograms of monomer/oil ratio (M/O) for control reactions. **B**) Histograms of monomer/oil ratio (M/O) for poplar variant population reactions. **C**) Scatter plot of oil yield versus monomer yield.

Follow-up RCF experiments at 75 mL reaction scale

Given that the extractability differences have only been measured under a single condition, we next sought to clarify the implication of extractability differences for the biorefinery by screening poplar genotypes with a range of measured extractability at various reaction RCF conditions. To do this at a larger scale in 75 mL reactions, we acquired additional substrate material of the desired poplar samples from a recent harvest (2022). Reactions were first conducted at 200 °C for three hours in pure methanol as a corollary to the HTP-RCF reactions. A range of monomer yields was obtained for the various genotypes, from $21.8 \pm 0.2\%$ for BESC-151 to $27.71 \pm 0.01\%$ for BESC-392 (**Figure 25A**). The poplar used for control reactions in the HTP-RCF campaign, GW-9947, showed a low monomer yield of $22.45 \pm 0.02\%$ as expected given the HTP-RCF results. When reactions were conducted at 225 °C in methanol for 3 hours, the order of yields was mostly maintained, however a smaller gap was observed between the high/low variants of 2.2%. When reaction time is reduced to just 0.5 hour for these two extreme poplars, the yield differences are again larger (4.4%) (**Figure 25B**). These data point toward to the idea that extractability differences are differences in the rate of extraction. Therefore, if poplars are extracted to a high enough extent, their monomer yields will not depend on the extraction extent and will instead be governed by other factors (such as β-O-4 linkage abundance). This phenomenon is further emphasized through reactions results using 1:1 MeOH/H_2O (v/v) at 225 °C for a reaction time of 0.5 hours. Here, the previously lowest variant demonstrates the highest yield, however most poplars nearly identical yields, indicating that the extractability phenotype measured in the HTP-RCF experiment has little impact on the yields at near maximal extraction. Interestingly, at less severe conditions of 175 °C with the same solvent and residence time (1:1 MeOH/H_2O, 0.5 hours), yields for BESC-151 and BESC-392 are only separated by 1.6% despite the much lower extraction extents compared to the other reactions (**Figure 25A**). The small sample size limits firm conclusions to be drawn, however this tentatively could mean that the genotype dependent extractability differences could be caused by a component that is more efficiently extracted in with the water co-solvent compared to pure methanol. In the same vein, the addition of water to the solvent may be

a strategy to alleviate substrate dependence in an RCF biorefinery.
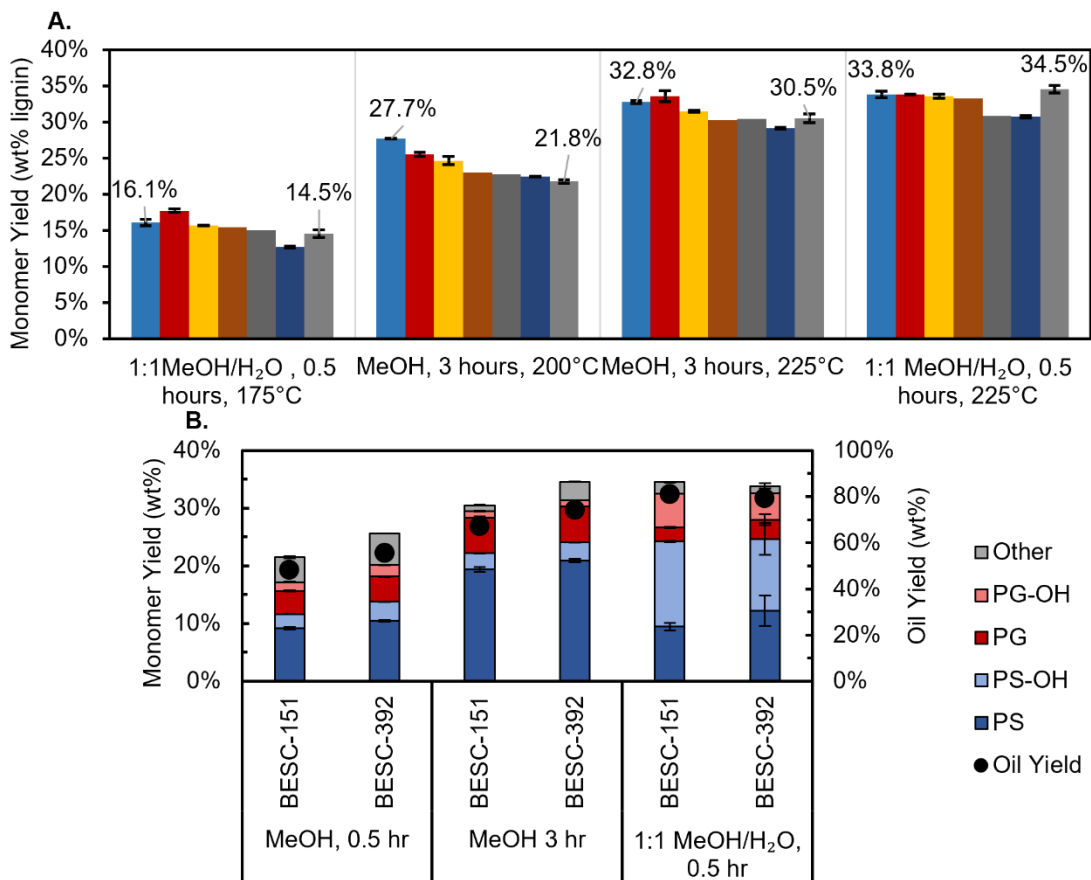
Figure 26. Follow up 75 mL batch experiments further exploring extractability differences. **A**) Total monomer yield of seven variants at four different operating conditions. **B**) Variation in extreme variant (BESC-151 and BESC-392) RCF monomer yield for time course reactions in methanol at 0.5 and 3 hours compared to reactions in 1:1 MeOH/H_2O.

Towards mechanistic understanding of delignification

       Interestingly, the monomer yields from the follow-up experiments at 200 °C in pure methanol for

three hours showed a negative correlation with cellulose content (**Figure 26**). Weak correlations with other
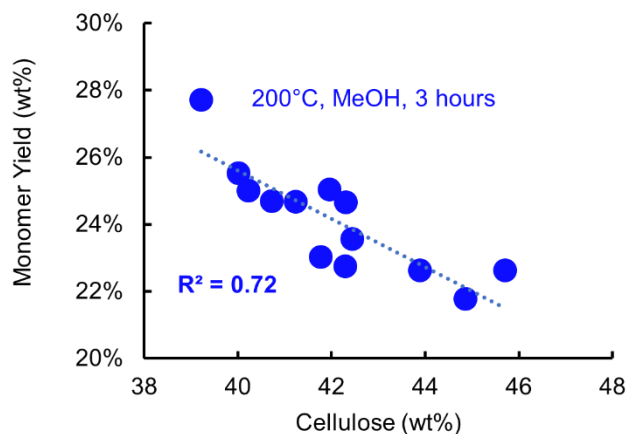
Figure 27. Correlation of cellulose content measured from compositional analysis with the lignin monomer yield at 200 °C, 30 mL methanol, and 3 hours of reaction time.

compositional characteristics such as total lignin content or hemicellulose were present, but not as robust as the cellulose correlation. The relationship of cellulose content and lignin monomer yield may shed light on the physical basis for the observed differential extractability. Most of the lignin in the plant resides in the secondary cell wall despite being enriched in the middle lamella and cell corners.[27] We hypothesize that higher cellulose content may manifest in cell wall differences between poplars affecting delignification. Specifically, it could be a result of thicker cell walls, increasing the distance that lignin must diffuse through to be extracted. This would cause the density of the poplar to increase, which has been experimentally observed.[166]

5.5 Conclusions

In this work through HTP-RCF of approximately 600 trees we demonstrated that lignin phenotypes of monomer yield, oil yield, and S/G ratio show substantial variability in a population natural variant from Corvallis, OR. Surprisingly, the monomer yield was directly correlated with the oil yield, indicating that extractability, rather than linkage abundance, is limiting RCF monomer yields under the studied conditions. Follow up experiments showed that the differential extractability decreased at higher extents of extraction and in the presence of 50% water as a co-solvent. Extractability was negatively correlated with cellulose content, potentially indicating that cell wall thickness may be a determining factor in lignin extractability

Chapter 6: Outlook

In this thesis, we have attempted to push RCF and the characterization of lignin further. In the first study on H_2-free, we demonstrated that achieving high monomer yields is depends on catalyst choice. Furthermore, the stabilization process gap from H_2-free to reactions with exogenous H_2 does not seem to be dependent by reforming ability alone. Overall, this highlights the interdependence of process parameters, and will likely have to be revisited when moving to more realistic systems.[139]

We next simplified phenolic quantification through the development of a derivatization and analysis procedure complementary but alternative to the ^{31}P gold standard method. Pentafluoropyridine is less dangerous to work with compared to the phosphorus agent, making the method more accessible to novice chemists. Furthermore, the method is cheaper and potentially faster than the ^{31}P method, all while maintaining the resolution of S, G, H, and 5-substititued groups.[167]

Lastly, a half decade long project to screen the substrate dependence of RCF for a natural variant population was executed. Over 2500 individual reactions were performed to isolate the required conditions, validate the small-scale HTP-RCF method, and finally screen 572 poplar trees. A major result was that RCF appears to be limited by extractability differences, rather than linkage abundance. Furthermore, this differential extractability is linked to cellulose content, and is perhaps indicative that cell wall structure impacts the rate of lignin transport through the cell wall. In the next phase of the work, our computational collaborators will attempt to correlate specific genes responsible for controlling the extractability phenotype.

Lignin, and biomass as a whole, contains enormous complexity. Therefore, it is a wonder that despite this, reductive catalytic fractionation can provide nearly 50% of the starting lignin as aromatic monomers with high selectivity to only two analogous products, and a single product from sugars in the form of ethanol. RCF is attractive in part because it is reliable and somewhat simple to obtain these near "quantitative" monomer yields in laboratory experiments. Countless additional papers and PhD theses could be had studying the intricacies of extraction and stabilization phenomenon by applying standard conditions with high pressure, high catalyst loadings, full exhaustive liquid-liquid extraction, pristine feedstocks, and

unrecycled chemicals. And yet at the end of these studies, the world may be no closer to viable fuels and chemicals from lignin. Academia tends to push for marginal progress – changing a single variable at a time to irrefutably isolate its effect, as science education has taught us to do. However, a wave of advances in the field have been recently published that alter what the standard conditions for RCF should be, each crystalizing the fact that the impacts of process parameters are interrelated, not independent. First, recycling the RCF liquor into the reaction solvent can minimizing the solvent loading without yield penalty, and possibly even improving extraction.[78] Second the use of water as a solvent under hydrogen-free conditions can eliminate the need to organic solvents and external hydrogen gas at the expense of the hemicellulose fraction.[168] To realize the potential of the RCF biorefinery, practitioners need to push to lower cost processes by assimilating these recent advances in the field. Unfortunately, this instills additional complexity on running RCF reactions. Using a recycled RCF liquor solvent requires large amount RCF oil and complicates the analysis of the marginal increase in monomers given their already high concentration. Using water may introduce phase separation and solubility issues that will require tedious tracking throughout the workup procedure. Nonetheless, the pace at which technology needs to advance to produce renewable products from biomass, especially lignin, is high. This therefore demands that practitioners take this leap to more realistic and transferrable conditions. With this, we may take one step towards a brighter future, and may even just prove wrong the phrase that haunts lignin chemists: "you can make anything from lignin except money."

References

(1)   Steffen, W.; Richardson, K.; Rockström, J.; Cornell, S. E.; Fetzer, I.; Bennett, E. M.; Biggs, R.; Carpenter, S. R.; De Vries, W.; De Wit, C. A.; Folke, C.; Gerten, D.; Heinke, J.; Mace, G. M.; Persson, L. M.; Ramanathan, V.; Reyers, B.; Sörlin, S. Planetary Boundaries: Guiding Human Development on a Changing Planet. *Science (80-.).* **2015**, *347* (6223). https://doi.org/10.1126/science.1259855.

(2)   Hallegatte, S.; Rogelj, J.; Allen, M.; Clarke, L.; Edenhofer, O.; Field, C. B.; Friedlingstein, P.; Van Kesteren, L.; Knutti, R.; Mach, K. J.; Mastrandrea, M.; Michel, A.; Minx, J.; Oppenheimer, M.; Plattner, G. K.; Riahi, K.; Schaeffer, M.; Stocker, T. F.; Van Vuuren, D. P. Mapping the Climate Change Challenge. *Nat. Clim. Chang.* **2016**, *6* (7), 663–668. https://doi.org/10.1038/nclimate3057.

(3)   Lenton, T. M.; Xu, C.; Abrams, J. F.; Ghadiali, A.; Loriani, S.; Sakschewski, B.; Zimm, C.; Ebi, K. L.; Dunn, R. R.; Svenning, J. C.; Scheffer, M. Quantifying the Human Cost of Global Warming. *Nat. Sustain.* **2023**. https://doi.org/10.1038/s41893-023-01132-6.

(4)   Smith, C. J.; Forster, P. M.; Allen, M.; Fuglestvedt, J.; Millar, R. J.; Rogelj, J.; Zickfeld, K. Current Fossil Fuel Infrastructure Does Not yet Commit Us to 1.5 °C Warming. *Nat. Commun.* **2019**, *10* (1), 1–10. https://doi.org/10.1038/s41467-018-07999-w.

(5)   Nemet, G. F. Beyond the Learning Curve: Factors Influencing Cost Reductions in Photovoltaics. *Energy Policy* **2006**, *34* (17), 3218–3232. https://doi.org/10.1016/j.enpol.2005.06.020.

(6)   Braff, W. A.; Mueller, J. M.; Trancik, J. E. Value of Storage Technologies for Wind and Solar Energy. *Nat. Clim. Chang.* **2016**, *6* (10), 964–969. https://doi.org/10.1038/nclimate3045.

(7)   Sacchi, R.; Becattini, V.; Gabrielli, P.; Cox, B.; Dirnaichner, A.; Bauer, C.; Mazzotti, M. How to Make Climate-Neutral Aviation Fly. *Nat. Commun.* **2023**, *14* (1), 3989. https://doi.org/10.1038/s41467-023-39749-y.

(8)   Ragauskas, A. J.; Williams, C. K.; Davison, B. H.; Britovsek, G.; Cairney, J.; Eckert, C. A.; Frederick, W. J.; Hallett, J. P.; Leak, D. J.; Liotta, C. L.; Mielenz, J. R.; Murphy, R.; Templer, R.; Tschaplinski, T. The Path Forward for Biofuels and Biomaterials. *Renew. Energy Four Vol. Set* **2006**, *311* (January), 271–283.

(9)   DelSesto, M. People–Plant Interactions and the Ecological Self. *Plants People Planet* **2020**, *2* (3), 201–211. https://doi.org/10.1002/ppp3.10087.

(10)   Bar-On, Y. M.; Phillips, R.; Milo, R. The Biomass Distribution on Earth. *Proc. Natl. Acad. Sci. U. S. A.* **2018**, *115* (25), 6506–6511. https://doi.org/10.1073/pnas.1711842115.

(11)   2003., A. I. An Update of the Angiosperm Phylogeny Group Classification for the Orders and Families of Flowering Plants: APG II. *Bot. J. Linn. Soc.* **2003**, *141* (4), 399–436. https://doi.org/10.1046/j.1095-8339.2003.t01-1-00158.x.

(12)   Chase, M. W.; Reveal, J. L. A Phylogenetic Classification of the Land Plants to Accompany APG III. *Bot. J. Linn. Soc.* **2009**, *161* (2), 122–127. https://doi.org/10.1111/j.1095-8339.2009.01002.x.

(13)   Tuck, C. O.; Pérez, E.; Horváth, I. T.; Sheldon, R. A.; Poliakoff, M. Valorization of Biomass: Deriving More Value from Waste. *Science (80-.).* **2012**, *337*, 695–699. https://doi.org/10.1126/science.338.6107.604-b.

(14)   Mohr, A.; Raman, S. Lessons from First Generation Biofuels and Implications for the Sustainability Appraisal of Second Generation Biofuels. *Effic. Sustain. Biofuel Prod. Environ. Land-Use Res.* **2015**, *63*, 281–310. https://doi.org/10.1016/j.enpol.2013.08.033.

(15)   Langholtz, M. H.; Stokes, B. J.; Eaton, L. M.; (Leads). *U.S. Department of Energy.2016 Billion-Ton Report: Advancing Domestic Resources for a Thriving Bioeconomy, Volume 1: Economic Availability of Feedstocks*; 2016; Vol. I.

(16)   Gilna, P.; Lynd, L. R.; Mohnen, D.; Davis, M. F.; Davison, B. H. Progress in Understanding and Overcoming Biomass Recalcitrance: A BioEnergy Science Center (BESC) Perspective Mike Himmel. *Biotechnol. Biofuels* **2017**, *10* (1), 1–7. https://doi.org/10.1186/s13068-017-0971-1.

(17)   Jessup, R. W. Development and Status of Dedicated Energy Crops in the United States. *Vitr. Cell. Dev. Biol. - Plant* **2009**, *45* (3), 282–290. https://doi.org/10.1007/s11627-009-9221-y.

(18) Meerts, P. Mineral Nutrient Concentrations in Sapwood and Heartwood: A Literature Review. *Ann. For. Sci.* **2002**, *59* (7), 713–722. https://doi.org/10.1051/forest:2002059.

(19) Cosgrove, D. J. Growth of the Plant Cell Wall. *Nat. Rev. Mol. Cell Biol.* **2005**, *6* (11), 850–861. https://doi.org/10.1038/nrm1746.

(20) Nishiyama, Y. Structure and Properties of the Cellulose Microfibril. *J. Wood Sci.* **2009**, *55* (4), 241–249. https://doi.org/10.1007/s10086-009-1029-1.

(21) Rao, J.; Lv, Z.; Chen, G.; Peng, F. Hemicellulose: Structure, Chemical Modification, and Application. *Prog. Polym. Sci.* **2023**, *140*, 101675.

(22) Vanholme, R.; Demedts, B.; Morreel, K.; Ralph, J.; Boerjan, W. Lignin Biosynthesis and Structure. *Plant Physiol.* **2010**, *153* (3), 895–905. https://doi.org/10.1104/pp.110.155119.

(23) Boerjan, W.; Ralph, J.; Baucher, M. Lignin Biosynthesis. *Annu. Rev. Plant Biol.* **2003**, *54*, 519–546. https://doi.org/10.1146/annurev.arplant.54.031902.134938.

(24) Ralph, J.; Lundquist, K.; Brunow, G.; Lu, F.; Kim, H.; Schatz, P. F.; Marita, J. M.; Hatfield, R. D.; Ralph, S. A.; Christensen, J. H.; Boerjan, W. Lignins: Natural Polymers from Oxidative Coupling of 4-Hydroxyphenyl- Propanoids. *Phytochem. Rev.* **2004**, *3* (1–2), 29–60. https://doi.org/10.1023/B:PHYT.0000047809.65444.a4.

(25) del Río, J. C.; Rencoret, J.; Gutierrez, A.; Elder, T.; Kim, H.; Ralph, J. Lignin Monomers from beyond the Canonical Monolignol Biosynthetic Pathway – Another Brick in the Wall. *ACS Sustain. Chem. Eng.* **2020**, *8*, 4997–5012. https://doi.org/10.1021/acssuschemeng.0c01109.

(26) Gierlinger, N.; Schwanninger, M. Chemical Imaging of Poplar Wood Cell Walls by Confocal Raman Microscopy. *Plant Physiol.* **2006**, *140* (4), 1246–1254. https://doi.org/10.1104/pp.105.066993.

(27) Zhang, X. Visualising Lignin Quantitatively in Plant Cell Walls by Micro-Raman Spectroscopy. *RSC Adv.* **2021**, *11* (22), 13124–13129. https://doi.org/10.1039/d1ra01825f.

(28) Zhou, C.; Li, Q.; Chiang, V. L.; Lucia, L. A.; Griffis, D. P. Chemical and Spatial Differentiation of Syringyl and Guaiacyl Lignins in Poplar Wood via Time-of-Flight Secondary Ion Mass Spectrometry. *Anal. Chem.* **2011**, *83* (18), 7020–7025. https://doi.org/10.1021/ac200903y.

(29) Zhao, Y.; Yu, X.; Lam, P.; Zhang, K.; Tobimatsu, Y.; Liu, C. Monolignol Acyltransferase for Lignin P-Hydroxybenzoylation in Populus. *Nat. Plants* **2021**, *7*, 1288–1300.

(30) Chen, M.; Li, Y.; Lu, F.; Luterbacher, J. S.; Ralph, J. Lignin Hydrogenolysis: Phenolic Monomers from Lignin and Associated Phenolates across Plant Clades. *ACS Sustain. Chem. Eng.* **2023**, *11* (27), 10001–10017.

(31) Solomon, B. D.; Barnes, J. R.; Halvorsen, K. E. Grain and Cellulosic Ethanol: History, Economics, and Energy Policy. *Biomass and Bioenergy* **2007**, *31* (6), 416–425. https://doi.org/10.1016/j.biombioe.2007.01.023.

(32) Lynd, L. R.; Liang, X.; Biddy, M. J.; Allee, A.; Cai, H.; Foust, T.; Himmel, M. E.; Laser, M. S.; Wang, M.; Wyman, C. E. Cellulosic Ethanol: Status and Innovation. *Curr. Opin. Biotechnol.* **2017**, *45*, 202–211. https://doi.org/10.1016/j.copbio.2017.03.008.

(33) Hannon, J. R.; Lynd, L. R.; Andrade, O.; Benavides, P. T.; Beckham, G. T.; Biddy, M. J.; Brown, N.; Chagas, M. F.; Davison, B. H.; Foust, T.; Junqueira, T. L.; Laser, M. S.; Li, Z.; Richard, T.; Tao, L.; Tuskan, G. A.; Wang, M.; Woods, J.; Wyman, C. E. Technoeconomic and Life-Cycle Analysis of Single-Step Catalytic Conversion of Wet Ethanol into Fungible Fuel Blendstocks. *Proc. Natl. Acad. Sci. U. S. A.* **2020**, *117* (23), 12576–12583. https://doi.org/10.1073/pnas.1821684116.

(34) Lynd, L. R.; Beckham, G. T.; Guss, A. M.; Jayakody, L. N.; Karp, E. M.; Maranas, C.; McCormick, R. L.; Amador-Noguez, D.; Bomble, Y. J.; Davison, B. H.; Foster, C.; Himmel, M. E.; Holwerda, E. K.; Laser, M. S.; Ng, C. Y.; Olson, D. G.; Román-Leshkov, Y.; Trinh, C. T.; Tuskan, G. A.; Upadhayay, V.; Vardon, D. R.; Wang, L.; Wyman, C. E. Toward Low-Cost Biological and Hybrid Biological/Catalytic Conversion of Cellulosic Biomass to Fuels†. *Energy Environ. Sci.* **2022**, *15* (3), 938–990. https://doi.org/10.1039/d1ee02540f.

(35) Bartling, A. W.; Stone, M. L.; Hanes, R. J.; Bhatt, A.; Zhang, Y.; Biddy, M. J.; Davis, R.; Kruger, J. S.; Thornburg, N. E.; Luterbacher, J. S.; Rinaldi, R.; Samec, J. S. M.; Sels, B. F.; Román-Leshkov,

Y.; Beckham, G. T. Techno-Economic Analysis and Life Cycle Assessment of a Biorefinery Utilizing Reductive Catalytic Fractionation. *Energy Environ. Sci.* **2021**, *14* (8), 4147–4168. https://doi.org/10.1039/d1ee01642c.

(36)   Kang, X.; Kirui, A.; Dickwella Widanage, M. C.; Mentink-Vigier, F.; Cosgrove, D. J.; Wang, T. Lignin-Polysaccharide Interactions in Plant Secondary Cell Walls Revealed by Solid-State NMR. *Nat. Commun.* **2019**, *10* (1), 1–9. https://doi.org/10.1038/s41467-018-08252-0.

(37)   Barros, J.; Serk, H.; Granlund, I.; Pesquet, E. The Cell Biology of Lignification in Higher Plants. *Ann. Bot.* **2015**, *115* (7), 1053–1074. https://doi.org/10.1093/aob/mcv046.

(38)   Balakshin, M.; Capanema, E.; Gracz, H.; Chang, H. min; Jameel, H. Quantification of Lignin-Carbohydrate Linkages with High-Resolution NMR Spectroscopy. *Planta* **2011**, *233* (6), 1097–1110. https://doi.org/10.1007/s00425-011-1359-2.

(39)   Giummarella, N.; Lawoko, M. Structural Basis for the Formation and Regulation of Lignin-Xylan Bonds in Birch. *ACS Sustain. Chem. Eng.* **2016**, *4* (10), 5319–5326. https://doi.org/10.1021/acssuschemeng.6b00911.

(40)   Mosier, N.; Wyman, C.; Dale, B.; Elander, R.; Lee, Y. Y.; Holtzapple, M.; Ladisch, M. Features of Promising Technologies for Pretreatment of Lignocellulosic Biomass. *Bioresour. Technol.* **2005**, *96* (6), 673–686. https://doi.org/10.1016/j.biortech.2004.06.025.

(41)   Abu-Omar, M. M.; Barta, K.; Beckham, G. T.; Luterbacher, J. S.; Ralph, J.; Rinaldi, R.; Román-Leshkov, Y.; Samec, J. S. M.; Sels, B. F.; Wang, F. Guidelines for Performing Lignin-First Biorefining. *Energy Environ. Sci.* **2021**, *14* (1), 262–292. https://doi.org/10.1039/d0ee02870c.

(42)   Wyman, C. E.; Dale, B. E.; Balan, V.; Elander, R. T.; Holtzapple, M. T.; Ramirez, R. S.; Ladisch, M. R.; Mosier, N. S.; Lee, Y. Y.; Gupta, R.; Thomas, S. R.; Hames, B. R.; Warner, R.; Kumar, R. *Comparative Performance of Leading Pretreatment Technologies for Biological Conversion of Corn Stover, Poplar Wood, and Switchgrass to Sugars*; 2013. https://doi.org/10.1002/9780470975831.ch12.

(43)   Chakar, F. S.; Ragauskas, A. J. Review of Current and Future Softwood Kraft Lignin Process Chemistry. *Ind. Crops Prod.* **2004**, *20* (2), 131–141. https://doi.org/10.1016/j.indcrop.2004.04.016.

(44)   Studer, M. H.; DeMartini, J. D.; Davis, M. F.; Sykes, R. W.; Davison, B.; Keller, M.; Tuskan, G. A.; Wyman, C. E. Lignin Content in Natural Populus Variants Affects Sugar Release. *Proc. Natl. Acad. Sci. U. S. A.* **2011**, *108* (15), 6300–6305. https://doi.org/10.1073/pnas.1009252108.

(45)   Wrasman, C. J.; Wilson, A. N.; Mante, O. D.; Iisa, K.; Dutta, A.; Talmadge, M. S.; Dayton, D. C.; Uppili, S.; Watson, M. J.; Xu, X.; Griffin, M. B.; Mukarakate, C.; Schaidle, J. A.; Nimlos, M. R. Catalytic Pyrolysis as a Platform Technology for Supporting the Circular Carbon Economy. *Nat. Catal.* **2023**, *6* (July), 563–573.

(46)   Mukarakate, C.; Iisa, K.; Habas, S. E.; Orton, K. A.; Xu, M.; Nash, C.; Wu, Q.; Happs, R. M.; French, R. J.; Kumar, A.; Miller, E. M.; Nimlos, M. R.; Schaidle, J. A. Accelerating Catalyst Development for Biofuel Production through Multiscale Catalytic Fast Pyrolysis of Biomass over Mo2C. *Chem Catal.* **2022**, *2*, 1819–1831.

(47)   Corona, A.; Biddy, M. J.; Vardon, D. R.; Birkved, M.; Hauschild, M. Z.; Beckham, G. T. Life Cycle Assessment of Adipic Acid Production from Lignin. *Green Chem.* **2018**, *20* (16), 3857–3866. https://doi.org/10.1039/c8gc00868j.

(48)   Ragauskas, A. J.; Beckham, G. T.; Biddy, M. J.; Chandra, R.; Chen, F.; Davis, M. F.; Davison, B. H.; Dixon, R. A.; Gilna, P.; Keller, M.; Langan, P.; Naskar, A. K.; Saddler, J. N.; Tschaplinski, T. J.; Tuskan, G. A.; Wyman, C. E. Lignin Valorization: Improving Lignin Processing in the Biorefinery. *Science (80-.).* **2014**, *344*.

(49)   Van Den Bosch, S.; Schutyser, W.; Koelewijn, S. F.; Renders, T.; Courtin, C. M.; Sels, B. F. Tuning the Lignin Oil OH-Content with Ru and Pd Catalysts during Lignin Hydrogenolysis on Birch Wood. *Chem. Commun.* **2015**, *51* (67), 13158–13161. https://doi.org/10.1039/c5cc04025f.

(50)   Schutyser, W.; Van Den Bosch, S.; Renders, T.; De Boe, T.; Koelewijn, S. F.; Dewaele, A.; Ennaert, T.; Verkinderen, O.; Goderis, B.; Courtin, C. M.; Sels, B. F. Influence of Bio-Based Solvents on the Catalytic Reductive Fractionation of Birch Wood. *Green Chem.* **2015**, *17* (11), 5035–5045.

https://doi.org/10.1039/c5gc01442e.

(51) Renders, T.; Van Den Bosch, S.; Vangeel, T.; Ennaert, T.; Koelewijn, S. F.; Van Den Bossche, G.; Courtin, C. M.; Schutyser, W.; Sels, B. F. Synergetic Effects of Alcohol/Water Mixing on the Catalytic Reductive Fractionation of Poplar Wood. *ACS Sustain. Chem. Eng.* **2016**, *4* (12), 6894–6904. https://doi.org/10.1021/acssuschemeng.6b01844.

(52) Anderson, E. M.; Stone, M. L.; Hu, M. J.; Beckham, G. T.; Román-Leshkov, Y. Kinetic Studies of Lignin Solvolysis and Reduction by Reductive Catalytic Fractionation Decoupled in Flow-Through Reactors. *ACS Sustain. Chem. Eng.* **2018**, *6*, 7951–7959. https://doi.org/10.1021/acssuschemeng.8b01256.

(53) Li, Y.; Shuai, L.; Kim, H.; Motagamwala, A. H.; Mobley, J. K.; Yue, F.; Tobimatsu, Y.; Havkin-Frenkel, D.; Chen, F.; Dixon, R. A.; Luterbacher, J. S.; Dumesic, J. A.; Ralph, J. An Ideal Lignin Facilitates Full Biomass Utilization. *Sci. Adv.* **2018**, *4* (9).

(54) Renders, T.; Cooreman, E.; Van Den Bosch, S.; Schutyser, W.; Koelewijn, S. F.; Vangeel, T.; Deneyer, A.; Van Den Bossche, G.; Courtin, C. M.; Sels, B. F. Catalytic Lignocellulose Biorefining in n -Butanol/Water: A One-Pot Approach toward Phenolics, Polyols, and Cellulose. *Green Chem.* **2018**, *20* (20), 4607–4619. https://doi.org/10.1039/c8gc01031e.

(55) Yan, N.; Zhao, C.; Dyson, P. J.; Wang, C.; Liu, L. T.; Kou, Y. Selective Degradation of Wood Lignin over Noble-Metal Catalysts in a Two-Step Process. *ChemSusChem* **2008**, *1* (7), 626–629. https://doi.org/10.1002/cssc.200800080.

(56) Ouyang, X.; Huang, X.; Zhu, J.; Boot, M. D.; Hensen, E. J. M. Catalytic Conversion of Lignin in Woody Biomass into Phenolic Monomers in Methanol/Water Mixtures without External Hydrogen. *ACS Sustain. Chem. Eng.* **2019**, *7* (16), 13764–13773. https://doi.org/10.1021/acssuschemeng.9b01497.

(57) Anderson, E. M.; Michael, L.; Katahira, R.; Beckham, G. T.; Anderson, E. M.; Stone, M. L.; Katahira, R.; Reed, M.; Beckham, G. T.; Román-Leshkov, Y. Flowthrough Reductive Catalytic Fractionation of Biomass Flowthrough Reductive Catalytic Fractionation of Biomass. *Joule* **2017**, No. 1, 613–622.

(58) Zijlstra, D. S.; Lahive, C. W.; Analbers, C. A.; Figueirêdo, M. B.; Wang, Z.; Lancefield, C. S.; Deuss, P. J. Mild Organosolv Lignin Extraction with Alcohols: The Importance of Benzylic Alkoxylation. *ACS Sustain. Chem. Eng.* **2020**, *8* (13), 5119–5131. https://doi.org/10.1021/acssuschemeng.9b07222.

(59) Renders, T.; Van den Bossche, G.; Vangeel, T.; Van Aelst, K.; Sels, B. Reductive Catalytic Fractionation: State of the Art of the Lignin-First Biorefinery. *Curr. Opin. Biotechnol.* **2019**, *56*, 193–201. https://doi.org/10.1016/j.copbio.2018.12.005.

(60) Kumaniaev, I.; Subbotina, E.; Sävmarker, J.; Larhed, M.; Galkin, M. V.; Samec, J. S. M. Lignin Depolymerization to Monophenolic Compounds in a Flow-through System. *Green Chem.* **2017**, *19* (24), 5767–5771. https://doi.org/10.1039/c7gc02731a.

(61) Brandner, D. G.; Kruger, J. S.; Thornburg, N. E.; Facas, G. G.; Kenny, J. K.; Dreiling, R. J.; Morais, A. R. C.; Renders, T.; Cleveland, N. S.; Happs, R. M.; Katahira, R.; Vinzant, T. B.; Wilcox, D. G.; Román-Leshkov, Y.; Beckham, G. T. Flow-through Solvolysis Enables Production of Native-like Lignin from Biomass. *Green Chem.* **2021**, *23* (15), 5437–5441. https://doi.org/10.1039/D1GC01591E.

(62) Thornburg, N. E.; Pecha, M. B.; Brandner, D. G.; Reed, M. L.; Vermaas, J. V.; Michener, W. E.; Katahira, R.; Vinzant, T. B.; Foust, T. D.; Donohoe, B. S.; Román-Leshkov, Y.; Ciesielski, P. N.; Beckham, G. Mesoscale Reaction-Diffusion Phenomena Governing Lignin-First Biomass Fractionation. *ChemSusChem* **2020**, *13* (17), 4495–4509. https://doi.org/10.1002/cssc.202000558.

(63) Chen, L.; Muyden, A. P. Van; Cui, X.; Fei, Z.; Yan, N.; Laurenczy, G.; Dyson, P. J. Lignin First: Confirming the Role of the Metal Catalyst in Reductive Fractionation. *J. Am. Chem. Soc. Au* **2021**, *1*, 7239–7733.

(64) Liu, X.; Feng, S.; Fang, Q.; Jiang, Z.; Hu, C. Reductive Catalytic Fractionation of Lignin in Birch Sawdust to Monophenolic Compounds with High Selectivity. *Molecular Catalysis*. 2020.

https://doi.org/10.1016/j.mcat.2020.111164.

(65) Li, Y.; Demir, B.; Vázquez Ramos, L. M.; Chen, M.; Dumesic, J. A.; Ralph, J. Kinetic and Mechanistic Insights into Hydrogenolysis of Lignin to Monomers in a Continuous Flow Reactor. *Green Chem.* **2019**, *21* (13), 3561–3572. https://doi.org/10.1039/c9gc00986h.

(66) Klein, I.; Marcum, C.; Kenttämaa, H.; Abu-Omar, M. M. Mechanistic Investigation of the Zn/Pd/C Catalyzed Cleavage and Hydrodeoxygenation of Lignin. *Green Chem.* **2016**, *18* (8), 2399–2405. https://doi.org/10.1039/c5gc01325a.

(67) Su, S.; Xiao, L.-P.; Chen, X.; Wang, S.; Chen, X.-H.; Guo, Y.; Zhai, S.-R. Lignin-First Depolymerization of Lignocellulose into Monophenols over Carbon Nanotube Supported Ruthenium: Impact of Lignin Sources. *ChemSusChem* **2022**, *15*. https://doi.org/10.1002/cssc.202200365.

(68) Klein, I.; Saha, B.; Abu-Omar, M. M. Lignin Depolymerization over Ni/C Catalyst in Methanol, a Continuation: Effect of Substrate and Catalyst Loading. *Catal. Sci. Technol.* **2015**, *5* (6), 3242–3245. https://doi.org/10.1039/c5cy00490j.

(69) Jang, J. H.; Morais, A. R. C.; Browning, M.; Brandner, D. G.; Kenny, J. K.; Stanley, L. M.; Happs, R. M.; Kovvali, A. S.; Cutler, J. I.; Román-Leshkov, Y.; Bielenberg, J. R.; Beckham, G. T. Feedstock-Agnostic Reductive Catalytic Fractionation in Alcohol and Alcohol-Water Mixtures. *Green Chem.* **2023**, *25* (9), 3660–3670. https://doi.org/10.1039/d2gc04464a.

(70) Galkin, M. V.; Smit, A. T.; Subbotina, E.; Artemenko, K. A.; Bergquist, J.; Huijgen, W. J. J.; Samec, J. S. M. Hydrogen-Free Catalytic Fractionation of Woody Biomass. *ChemSusChem* **2016**, *9* (23), 3280–3287. https://doi.org/10.1002/cssc.201600648.

(71) Orella, M. J.; Gani, T. Z. H.; Vermaas, J. V; Stone, M. L.; Anderson, E. M.; Beckham, G. T.; Brushett, F. R.; Roma, Y. Lignin-KMC : A Toolkit for Simulating Lignin Biosynthesis. *ACS Sustain. Chem. Eng.* **2019**, *7* (18313–18322). https://doi.org/10.1021/acssuschemeng.9b03534.

(72) Anderson, E. M.; Stone, M. L.; Katahira, R.; Reed, M.; Muchero, W.; Ramirez, K. J.; Beckham, G. T.; Román-leshkov, Y. Differences in S/G Ratio in Natural Poplar Variants Do Not Predict Catalytic Depolymerization Monomer Yields. *Nat. Commun.* **2019**, *10*, 1–10. https://doi.org/10.1038/s41467-019-09986-1.

(73) Duarte, C. M.; Agusti, S.; Chang, J.; Harrison, W. G.; Head, E. J. H.; Goericke, R.; Chisholm, S. W.; Hassett, R. P.; Chisholm, S. W.; Landry, M. R.; Hole, W.; Post, A. F.; Peacock, E. E.; Sosik, H. M.; Boss, E. S.; Falkowski, P. G.; Woodhead, A. D.; Vivirito, K.; Peacock, E.; Fredericks, J.; Team, O.; Members, C. Formaldehyde Stabilization Facilitates Lignin Monomer Production during Biomass Depolymerization. *Science (80-.).* **2016**, *354* (6310), 329–334.

(74) Stone, M. L.; Webber, M. S.; Mounfield III, W. P.; Bell, D. C.; Christensen, E.; Morais, A. R. C.; Li, Y.; Anderson, E. M.; Heyne, J. S.; Beckham, G. T.; Román-Leshkov, Y. Continuous Hydrodeoxygenation of Lignin to Jet-Range Aromatic Hydrocarbons. *Joule* **2022**, 1–14.

(75) Pedersen, S. S.; Batista, G. M. F.; Henriksen, M. L.; Hammershøj, H. C. D.; Hopmann, K. H.; Skrydstrup, T. Lignocellulose Conversion via Catalytic Transformations Yields Methoxyterephthalic Acid Directly from Sawdust. *JACS Au* **2023**, *3* (4), 1221–1229. https://doi.org/10.1021/jacsau.3c00092.

(76) Liao, Y.; Koelewijn, S. F.; van den Bossche, G.; van Aelst, J.; van den Bosch, S.; Renders, T.; Navare, K.; Nicolaï, T.; van Aelst, K.; Maesen, M.; Matsushima, H.; Thevelein, J. M.; van Acker, K.; Lagrain, B.; Verboekend, D.; Sels, B. F. A Sustainable Wood Biorefinery for Low-Carbon Footprint Chemicals Production. *Science (80-.).* **2020**, *367* (6484), 1385–1390. https://doi.org/10.1126/science.aau1567.

(77) Tschulkow, M.; Compernolle, T.; Van den Bosch, S.; Van Aelst, J.; Storms, I.; Van Dael, M.; Van den Bossche, G.; Sels, B.; Van Passel, S. Integrated Techno-Economic Assessment of a Biorefinery Process: The High-End Valorization of the Lignocellulosic Fraction in Wood Streams. *J. Clean. Prod.* **2020**, *266*. https://doi.org/10.1016/j.jclepro.2020.122022.

(78) Arts, W.; Van Aelst, K.; Cooreman, E.; Van Aelst, J.; Van den Bosch, S.; Sels, B. F. Stepping Away from Purified Solvents in Reductive Catalytic Fractionation: A Step Forwards towards a Disruptive

Wood Biorefinery Process. *Energy Environ. Sci.* **2023**, *16*, 2518–2539. https://doi.org/10.1039/d3ee00965c.

(79) Jang, J. H.; Brandner, D. G.; Dreiling, R. J.; Ringsby, A. J.; Bussard, J. R.; Stanley, L. M.; Happs, R. M.; Kovvali, A. S.; Cutler, J. I.; Renders, T.; Bielenberg, J. R.; Román-Leshkov, Y.; Beckham, G. T. Multi-Pass Flow-through Reductive Catalytic Fractionation. *Joule* **2022**, *6* (8), 1859–1875. https://doi.org/10.1016/j.joule.2022.06.016.

(80) Cooreman, E.; Nicola, T.; Arts, W.; Aelst, K. Van; Vangeel, T.; Bosch, S. Van Den; Aelst, J. Van; Lagrain, B.; Thiele, K.; Thevelein, J.; Sels, B. F. The Future Biorefinery: The Impact of Upscaling the Reductive Catalytic Fractionation of Lignocellulose Biomass on the Quality of the Lignin Oil, Carbohydrate Products, and Pulp. *ACS Sustain. Chem. Eng.* **2023**.

(81) Galkin, M. V.; Sawadjoon, S.; Rohde, V.; Dawange, M.; Samec, J. S. M. Mild Heterogeneous Palladium-Catalyzed Cleavage of β-o-4'-Ether Linkages of Lignin Model Compounds and Native Lignin in Air. *ChemCatChem* **2014**, *6* (1), 179–184. https://doi.org/10.1002/cctc.201300540.

(82) Galkin, M. V.; Samec, J. S. M. Selective Route to 2-Propenyl Aryls Directly from Wood by a Tandem Organosolv and Palladium-Catalysed Transfer Hydrogenolysis. *ChemSusChem* **2014**, *7* (8), 2154–2158. https://doi.org/10.1002/cssc.201402017.

(83) Ferrini, P.; Rinaldi, R. Catalytic Biorefining of Plant Biomass to Non-Pyrolytic Lignin Bio-Oil and Carbohydrates through Hydrogen Transfer Reactions. *Angew. Chemie* **2014**, *126* (33), 8778–8783. https://doi.org/10.1002/ange.201403747.

(84) Graça, I.; Woodward, R. T.; Kennema, M.; Rinaldi, R. Formation and Fate of Carboxylic Acids in the Lignin-First Biorefining of Lignocellulose via H-Transfer Catalyzed by Raney Ni. *ACS Sustain. Chem. Eng.* **2018**, *6* (10), 13408–13419. https://doi.org/10.1021/acssuschemeng.8b03190.

(85) Ren, T.; You, S.; Zhang, Z.; Wang, Y.; Qi, W.; Su, R.; He, Z. Highly Selective Reductive Catalytic Fractionation at Atmospheric Pressure without Hydrogen. *Green Chem.* **2021**, *23* (4), 1648–1657. https://doi.org/10.1039/d0gc03314f.

(86) Sluiter, A.; Hames, B.; Ruiz, R. O.; Scarlata, C.; Sluiter, J.; Templeton, D.; Crocker, D. P. *Determination of Structural Carbohydrates and Lignin in Biomass*; 2008.

(87) Schutyser, W.; Renders, T.; Van Den Bosch, S.; Koelewijn, S. F.; Beckham, G. T.; Sels, B. F. Chemicals from Lignin: An Interplay of Lignocellulose Fractionation, Depolymerisation, and Upgrading. *Chem. Soc. Rev.* **2018**, *47* (3), 852–908. https://doi.org/10.1039/c7cs00566k.

(88) Singh, N.; Campbell, C. T. A Simple Bond-Additivity Model Explains Large Decreases in Heats of Adsorption in Solvents Versus Gas Phase: A Case Study with Phenol on Pt(111) in Water. *ACS Catal.* **2019**, *9*, 8116–8127. https://doi.org/10.1021/acscatal.9b01870.

(89) Shangguan, J.; Hensley, A. J. R.; Gradiski, M. V.; Pfriem, N.; McEwen, J. S.; Morris, R. H.; Chin, Y. H. C. The Role of Protons and Hydrides in the Catalytic Hydrogenolysis of Guaiacol at the Ruthenium Nanoparticle-Water Interface. *ACS Catal.* **2020**, *10* (20), 12310–12332. https://doi.org/10.1021/acscatal.0c01963.

(90) Demir, B.; Kropp, T.; Gilcher, E. B.; Mavrikakis, M.; Dumesic, J. A. Effects of Water on the Kinetics of Acetone Hydrogenation over Pt and Ru Catalysts. *Journal of Catalysis*. 2021, pp 215–227. https://doi.org/10.1016/j.jcat.2021.03.013.

(91) Van Den Bosch, S.; Renders, T.; Kennis, S.; Koelewijn, S. F.; Van Den Bossche, G.; Vangeel, T.; Deneyer, A.; Depuydt, D.; Courtin, C. M.; Thevelein, J. M.; Schutyser, W.; Sels, B. F. Integrating Lignin Valorization and Bio-Ethanol Production: On the Role of Ni-Al2O3 Catalyst Pellets during Lignin-First Fractionation. *Green Chem.* **2017**, *19* (14), 3313–3326. https://doi.org/10.1039/c7gc01324h.

(92) Li, H.; Song, G. Ru-Catalyzed Hydrogenolysis of Lignin: Base-Dependent Tunability of Monomeric Phenols and Mechanistic Study. *ACS Catal.* **2019**, *9* (5), 4054–4064. https://doi.org/10.1021/acscatal.9b00556.

(93) Davis, J. L.; Barteau, M. A. Decarbonylation and Decomposition Pathways of Alcohol's on Pd(111). *Surf. Sci.* **1987**, *187* (2–3), 387–406. https://doi.org/10.1016/S0039-6028(87)80064-X.

(94) Mavrikakis, M.; Barteau, M. A. Oxygenate Reaction Pathways on Transition Metal Surfaces. *J. Mol.*

Catal. A Chem. **1998**, *131* (1–3), 135–147. https://doi.org/10.1016/S1381-1169(97)00261-6.

(95) Rinaldi, R.; Jastrzebski, R.; Clough, M. T.; Ralph, J.; Kennema, M.; Bruijnincx, P. C. A.; Weckhuysen, B. M. Paving the Way for Lignin Valorisation: Recent Advances in Bioengineering, Biorefining and Catalysis. *Angew. Chemie - Int. Ed.* **2016**, *55* (29), 8164–8215. https://doi.org/10.1002/anie.201510351.

(96) Laurichesse, S.; Avérous, L. Chemical Modification of Lignins: Towards Biobased Polymers. *Progress in Polymer Science.* 2014, pp 1266–1290. https://doi.org/10.1016/j.progpolymsci.2013.11.004.

(97) Duval, A.; Lawoko, M. Reactive & Functional Polymers A Review on Lignin-Based Polymeric , Micro- and Nano-Structured Materials. *React. Funct. Polym.* **2014**, *85*, 78–96. https://doi.org/https://doi.org/10.1016/.

(98) Balakshin, M.; Capanema, E. On the Quantification of Lignin Hydroxyl Groups with ^{31}P and ^{13}C NMR Spectroscopy. *J. Wood Chem. Technol.* **2015**, *35* (3), 220–237. https://doi.org/10.1080/02773813.2014.928328.

(99) Jääskeläinen, A. S.; Sun, Y.; Argyropoulos, D. S.; Tamminen, T.; Hortling, B. The Effect of Isolation Method on the Chemical Structure of Residual Lignin. *Wood Sci. Technol.* **2003**, *37* (2), 91–102. https://doi.org/10.1007/s00226-003-0163-y.

(100) Lin, Y. S. ;; Dence, W. C. *Methods in Lignin Chemistry*; 1992.

(101) Faix, O.; Argyropoulos, D. S.; Robert, D.; Neirinck, V. Determination of Hydroxyl Groups in Lignins Evaluation of 1H- 13C-, 31P-NMR, FTIR and Wet Chemical Methods. *Holzforschung* **1994**, *48* (5), 387–394. https://doi.org/10.1515/hfsg.1994.48.5.387.

(102) Michel Barrelle. A New Method for the Quantitative 19F NMR Spectroscopic Analysis of Hydroxyl Groups in Lignins. *Holzforschung* **1993**, *47* (3), 261–267. https://doi.org/https://doi.org/10.1515/hfsg.1993.47.3.261.

(103) Barrelle, M. Improvements in the Structural Investigation of Lignins by ^{19}F NMR Spectroscopy. *J. Wood Chem. Technol.* **1995**, *15* (2), 179–188. https://doi.org/10.1080/02773819508009506.

(104) Esakkimuthu, E. S.; Marlin, N.; Brochier-Salon, M.-C.; Mortha, G. Study of the Reactivity of Lignin Model Compounds to Fluorobenzylation Using 13C and 19F NMR : *Molecules* **2020**, *25*, 3211. https://doi.org/https://doi.org/10.3390/molecules25143211.

(105) Capanema, E. A.; Balakshin, M. Y.; Kadla, J. F. Quantitative Characterization of a Hardwood Milled Wood Lignin by Nuclear Magnetic Resonance Spectroscopy. *J. Agric. Food Chem.* **2005**, *53* (25), 9639–9649. https://doi.org/10.1021/jf0515330.

(106) Capanema, E. A.; Balakshin, M. Y.; Kadla, J. F. A Comprehensive Approach for Quantitative Lignin Characterization by NMR Spectroscopy. *J. Agric. Food Chem.* **2004**, *52* (7), 1850–1860. https://doi.org/10.1021/jf035282b.

(107) Mansfield, S. D.; Kim, H.; Lu, F.; Ralph, J. Whole Plant Cell Wall Characterization Using Solution-State 2D NMR. *Nat. Protoc.* **2012**, *7* (9), 1579–1589. https://doi.org/10.1038/nprot.2012.064.

(108) Meng, X.; Crestini, C.; Ben, H.; Hao, N.; Pu, Y.; Ragauskas, A. J.; Argyropoulos, D. S. Determination of Hydroxyl Groups in Biorefinery Resources via Quantitative ^{31}P NMR Spectroscopy. *Nat. Protoc.* **2019**, *14* (9), 2627–2647. https://doi.org/10.1038/s41596-019-0191-1.

(109) Schiff, D. E.; Verkade, J. G.; Metzler, R. M.; Squires, T. G.; Venier, C. G. Determination of Alcohols, Phenols, and Carboxylic Acids Using Phosphorus-31 Nmr Spectroscopy. *Appl. Spectrosc.* **1986**, *40* (3), 348–351. https://doi.org/10.1366/0003702864509268.

(110) Lensink, C.; Markuszewski, R.; Verkade, J. G.; Wroblewski, A. E. ^{31}P NMR Spectroscopic Analysis of Coal Pyrolysis Condensates and Extracts for Heteroatom Functionalities Possessing Labile Hydrogen. *Energy and Fuels* **1988**, *2* (6), 765–774. https://doi.org/10.1021/ef00012a008.

(111) Argyropoulos, D. S. Quantitative Phosphorus-31 Nmr Analysis of Lignins, a New Tool for the Lignin Chemist. *J. Wood Chem. Technol.* **1994**, *14* (1), 45–63. https://doi.org/10.1080/02773819408003085.

(112) Archipov, Y.; Argyropoulos, D. S.; Bolker, H. I.; Heitner, C. ^{31}P NMR Spectroscopy in Wood Chemistry . I . Model Compounds. *J. Wood Chem. Technol.* **1991**, *11* (2), 137–151.

https://doi.org/10.1080/02773819108050267.

(113) Argyropoulos, D. S.; Bolker, H. I.; Heitner, C.; Archipov, Y. ^{31}P NMR Spectroscopy in Wood Chemistry. Part V. Qualitative Analysis of Lignin Functional Groups. *J. Wood Chem. Technol.* **1993**, *13* (2), 187–212. https://doi.org/10.1080/02773819308020514.

(114) Ben, H.; Ferrell, J. R. In-Depth Investigation on Quantitative Characterization of Pyrolysis Oil by ^{31}P NMR. *RSC Adv.* **2016**, *6* (21), 17567–17573. https://doi.org/10.1039/c5ra23939g.

(115) Brittain, W. D. G.; Cobb, S. L. Tetrafluoropyridyl (TFP): A General Phenol Protecting Group Readily Cleaved under Mild Conditions. *Org. Biomol. Chem.* **2019**, *17* (8), 2110–2115. https://doi.org/10.1039/C8OB02899K.

(116) Meng, X.; Pu, Y.; Yoo, C. G.; Li, M.; Bali, G.; Park, D. Y.; Gjersing, E.; Davis, M. F.; Muchero, W.; Tuskan, G. A.; Tschaplinski, T. J.; Ragauskas, A. J. An In-Depth Understanding of Biomass Recalcitrance Using Natural Poplar Variants as the Feedstock. *ChemSusChem* **2017**, *10* (1), 139–150. https://doi.org/10.1002/cssc.201601303.

(117) Kojima, M.; Tsunoi, S.; Tanaka, M. Determination of 4-Alkylphenols by Novel Derivatization and Gas Chromatography-Mass Spectrometry. *J. Chromatogr. A* **2003**, *984* (2), 237–243. https://doi.org/10.1016/S0021-9673(02)01836-8.

(118) Fuhrer, T. J.; Houck, M.; Corley, C. A.; Iacono, S. T. Theoretical Explanation of Reaction Site Selectivity in the Addition of a Phenoxy Group to Perfluoropyridine. *J. Phys. Chem. A* **2019**, *123* (44), 9450–9455. https://doi.org/10.1021/acs.jpca.9b06413.

(119) Li, X.; Russell, R. K. Using Potassium Carbonate to Scavenge Hydrogen Fluoride: A Scale-up Process for Quantitative Production of (1-Cyclopropyl-6,7-Difluoro-1,4-Dihydro-8- Methoxy-4-(0x0-K0)-3-Quinolinecarboxylato-K03)Difluoro Boron. *Org. Process Res. Dev.* **2008**, *12* (3), 464–466. https://doi.org/10.1021/op8000228.

(120) Ragnar, M.; Lindgren, C. T.; Nilvebrant, N.-O. PKa-Values of Guaiacyl and Syringyl Phenols Related to Lignin. *J. Wood Chem. Technol.* **2000**, *20* (3), 277–305. https://doi.org/10.1080/02773810009349637.

(121) Ahvazi, B. C.; Crestini, C.; Argyropoulos, D. S. [19]F Nuclear Magnetic Resonance Spectroscopy for the Quantitative Detection and Classification of Carbonyl Groups in Lignins. *J. Agric. Food Chem.* **1999**, *47* (1), 190–201. https://doi.org/10.1021/jf980431p.

(122) Sameni, J.; Krigstin, S.; Sain, M. Solubility of Lignin and Acetylated Lignin in Organic Solvents. *BioResources* **2017**, *12* (1), 1548–1565. https://doi.org/10.15376/biores.12.1.1548-1565.

(123) Duval, A.; Vilaplana, F.; Crestini, C.; Lawoko, M. Solvent Screening for the Fractionation of Industrial Kraft Lignin. *Holzforschung* **2016**, *70* (1), 11–20. https://doi.org/10.1515/hf-2014-0346.

(124) Dastpak, A.; Lourençon, T. V.; Balakshin, M.; Farhan Hashmi, S.; Lundström, M.; Wilson, B. P. Solubility Study of Lignin in Industrial Organic Solvents and Investigation of Electrochemical Properties of Spray-Coated Solutions. *Ind. Crops Prod.* **2020**, *148* (October 2019). https://doi.org/10.1016/j.indcrop.2020.112310.

(125) Miguel, E. L. M.; Santos, C. I. L.; Silva, C. M.; Pliego, J. R. How Accurate Is the SMD Model for Predicting Free Energy Barriers for Nucleophilic Substitution Reactions in Polar Protic and Dipolar Aprotic Solvents? *J. Braz. Chem. Soc.* **2016**, *27* (11), 2055–2061. https://doi.org/10.5935/0103-5053.20160095.

(126) Pliego, J. R.; Piló-Veloso, D. Effects of Ion-Pairing and Hydration on the SNAr Reaction of the F- with p-Chlorobenzonitrile in Aprotic Solvents. *Phys. Chem. Chem. Phys.* **2008**, *10* (8), 1118–1124. https://doi.org/10.1039/b716159j.

(127) Li, M.; Constantinescu, D.; Wang, L.; Mohs, A.; Gmehling, J. Solubilities of NaCl, KCl, LiCl, and LiBr in Methanol, Ethanol, Acetone, and Mixed Solvents and Correlation Using the Liquac Model. *Ind. Eng. Chem. Res.* **2010**, *49* (10), 4981–4988. https://doi.org/10.1021/ie100027c.

(128) Long, B. Experimental Studies and Thermodynamic Modeling of the Solubilities of Potassium Nitrate, Potassium Chloride, Potassium Bromide, and Sodium Chloride in Dimethyl Sulfoxide. *Ind. Eng. Chem. Res.* **2011**, *50* (11), 7019–7026. https://doi.org/10.1021/ie102134g.

(129) Brittain, W. D. G.; Cobb, S. L. Carboxylic Acid Deoxyfluorination and One-Pot Amide Bond

Formation Using Pentafluoropyridine (PFP). *Org. Lett.* **2021**, *23* (15), 5793–5798. https://doi.org/https://doi.org/10.1021/acs.orglett.1c01953.

(130) Vlasov, V. M. Fluoride Ion as a Nucleophile and a Leaving Group in Aromatic Nucleophilic Substitution Reactions. *J. Fluor. Chem.* **1993**, *61* (3), 193–216. https://doi.org/10.1016/S0022-1139(00)80104-9.

(131) Honda, S.; Ishida, R.; Hidaka, K.; Masuda, T. Stability of Polyphenols under Alkaline Conditions and the Formation of a Xanthine Oxidase Inhibitor from Gallic Acid in a Solution at PH 7.4. *Food Sci. Technol. Res.* **2019**, *25* (1), 123–129. https://doi.org/10.3136/fstr.25.123.

(132) Jinhua, Z.; Kleinöder, T.; Gasteiger, J. Prediction of PKa Values for Aliphatic Carboxylic Acids and Alcohols with Empirical Atomic Charge Descriptors. *J. Chem. Inf. Model.* **2006**, *46* (6), 2256–2266. https://doi.org/10.1021/ci060129d.

(133) Cabrera, Y.; Cabrera, A.; Jensen, A.; Felby, C. Purification of Biorefinery Lignin with Alcohols. *J. Wood Chem. Technol.* **2016**, *36* (5), 339–352. https://doi.org/10.1080/02773813.2016.1148168.

(134) Granata, A.; Argyropoulos, D. S. 2-Chloro-4,4,5,5-Tetramethyl-1,3,2-Dioxaphospholane, a Reagent for the Accurate Determination of the Uncondensed and Condensed Phenolic Moieties in Lignins. *J. Agric. Food Chem.* **1995**, *43* (6), 1538–1544. https://doi.org/10.1021/jf00054a023.

(135) Schutyser, W.; Kruger, J. S.; Robinson, A. M.; Katahira, R.; Brandner, D. G.; Cleveland, N. S.; Mittal, A.; Peterson, D. J.; Meilan, R.; Román-leshkov, Y.; Beckham, G. T. Revisiting Aerobic Lignin Oxidation. *Green Chem.* **2018**, 3828–3844. https://doi.org/10.1039/c8gc00502h.

(136) Dao Thi, H.; Van Aelst, K.; Van den Bosch, S.; Katahira, R.; Beckham, G. T.; Sels, B. F.; Van Geem, K. M. Identification and Quantification of Lignin Monomers and Oligomers from Reductive Catalytic Fractionation of Pine Wood with GC × GC – FID/MS. *Green Chem.* **2022**. https://doi.org/10.1039/d1gc03822b.

(137) Mottiar, Y.; Karlen, S. D.; Goacher, R. E.; Ralph, J.; Mansfield, S. D. Metabolic Engineering of P-Hydroxybenzoate in Poplar Lignin. *Plant Biotechnol. J.* **2022**, 1–13. https://doi.org/10.1111/pbi.13935.

(138) Goacher, R. E.; Mottiar, Y.; Mansfield, S. D. ToF-SIMS Imaging Reveals That p-Hydroxybenzoate Groups Specifically Decorate the Lignin of Fibres in the Xylem of Poplar and Willow. *Holzforschung* **2021**, *75* (5), 452–462. https://doi.org/10.1515/hf-2020-0130.

(139) Kenny, J. K.; Brandner, D. G.; Neefe, S. R.; Michener, W. E.; Román-leshkov, Y.; Beckham, G. T.; Medlin, J. W. Catalyst Choice Impacts Aromatic Monomer Yields and Selectivity in Hydrogen-Free Reductive Catalytic Fractionation. *React. Chem. Eng.* **2022**, *7* (7), 2527–2533. https://doi.org/10.1039/d2re00275b.

(140) Lancefield, C. S.; Wienk, H. J.; Boelens, R.; Weckhuysen, B. M.; Bruijnincx, P. C. A. Identification of a Diagnostic Structural Motif Reveals a New Reaction Intermediate and Condensation Pathway in Kraft Lignin Formation. *Chem. Sci.* **2018**, *9* (30), 6348–6360. https://doi.org/10.1039/c8sc02000k.

(141) Crestini, C.; Lange, H.; Sette, M.; Argyropoulos, D. S. On the Structure of Softwood Kraft Lignin. *Green Chem.* **2017**, *19* (17), 4104–4121. https://doi.org/10.1039/c7gc01812f.

(142) Balakshin, M.; Capanema, E. A.; Zhu, X.; Sulaeva, I.; Potthast, A.; Rosenau, T.; Rojas, O. J. Spruce Milled Wood Lignin: Linear, Branched or Cross-Linked? *Green Chem.* **2020**, *22* (13), 3985–4001. https://doi.org/10.1039/d0gc00926a.

(143) Facas, G. G.; Brandner, D. G.; Bussard, J. R.; Rom, Y.; Beckham, G. T. Interdependence of Solvent and Catalyst Selection on Low Pressure Hydrogen-Free Reductive Catalytic Fractionation. *ACS Sustain. Chem. Eng.* **2023**.

(144) Huber, G. W.; Shabaker, J. W.; Dumesic, J. A. Raney Ni-Sn Catalyst for H_2 Production from Biomass-Derived Hydrocarbons. *Science (80-.).* **2003**, *300* (5628), 2075–2078. https://doi.org/10.1126/science.1085597.

(145) Hagemeyer, A.; Borade, R.; Desrosiers, P.; Guan, S.; Lowe, D. M.; Poojary, D. M.; Turner, H.; Weinberg, H.; Zhou, X.; Armbrust, R.; Fengler, G.; Notheis, U. Application of Combinatorial Catalysis for the Direct Amination of Benzene to Aniline. *Appl. Catal. A Gen.* **2002**, *227* (1–2), 43–

61. https://doi.org/10.1016/S0926-860X(01)00921-8.

(146) Corma, A.; Serra, J. M.; Chica, A. Discovery of New Paraffin Isomerization Catalysts Based on SO42-/ZrO2 and WOx/ZrO2 Applying Combinatorial Techniques. *Catal. Today* **2003**, *81* (3), 495–506. https://doi.org/10.1016/S0920-5861(03)00148-2.

(147) Liu, Y.; Cong, P.; Doolen, R. D.; Guan, S.; Markov, V.; Woo, L.; Zeyß, S.; Dingerdissen, U. Discovery from Combinatorial Heterogeneous Catalysis: A New Class of Catalyst for Ethane Oxidative Dehydrogenation at Low Temperatures. *Appl. Catal. A Gen.* **2003**, *254* (1), 59–66. https://doi.org/10.1016/S0926-860X(03)00263-1.

(148) Greeley, J.; Jaramillo, T. F.; Bonde, J.; Chorkendorff, I.; Nørskov, J. K. Computational High-Throughput Screening of Electrocatalytic Materials for Hydrogen Evolution. *Nat. Mater.* **2006**, *5* (11), 909–913. https://doi.org/10.1038/nmat1752.

(149) Selig, M. J.; Viamajala, S.; Decker, S. R.; Tucker, M. P.; Himmel, M. E.; Vinzant, T. B. Deposition of Lignin Droplets Produced during Dilute Acid Pretreatment of Maize Stems Retards Enzymatic Hydrolysis of Cellulose. *Biotechnol. Prog.* **2007**, *23* (6), 1333–1339. https://doi.org/10.1021/bp0702018.

(150) Lindedam, J.; Bruun, S.; Jørgensen, H.; Decker, S. R.; Turner, G. B.; DeMartini, J. D.; Wyman, C. E.; Felby, C. Evaluation of High Throughput Screening Methods in Picking up Differences between Cultivars of Lignocellulosic Biomass for Ethanol Production. *Biomass and Bioenergy* **2014**, *66*, 261–267. https://doi.org/10.1016/j.biombioe.2014.03.006.

(151) Decker, S. R.; Brunecky, R.; Tucker, M. P.; Himmel, M. E.; Selig, M. J. High-Throughput Screening Techniques for Biomass Conversion. *Bioenergy Res.* **2009**, *2* (4), 179–192. https://doi.org/10.1007/s12155-009-9051-0.

(152) Studer, M. H.; DeMartini, J. D.; Brethauer, S.; McKenzie, H. L.; Wyman, C. E. Engineering of a High-Throughput Screening System to Identify Cellulosic Biomass, Pretreatments, and Enzyme Formulations That Enhance Sugar Release. *Biotechnol. Bioeng.* **2010**, *105* (2), 231–238. https://doi.org/10.1002/bit.22527.

(153) Santoro, N.; Cantu, S. L.; Tornqvist, C. E.; Falbel, T. G.; Bolivar, J. L.; Patterson, S. E.; Pauly, M.; Walton, J. D. A High-Throughput Platform for Screening Milligram Quantities of Plant Biomass for Lignocellulose Digestibility. *Bioenergy Res.* **2010**, *3* (1), 93–102. https://doi.org/10.1007/s12155-009-9074-6.

(154) Happs, R. M.; Bartling, A. W.; Doeppke, C.; Harman-Ware, A. E.; Clark, R.; Webb, E. G.; Biddy, M. J.; Chen, J. G.; Tuskan, G. A.; Davis, M. F.; Muchero, W.; Davison, B. H. Economic Impact of Yield and Composition Variation in Bioenergy Crops: Populus Trichocarpa. *Biofuels, Bioprod. Biorefining* **2021**, *15* (1), 176–188. https://doi.org/10.1002/bbb.2148.

(155) Xiao, L.; Wei, H.; Himmel, M. E.; Jameel, H.; Kelley, S. S. NIR and Py-Mbms Coupled with Multivariate Data Analysis as a High-Throughput Biomass Characterization Technique: A Review. *Front. Plant Sci.* **2014**, *5* (AUG), 1–10. https://doi.org/10.3389/fpls.2014.00388.

(156) Ferrini, P.; Chesi, C.; Parkin, N.; Rinaldi, R. Effect of Methanol in Controlling Defunctionalization of the Propyl Side Chain of Phenolics from Catalytic Upstream Biorefining. *Faraday Discuss.* **2017**, *202*, 403–413. https://doi.org/10.1039/c7fd00069c.

(157) Ambrose, D.; Townsend, R. Thermodynamic Properties of Organic Oxygen Compounds. Part IX. The Critical Properties and Vapour Pressures, above Five Atmospheres, of Six Aliphatic Alcohols. *J. Chem. Soc.* **1963**, No. 3614, 3614–3625.

(158) Ambrose, D.; Sprake, C. H. S.; Townsend, R. Thermodynamic Properties of Organic Oxygen Compounds XXXVII. Vapour Pressures of Methanol, Ethanol, Penta-1-Ol, and Octan-l-O1 from the Normal Boiling Temperature to the Critical Temperature. *J. Chem. Thermodyn.* **1975**, *7* (2), 185–190.

(159) Van Den Bosch, S.; Schutyser, W.; Vanholme, R.; Driessen, T.; Koelewijn, S. F.; Renders, T.; De Meester, B.; Huijgen, W. J. J.; Dehaen, W.; Courtin, C. M.; Lagrain, B.; Boerjan, W.; Sels, B. F. Reductive Lignocellulose Fractionation into Soluble Lignin-Derived Phenolic Monomers and Dimers and Processable Carbohydrate Pulps. *Energy Environ. Sci.* **2015**, *8* (6), 1748–1763.

https://doi.org/10.1039/c5ee00204d.

(160) Su, S.; Xiao, L. P.; Chen, X.; Wang, S.; Chen, X. H.; Guo, Y.; Zhai, S. R. Lignin-First Depolymerization of Lignocellulose into Monophenols over Carbon Nanotube-Supported Ruthenium: Impact of Lignin Sources. *ChemSusChem* **2022**, *15* (12), 1–9. https://doi.org/10.1002/cssc.202200365.

(161) Chen, S. F.; Mowery, R. A.; Sevcik, R. S.; Scarlata, C. J.; Chambliss, C. K. Compositional Analysis of Water-Soluble Materials in Switchgrass. *J. Agric. Food Chem.* **2010**, *58* (6), 3251–3258. https://doi.org/10.1021/jf9033877.

(162) Harman-Ware, A. E.; Macaya-Sanz, D.; Abeyratne, C. R.; Doeppke, C.; Haiby, K.; Tuskan, G. A.; Stanton, B.; DiFazio, S. P.; Davis, M. F. Accurate Determination of Genotypic Variance of Cell Wall Characteristics of a Populus Trichocarpa Pedigree Using High-Throughput Pyrolysis-Molecular Beam Mass Spectrometry. *Biotechnol. Biofuels* **2021**, *14* (1), 1–15. https://doi.org/10.1186/s13068-021-01908-y.

(163) Van De Pas, D. J.; Nanayakkara, B.; Suckling, I. D.; Torr, K. M. Comparison of Hydrogenolysis with Thioacidolysis for Lignin Structural Analysis. *Holzforschung* **2014**, *68* (2), 151–155. https://doi.org/10.1515/hf-2013-0075.

(164) Sannigrahi, P.; Ragauskas, A. J.; Tuskan, G. A. Poplar as a Feedstock for Biofuels: A Review of Compositional Characteristics. *Biofuels, Bioprod. Biorefining* **2014**, *8* (6), 743. https://doi.org/10.1002/BBB.

(165) Bryant, N.; Zhang, J.; Feng, K.; Shu, M.; Ployet, R.; Chen, J.; Muchero, W.; Yoo, C. G.; Tschaplinski, T. J.; Pu, Y.; Ragauskas, A. J. Novel Candidate Genes for Lignin Structure Identi Fi Ed through Genome-Wide Association Study of Naturally Varying Populus Trichocarpa. *Front. Plant Sci.* **2023**, No. May, 1–10. https://doi.org/10.3389/fpls.2023.1153113.

(166) Quirk, J. T. Shrinkage and Related Properties of Cell Walls of Douglas-Fir. *IAWA Bull.* **1978**, No. 2–3, 48.

(167) Kenny, J. K.; Medlin, J. W.; Beckham, G. T. Quantification of Phenolic Hydroxyl Groups in Lignin via 19F NMR Spectroscopy. *ACS Sustain. Chem. Eng.* **2023**, *11* (14), 5644–5655. https://doi.org/10.1021/acssuschemeng.3c00115.

(168) Zhou, H.; Liu, X.; Guo, Y.; Wang, Y. Self-Hydrogen Supplied Catalytic Fractionation of Raw Biomass into Lignin-Derived Phenolic Monomers and Cellulose-Rich Pulps. *J. Am. Chem. Soc. Au* **2023**, *3* (7), 1911–1917.

(169) Iisa, K.; Kim, Y.; Orton, K. A.; Robichaud, D. J.; Katahira, R.; Watson, M. J.; Wegener, E. C.; Nimlos, M. R.; Schaidle, J. A.; Mukarakate, C.; Kim, S. Ga/ZSM-5 Catalyst Improves Hydrocarbon Yields and Increases Alkene Selectivity during Catalytic Fast Pyrolysis of Biomass with Co-Fed Hydrogen. *Green Chem.* **2020**, *22* (8), 2403–2418. https://doi.org/10.1039/c9gc03408k.

(170) Ayotte, Y.; Woo, S.; Laplante, S. R. Practical Considerations and Guidelines for Spectral Referencing for Fluorine NMR Ligand Screening. *ACS Omega* **2022**, *7* (15), 13155–13163. https://doi.org/10.1021/acsomega.2c00613.

(171) Hudlicky, M. Chemical Shifts of Fluorine in Hydrogen Fluoride and Fluoride Ion. *J.Fluorine.Chem.* **1985**, *28*, 461–472.

(172) Olarte, M. V; Burton, S. D.; Swita, M.; Padmaperuma, A. B.; Ferrell, J.; Ben, H. *Determination of Hydroxyl Groups in Pyrolysis Bio-Oils Using ^{31}P-NMR Laboratory Analytical Procedure (LAP)*; 2016; pp 1–9. http://www.nrel.gov/docs/fy16osti/65887.pdf.

Appendix

A.   Supplement to Chapter 2

Supplemental Figures
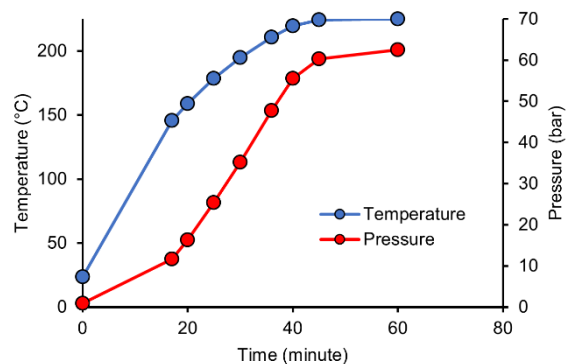
Figure A1. Heating and pressure profile of batch reactor heat-up during H_2-free RCF. Pressure during RCF with H_2 reached approximately 83 bar.
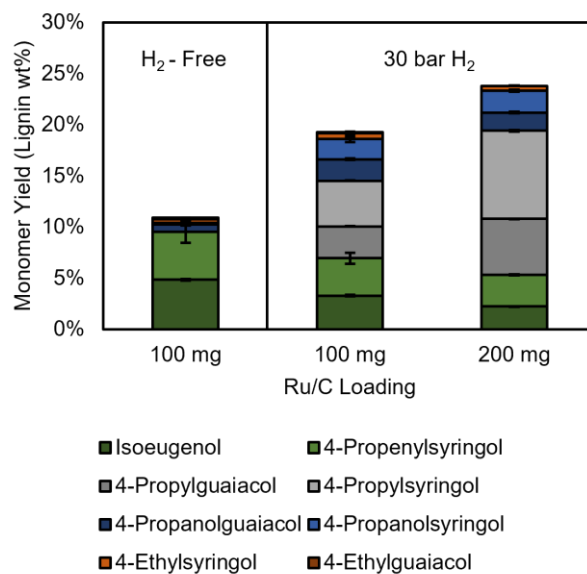
Figure A2. Comparison of monomer yields (not including methyl paraben or phenol as these presumably derive from para-hydroxy benzoate) with 100 and 200 mg Ru/C with 30 bar H2, showing increased monomer yields for the higher catalyst loading, indicating that reactions with 100 mg Ru/C are limited by the rate of hydrogenolysis. Note, reactions with 200 mg Ru/C were performed in duplicate, and error bars show the range of two experiments. Conditions are the same as those in Figure 2, except catalyst loading is as specified here.
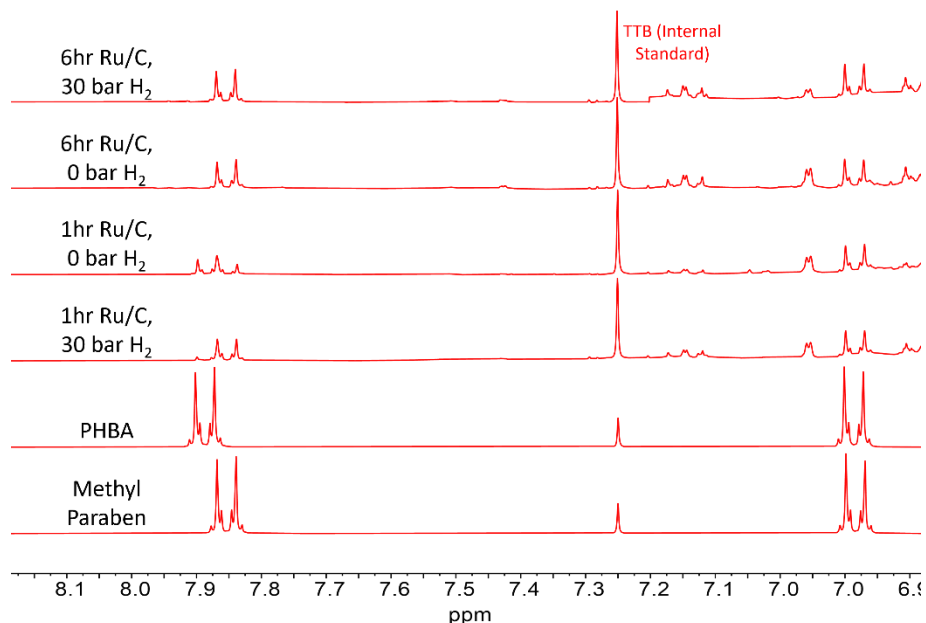
Figure A3. [1]H spectrum of para-hydroxy benzoate (PHBA), methyl paraben, and RCF oils from reactions with and without H_2. Solvent: d_6-acetone, approximately 15 mg/mL lignin oil.
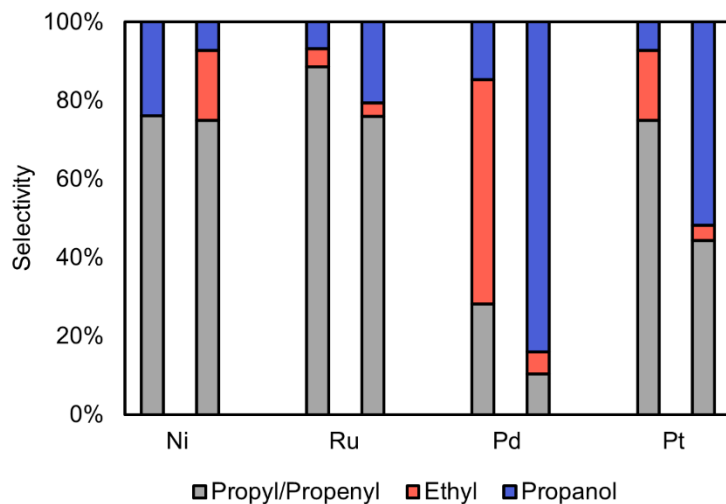
Figure A4. Selectivity to ethyl, propyl/propenyl, and propanol products calculated from **Figure A2**, normalized to 100%, showing that high selectivity to ethyl products consistently coincided with low selectivity to propanol products. Left bars are for reactions in H_2-free conditions, and right bars are for reactions with 30 bars H_2. For Ni and Ru, selectivity to propyl/propenyl products remains consistent even when external H_2 is added. For Pd and Pt, external H_2 has a large impact on selectivity.
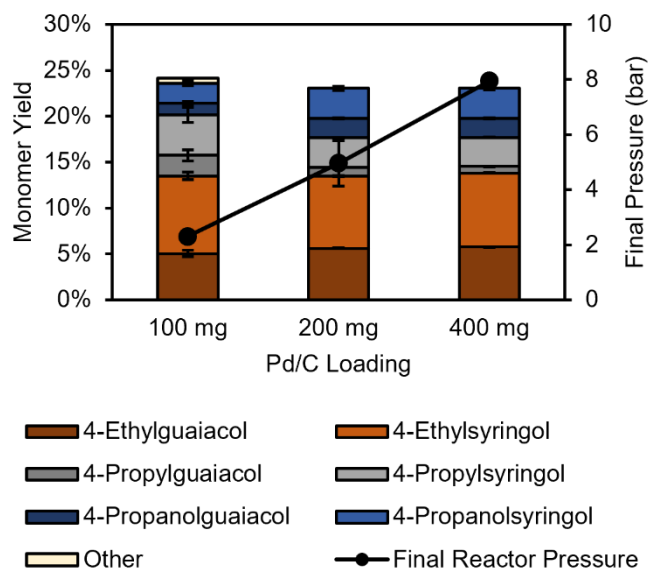
Figure A5. Lignin derived monomer yields (not including methyl paraben or phenol as these presumably derive from para-hydroxy benzoate) for H_2-free reactions with different amounts of Pd/C catalyst, showing that ethyl selectivity remains constant. Isoeugenol and propenyl syringol were not detected and are not included in the legend. Final reactor pressure refers to the pressure of the reactor post reaction after it had cooled down to room temperature. Conditions are the same as those in **Figure 2,** except catalyst loading is as specified here.
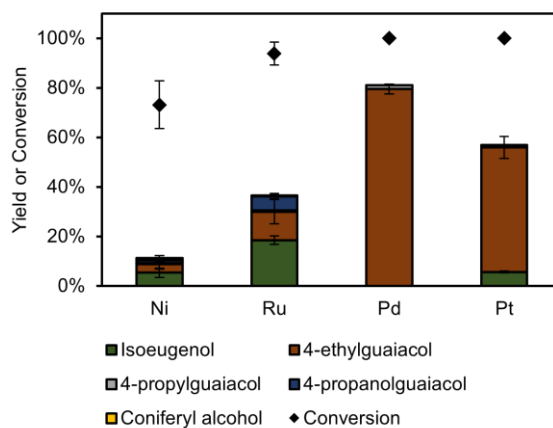
Figure A6. Monomer yields and conversions from coniferyl aldehyde. Conditions: 30 mg coniferyl aldehyde, 1 hour reaction after 30 minute heat-up, 20 mg catalyst, 30 mL methanol, 0 bar H_2, 225°C

B. Supplement to Chapter 3

Production of RCF oil from poplar

150 g of poplar biomass was added into a 2-gallon Parr reactor, along with 15 g of 5 wt% Ru/C and 3 L of methanol. The reactor was then sealed, and pressure tested up to 1,700 psig with N_2. The reactor was then flushed with N_2 three times, and then H_2 was added to a pressure of 435 psig. The reactor was heated to 225°C over the course of 90 minutes, and then held at temperature for 6 hours. After the reaction, an internal cooling water loop was used to cool the reactor to room temperature, and a peristaltic pump was used to separate the product solution from biomass and catalyst. The methanol was evaporated using a rotary evaporator, and an ethyl acetate/water extraction was performed. The organic layers were combined and dried with sodium sulfate. The ethyl acetate was then removed by rotary evaporation, yielding the poplar RCF oil.

Milled wood lignin isolation

Milled wood lignin from corn stover was produced via the Björkman method as previously reported.[169] The MWL was 86% lignin by mass according to compositional analysis.[86]

Assignment of α and γ resonances of GGE and VGE.

The assignment of resonances to hydroxyl groups in GGE and VGE are not immediately obvious due to the complex ^{19}F NMR. From time course reactions of VGE in acetone, we can see that the resonances located at -94.25 and -159.6 ppm belong to the same TFP ether from the fact that they integrate to the same value at low reaction times (**Figure B5**). Similar resonances are also observed in GGE reaction; however, they are complicated by the presence of the phenolic resonance. VGE resonances were compared to those from 4-hydroxy-3-methoxy-α-methylbenzyl alcohol and 1,2-diphenylethanol. These model compounds exhibited aliphatic TFP-ether resonances, which were downfield of typical G resonances, with similar positions to those seen in GGE and VGE, suggesting that the downfield resonances near -157.6 ppm observed in the β-O-4 model compounds belong to the α-hydroxyl groups. Interestingly, resonances are do not align with those from 3-(3,4-dimethoxyphenyl)-propanol and 3,4-dimethoxybenzyl alcohol, except for the fact that the γ resonance in 3-(3,4-dimethoxyphenyl)-propanol is significantly upfield from the α resonance in the 3,4-dimethoxybenzyl alcohol. This would lead to the conclusion that the resonance at -158.9 derives from the γ-hydroxyl group (**Figures S5-S6).**

Safety considerations

The prescribed method generates fluoride ions. Potassium fluoride (KF) is considered poisonous. The overall reaction is as follows:

$$R\text{-}OH + K_2CO_3 + PFP \rightarrow R\text{-}O\text{-}TFP + KHCO_3 + KF$$
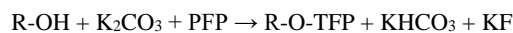
The inorganic products of the reaction can also participate in the equilibrium reaction:

$$KHCO_3 + KF \leftrightharpoons K_2CO_3 + HF$$
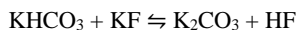
which forms HF, a highly poisonous and corrosive acid**.** The presence of HF in any appreciable amount would prevent the method from being considered safe. It is therefore necessary to consider the amount of KF and HF present in samples and waste streams. KF shows low solubility in organic solvents, which would prevent the equilibrium reaction from proceeding.[170] When derivatizations were performed in acetone or DMSO, no resonances in the expected range of -115 to -125 ppm were observed.[171] With the addition of water however, new peaks were observed in the range of -118 to -121 ppm, potentially indicating the formation and dissolution of KF or other fluoride salts. K_2CO_3, which is present in an excess in the reaction mixture, was shown to be an efficient scavenger of HF even in moderate excess (1.15 equivalents).[119]

^{31}P NMR measurements

Hydroxyl content of the three lignin substrates was measured with ^{31}P according to published procedures.[108,172] Briefly, approximately 20 mg of substrate was massed into a 4 mL vial. An internal standard solution consisting of $CDCl_3$, triphenylphosphine oxide, and Cr(acac)$_3$ was prepared, measuring the mass of each component added. Approximately 0.6 mL of the internal standard solution and 0.9 mL of anhydrous pyridine was added to the vial containing the substrate. Finally, approximately 200 μL of 2-Chloro-4,4,5,5-tetramethyl-1,3,2-dioxaphospholane (TMDP) was added. The vials was closed, shaken, and inspected for precipitate. Samples were transferred to NMR tubes, and a 1D ^{31}P NMR experiment was performed on a Bruker Avance III HD Nanobay 400 MHz instrument equipped with a nitrogen-cooled Prodigy cryoprobe using an inverse gated decoupling pulse sequence, 25 second pulse delay, and 128 scans at 25°C. Processing (including apodization with a LB of 5.0 Hz, phasing, baseline correction, and axis calibration) and quantification were performed using Bruker TopSpin 3.6 software. Figures were generated using MestreNova.
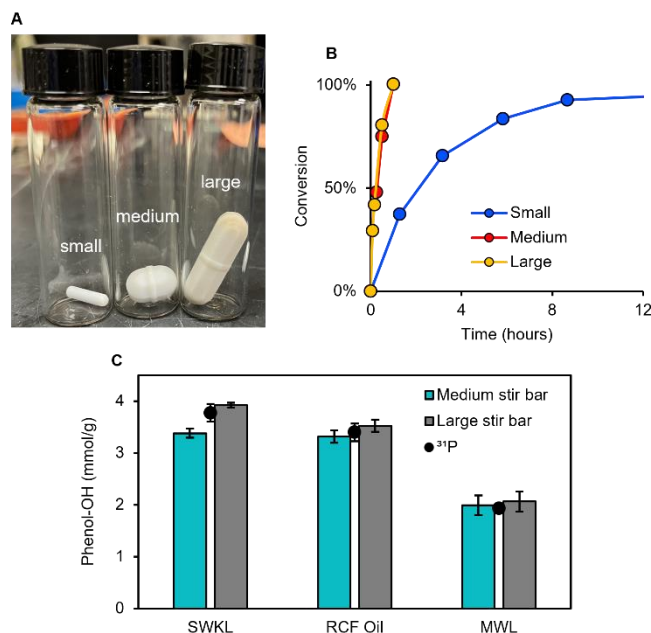
Figure B1. Impact of stir bar on reaction rate. (**A**) Picture of small (13 x 3 mm), medium (15 x 6 mm), and large (30 x 8 mm) stir bars used. (**B**) Comparison of time course derivatization of syringol using a small stir bar (blue circles), a medium stir bar (red circles), and a large stir bar (yellow circles). Error bars represent the range of duplicate experiments. (**C**) Comparison between total phenol content measured using medium stir bars (teal bars) and large stir bars (grey bars; data is same as in **Figure 6A**, 40% H_2O/DMSO). While the use of the large stir bar led to a greater quantification for all three substrates, the results are only statistically significant for SWKL (SWKL 3.43 ± 0.09 mmol/g versus 3.92 ± 0.05 mmol/g, p-value: 0.0045; RCF oil 3.32 ± 0.1 mmol/g versus 3.52 ± 0.1, p-value: 0.064; MWL 1.99 ± 0.2 mmol/g versus 2.06 ± 0.2 mmol/g, p-value 0.67). Conditions: 20-40 mg substrate, 1 mL 40% H_2O/DMSO, 4 equivalents of PFP & K_2CO_3 assuming a measurement of 4 mmol phenolic OH/g, 5 minutes reaction time, room temperature, 2 mL acetone added to resolubilize. Error bars represent the standard deviation of triplicate measurements.
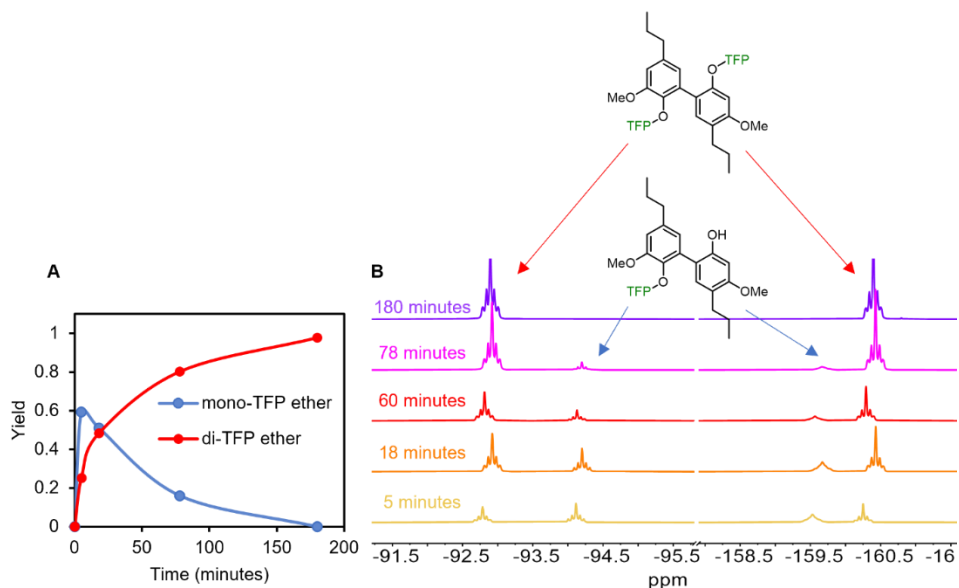
Figure B2. Time course reaction of the 5-5 model compound 3,3′-dimethoxy-5,5′-dipropyl[1,1′-biphenyl]-2,2′-diol (5-5 GG) in 40% H_2O/DMSO. (**A**) Yield of the mono and di -TFP ether (**B**) Partial ^{19}F NMR spectra showing the mono-derivatized model at -94.12 ppm. Three replicates are shown for the 5-minute reaction time point; all other time points are single measurements. Conditions: 1 mL 40% H_2O/DMSO, 4 equivalents PFP & K_2CO_3, 5 minutes reaction time, room temperature, 2 mL acetone added to the reaction vial to resolubilize products and internal standard.
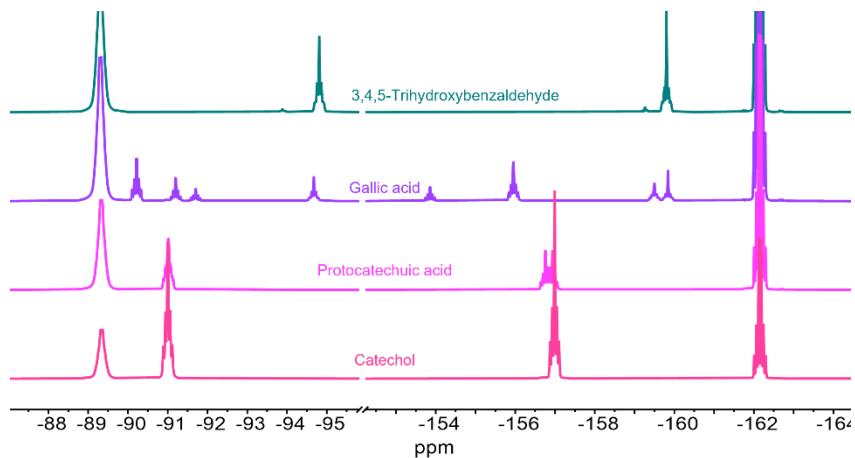
Figure B3. Partial ^{19}F NMR spectra for model compounds containing multiple phenolic hydroxyls. Conditions: 1 mL 40% H_2O/DMSO, 4 equivalents PFP & K_2CO_3, 5 minutes reaction time, room temperature, 2 mL acetone added to the reaction vial to resolubilize products and internal standard.
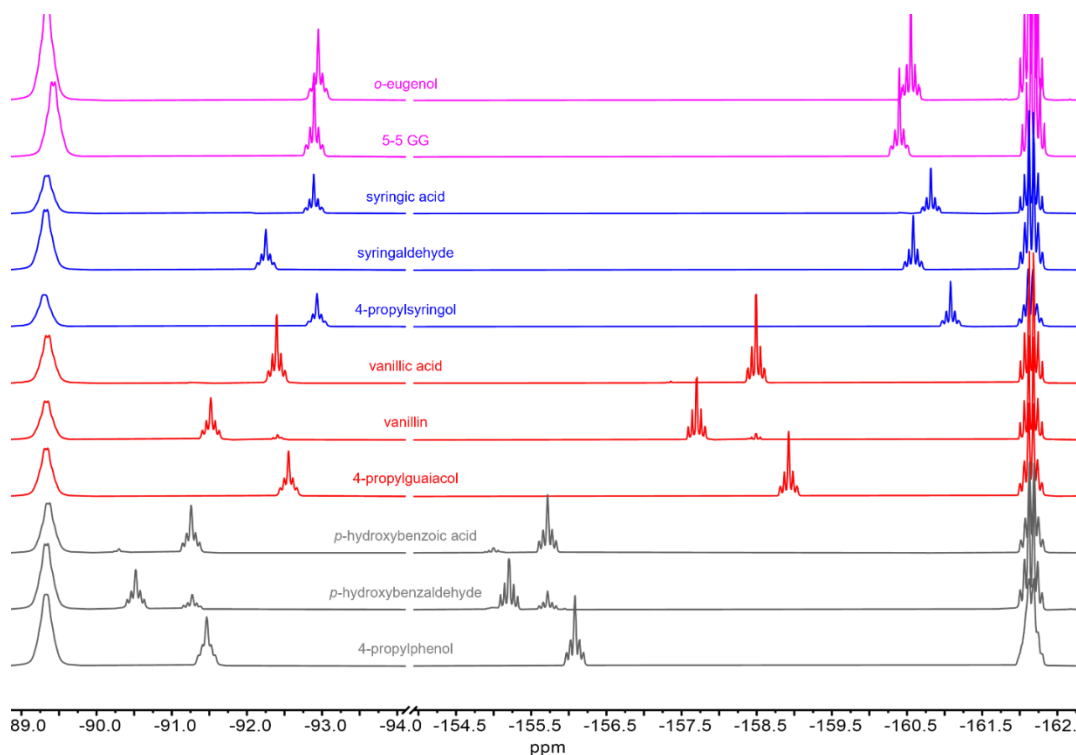
Figure B4. Partial ^{19}F NMR spectra of phenolic model compounds derivatized with PFP. Aldehydes show resonances that are further downfield than similarly substituted phenols. In the DF region, condensed-G (G$_c$) model compounds o-eugenol and 5-5 GG overlap completely with 4-propylsyringol, but this overlap is less severe in the UF region. Conditions: 1 mL 40% H2O/DMSO, 4 equivalents PFP & K$_2$CO$_3$, 5 minutes reaction time (except for 5-5 GG, in which reaction time was 3 hours), room temperature, 2 mL acetone added to the reaction vial to resolubilize products and internal standard. Conditions: 1 mL 40% H$_2$O/DMSO, 4 equivalents PFP & K$_2$CO$_3$, 5 minutes reaction time, room temperature, 2 mL acetone added to the reaction vial to resolubilize products and internal standard.
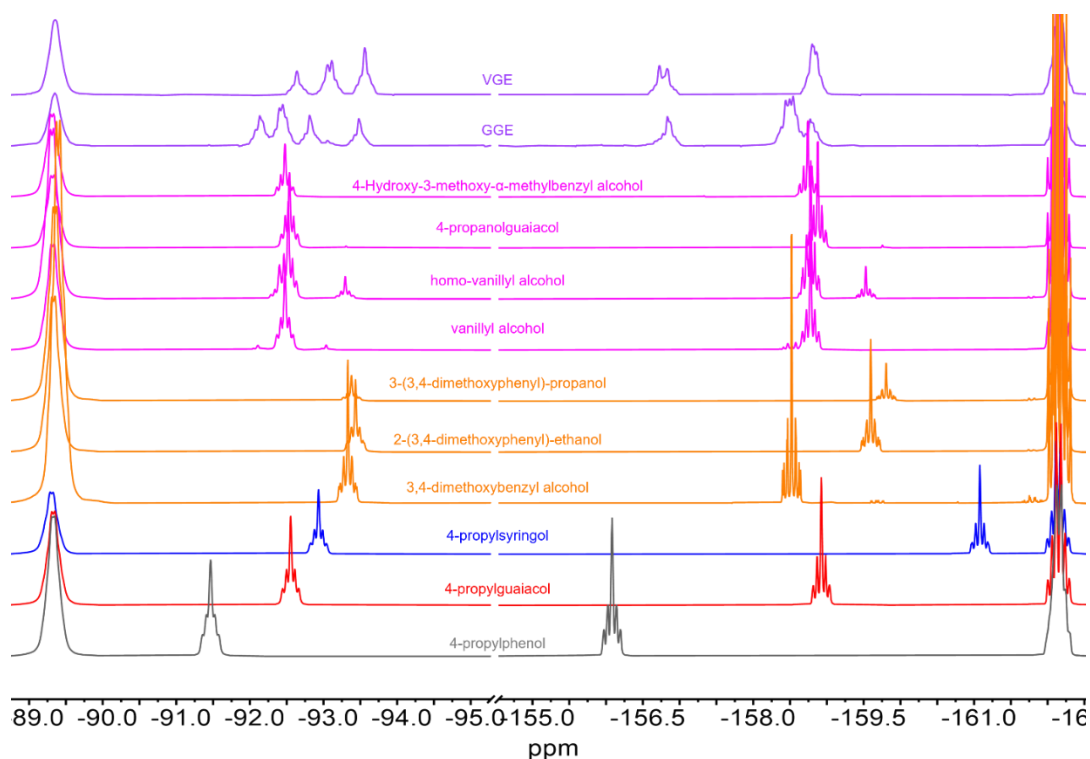
Figure B5. Partial ^{19}F NMR spectra of aliphatic model compounds, with 4-propylsyringol, 4-propylguaiacol included for reference. Orange spectra are non-phenolic model compounds, pink spectra are phenolic model compounds, and purple spectra are β-O-4 dimers. Conditions: 1 mL 40% H_2O/DMSO, 4 equivalents PFP & K_2CO_3, 5 minutes reaction time, room temperature, 2 mL acetone added to the reaction vial to resolubilize products and internal standard.
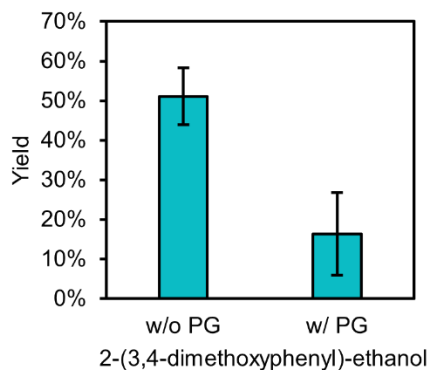
Figure B6. Aliphatic yield of 2-(3,4-dimethoxyphenyl) ethanol without (left bar) and with 4-propylguaiacol added, showing the influence of phenolic alcohols on the reaction rate of aliphatics. Conditions: 20 mg substrates, 1 mL 40% H_2O/DMSO, 4 equivalents PFP & K_2CO_3 with respect to total phenol content in reaction, room temperature, 2 mL acetone added to resolubilize.
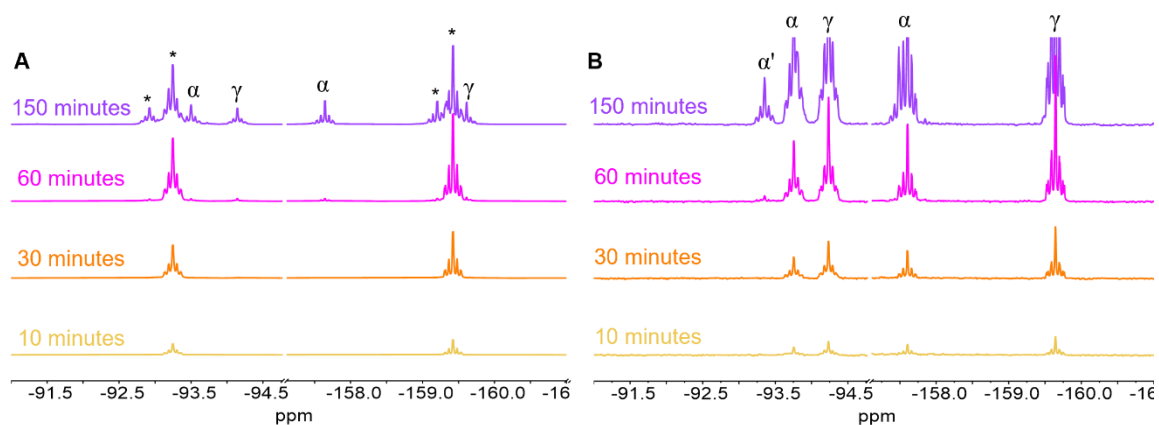
Figure B7. GGE and VGE time course reaction. (**A**) GGE reaction showing appearance of phenol resonance first (*), followed by the appearance of α and γ resonances. Derivatization at the α position coincides with the appearance a second phenolic resonance when the phenol and α hydroxyl are both derivatized (also marked with *). (**B**) Reaction of VGE showing fast derivatization of both α and γ hydroxyl. Conditions: 40 mg substrate, 4 mL acetone-d_6, 4 equivalents PFP & K_2CO_3, room temperature.
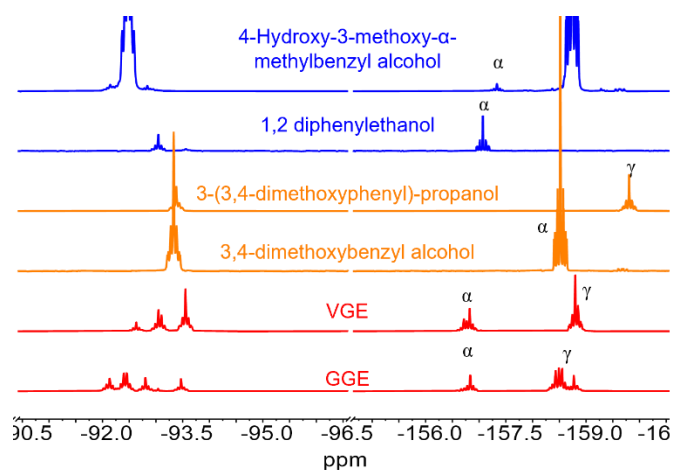
Figure B8. Assignment of VGE and GGE resonances through comparison to 1,2-diphenylethanol and 4-hydroxy-3-methoxy-α-methylbenzyl.

108
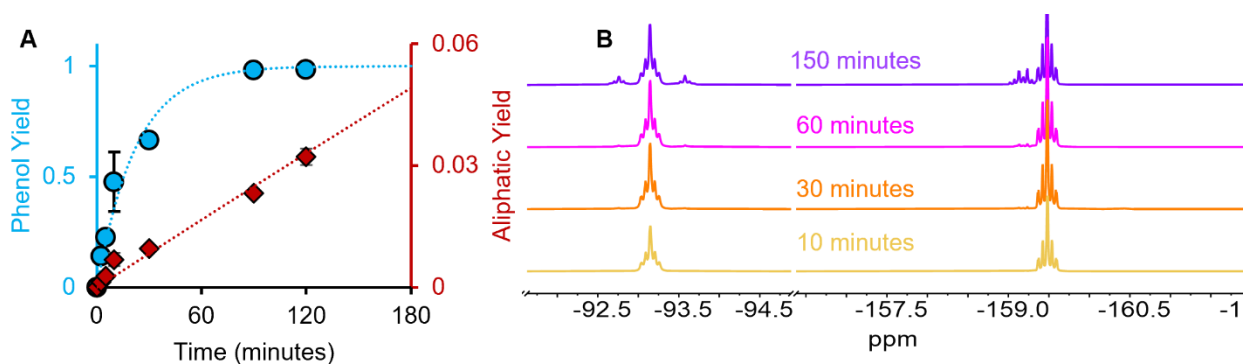
Figure B9. Vanillyl alcohol time course reaction. (**A**) Yield of phenol-TFP ether (blue) and aliphatic-TFP ether (red). (**B**) Partial ^{19}F NMR spectra showing the appearance of the aliphatic resonance at -93.1 ppm, and corresponding resonance for the phenol with derivatized aliphatic hydroxyl group downfield from the normal vanillyl alcohol resonance. Conditions for both **A** and **B**: 80 mg vanillyl alcohol, 4 mL acetone, 4 equivalents PFP & K_2CO_3, room temperature, conducted in 10 mL vial.
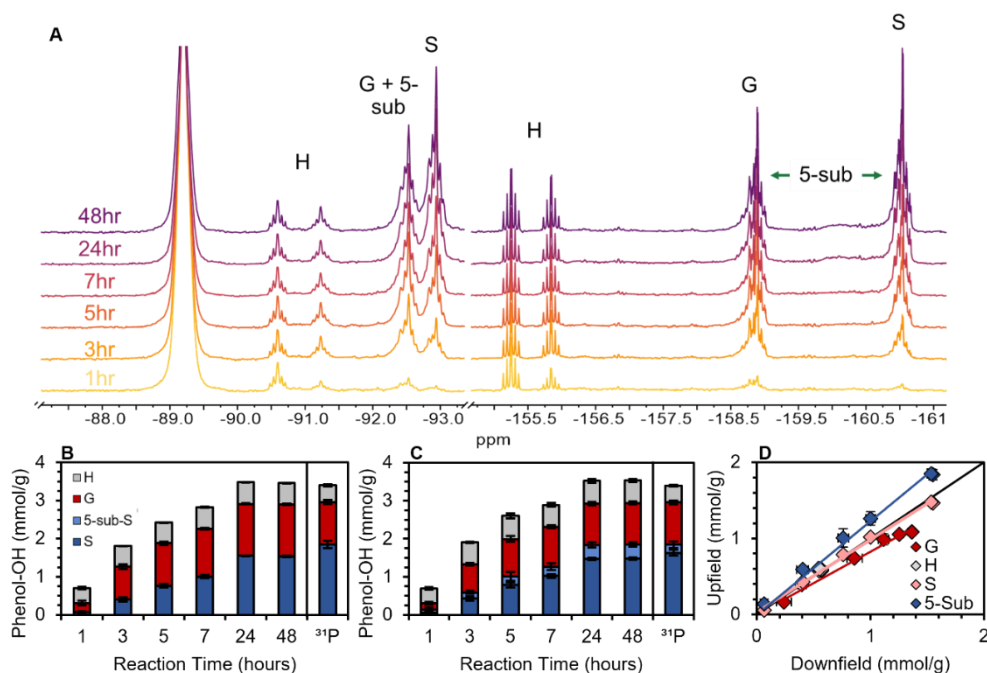
Figure B10. Time course derivatization of RCF oil with acetone solvent with small stir bar. (**A**) ^{19}F spectra, (**B**) downfield integration region, (**C**) upfield integration region, and (**D**) comparison of upfield versus downfield integration regions showing good agreement for H, total phenolics, but indicating that some 5-substitued phenolics appear to overlap with the G integral in the DF region. Approximately 200 mg of oil was massed into a 10 mL vial with a small stir bar. 2 equivalents PFP/K_2CO_3 was added assuming a phenol content of 3.4 mmol/g (the value obtained from ^{31}P), followed by 4 mL of acetone. The timer was started when 2 equivalents PFP was added to the reaction. Samples were taken from the same vial at various time points and filtered. 0.4 mL of the sample was combined with 0.4 acetone-d_6 in an NMR tube. A ^{19}F experiment was performed as described above, except the delay was set to 30 seconds since Cr(acac)$_3$ was not added, and 16 scans were recorded. Error bars indicate the standard deviation of three separate experiments.
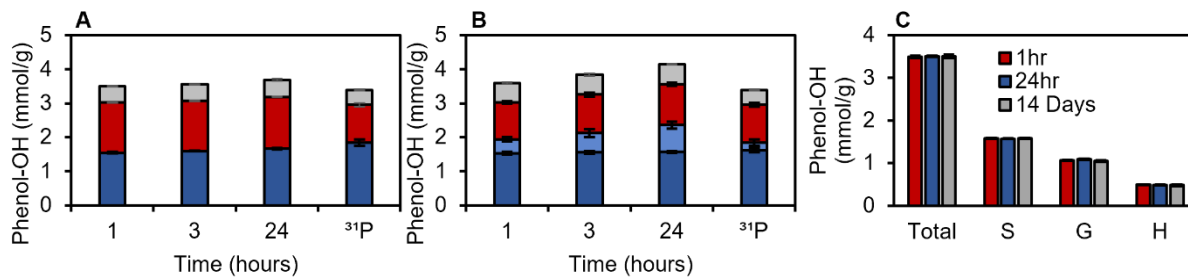
Figure B11. Time course reaction of RCF oil using DMSO as a solvent (A) Downfield region showing minimal increase in integrations, indicating that most aliphatics do not overlap with this region, (B) upfield region showing increase in total phenolics from aliphatics reacting and overlapping with 5-substituted region, and (C) stability of the 1-hour sample over 14 days.
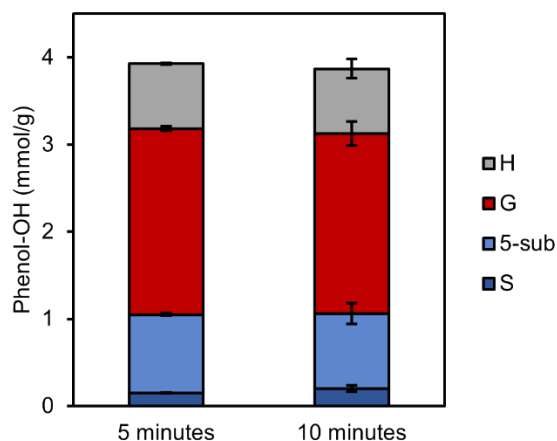
Figure B12. Comparison of phenolic measurements for SWKL with a reaction time of 5 minutes and 10 minutes. Conditions: 40 mg SWKL, 1 mL 40% H_2O/DMSO, 4 equivalents of PFP & K_2CO_3 assuming a measurement of 4 mmol phenolic OH/g, room temperature, 2 mL acetone added to resolubilize.
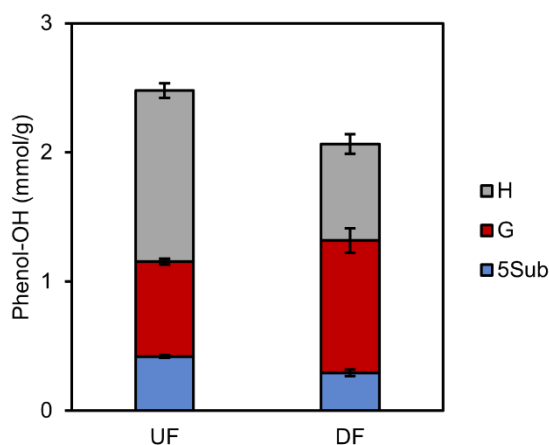
Figure B13. Comparison of measurements for MWL from the upfield and downfield regions. Conditions: 20 mg corn stover MWL, 1 mL 40% H_2O/DMSO, 4 equivalents of PFP & K_2CO_3 assuming a measurement of 4 mmol phenolic OH/g, 5 minutes reaction time, room temperature, 2 mL acetone added to resolubilize.
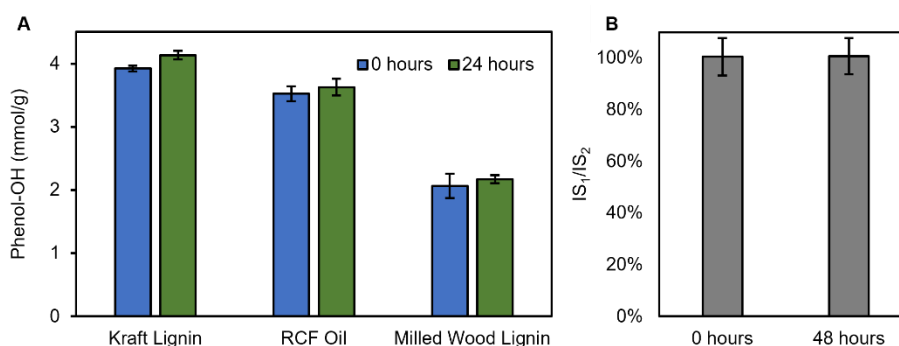
Figure B14. Sample stability of derivatized lignins from **Figure 6A** in NMR tube using 40% H_2O/DMSO solvent. (**A**) change in total phenolic measurement. (**B**) Ratio of two internal standards (4,4-difluorobenzophenone and 1,4-difluoro-2,5-dimethoxybenzene) normalized to the expected amount based on their mass measurement at the time of first measurement (0 hour) and after 48 hours in the NMR tube. Conditions: 20-40 mg substrate, 1 mL 40% H_2O/DMSO, 2 mL acetone added to resolubilize products and internal standard, 4 equivalents PFP & K_2CO_3, room temperature, samples were left in NMR tubes on benchtop for 24 hours for stability measurement, 5 minutes reaction time for **A**, 10 minutes reaction time for **B** (these are the same samples as from **Figure B10**).

Supplemental Tables

Table B1: ^{19}F NMR shifts for model compounds derivatized in 40% H_2O/DMSO organized by functional group. Chemical shifts are referenced to the 4,4 difluorobenzophenone at -107.4 ppm.

Functional Group	Model compound	Downfield Shift (ppm)	Upfield Shift (ppm)
S	syringol	-92.812	-161.016
	syringyl alcohol	-92.893	-160.992
	4-propylsyringol	-92.932	-161.079
	syringic acid	-92.889	-160.815
	syringaldehyde	-92.248	-160.581
G_c	5-5 GG dimer	-92.814	-160.293
	o-eugenol	-92.95	-160.551
G	guaiacol	-92.397	-158.758

	homovanillyl alcohol	-92.524	-158.778
	4-propylguaiacol	-92.553	-158.926
	4-propanolguaiacol	-92.538	-158.876
	vanillyl alcohol	-92.478	-158.786
	vanillin	-91.521	-157.902
	vanillic acid	-92.397	-158.491
	acetovanillone	-91.683	-157.881
	isoeugenol	-92.424	-158.816
	GGE	-92.412	-158.461
	4-hydroxy-3-methoxy-α-methylbenzyl alcohol	-92.477	-158.741
H	phenol	-91.295	-155.911
	2-(4-hydroxyphenyl)-ethanol	-91.392	-155.94
	4-propylphenol	-91.465	-156.08
	p-hydroxybenzoic acid	-91.255	-155.717
	p-hydroxybenzaldehyde	-90.520	-155.207
	methyl paraben	-90.659	-155.322
Catechols	1,2-dihydroxybenzene	-91.010	-156.990
	protocatechuic acid	-91.010	-156.870
Aliphatic	4-propanolguaiacol	-93.308	-159.755
	GGE α -1	-93.037	-156.834
	GGE α -2	-92.797	-156.834
	GGE γ	-93.475	-158.774
	VGE α -1	-92.665	-156.779
	VGE α -2	-93.127	-156.779
	VGE γ	-93.58	-158.85
	3,4 dimethoxybenzyl alcohol	-93.33	-158.52
	vanillyl alcohol	-93.038	-158.474
	syringyl alcohol	-92.996	-158.484
	hydroxy-3-methoxy-α-methylbenzyl alcohol	-92.85	-157.33

2-(4-hydroxyphenyl)-ethanol	-93.288	-159.53
homovanillyl alcohol	-93.295	-159.53
2-(3,4 dimethoxyphenyl)-ethanol	-93.435	-159.596
3-(3,4 dimethoxy phenyl)-propanol	-93.38	-159.806
4-methoxybenzyl alcohol	-93.267	-158.534

Table B2: ^{19}F NMR integration ranges for functional groups.

Region	Functional Group	Integral Range (ppm)
Upfield	Total phenol region	-90.45 to -93.2
	5-sub	-92.7 to - 93.2
	G	- 91.5 to - 92.7
	H	90.45 to -91.5
Downfield	Total Phenol Region	-155.17 to -161.35
	S	-159.1 to - 161.35
	5-sub	161.8 to -161.35
	G	157.5 to -159.1
	H	155.17 to -157.5

Table B3: Integration ranges for ^{31}P analysis of different functional groups. Shifts are referenced to TMDP peak at 175.514 ppm.

Functional Group	Integral Range (ppm)
Total Phenol Region	138-145
5-sub	141-145
S	142.8-144.5
G	139.1-141
H	138-139.1
Aliphatic	145-152

C. Supplement to Chapter 4

Optimization of transfer solvent

Due to the small reaction volume, small transfer losses can significantly impact product yield. We first sought to optimize the recovery of products during the post reaction workup to ensure accurate and repeatable sampling. The workup of HTP-RCF reactions requires the removal of solid particles and the isolation of lignin oil in a known final sample volume for analysis. To account for errors arising from transfer losses, octadecane (C_{18}) was used as a surrogate since it is an inert compound with no impact on the RCF reaction. Choosing a transfer solvent system that achieves a proportional transfer of lignin products and C_{18} allows the lignin monomer and oil yields to be scaled to the recovery factor of the surrogate. Solid particle removal was achieved by transferring the liquid product to a 24-well filter plate above a vacuum manifold containing collection vials. Much of the reaction solvent in which product is dissolved remains entrained in the biomass at the end of the reaction and is thus difficult to transfer. To increase total product recovery, a transfer solvent is used to wash the biomass, wells, and filters. To investigate the impact of the transfer solvent, identical reactions were worked up using different solvents. Several primary solvents (isopropanol, ethanol, methanol, ethyl acetate, and acetone) were identified as possibly being assistive in the monomer recovery process. Utilizing hexane to assist in the recovery of C18, these five primary solvents were mixed with various amounts of hexane to create 21 binary transfer-solvent systems. Systems with a wide range of polarity ensured that a solvent system which accurately represents product recovery was chosen as the transfer solvent. Results from reactions worked up with varying transfer solvents are shown in **Figure C3.** Choice of workup solvent had a large impact on monomer yields, ranging from 21% for pure hexane to 41% pure methanol. This is due to both greatly varying recoveries of both the lignin oil and C_{18} recoveries obtained. Several solvent systems gave acceptable results as concluded from the total recovery of C_{18} and lignin oil, as well as a positive correlation of C_{18} and lignin recovery (monomers and oil) indicating that they are co-recovered, rather than selectively. The 50% acetone/hexane gave the highest total recovery of reaction material, quantified as the sum of C_{18} recovery and total oil yield. Utilizing a

mixture of 75% ethyl acetate and 25% hexane by volume satisfied both constraints. Furthermore, the scaled lignin oil and monomers measurements most accurately reflected the expected yields and selectivity compared to 75-mL batch reactions run at high-throughput conditions (**Figure *C3,*** far right entry). The 75% ethyl acetate/hexane also conveniently system evaporates quickly, allowing for convenient workup conditions.

Supplemental Figures
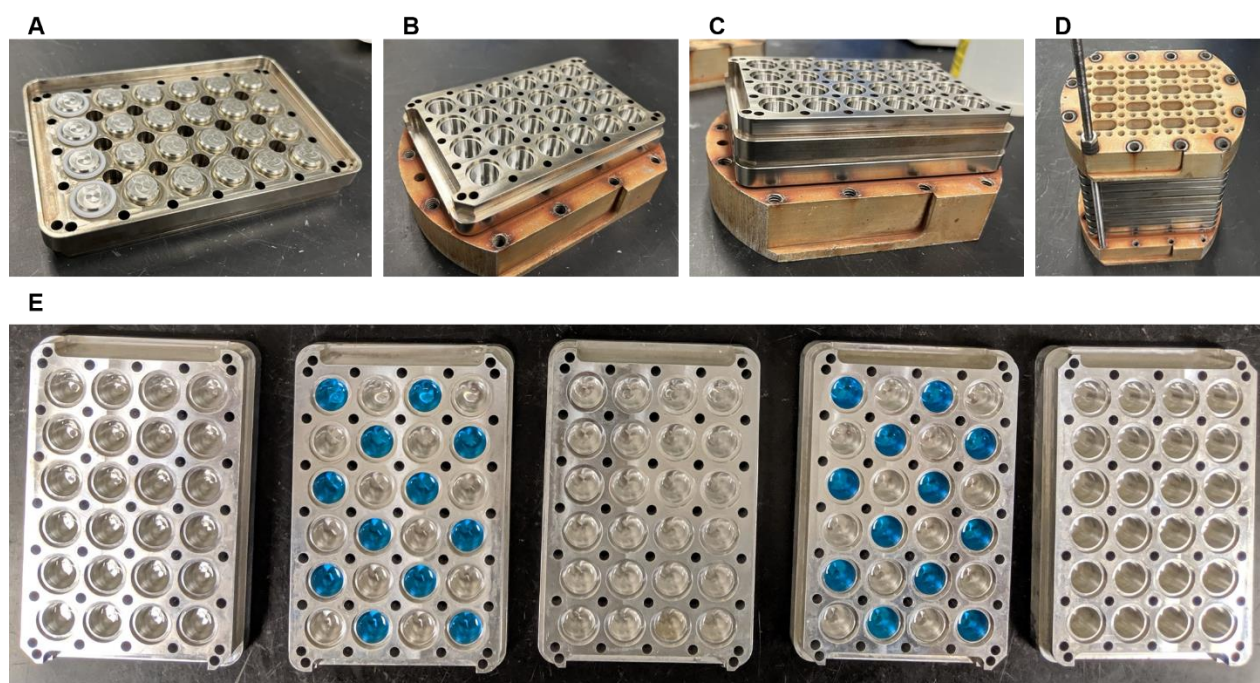
Figure C1. Images of reactor plates **A**) underside of reactor plate with O-rings affixed to first 4 pins **B**) First reactor plate (without catalyst/biomass) attached to bottom sealing plate **C**) First two reactor plates stacked **D**) Ten reactor plates stacked with top and bottom sealing plates, with 1 of 12 disc spring laden all-threads installed **E**) Plates with methanol post- leak test at 200°C for 6 hours, with blue dye in alternating wells demonstrating that there is no cross-contamination between wells.
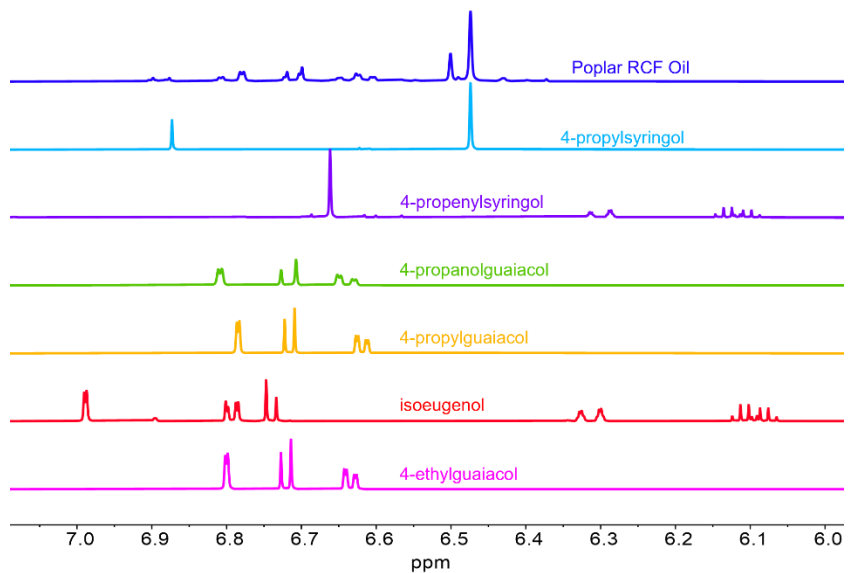
Figure C2: ^{1}H NMR spectra of lignin monomer model compounds compared to poplar RCF oil. RCF oil was generated from a standard parr reaction, leading to high selectivity for propyl substituted monomers.
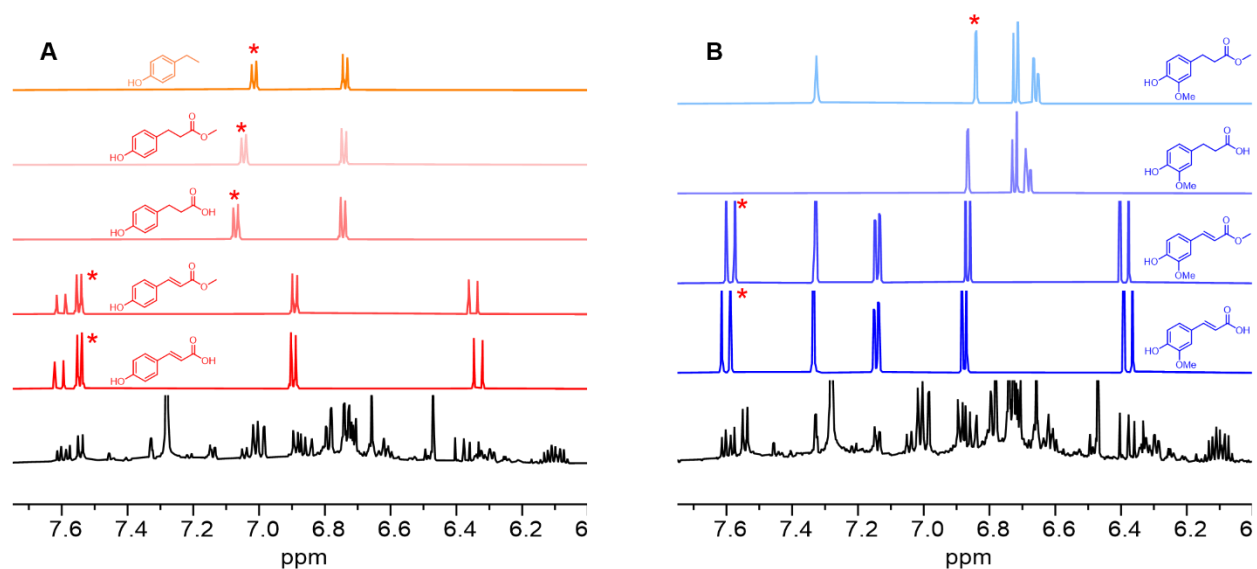
Figure C3. ^{1}H NMR spectra of compounds deriving from coumaric acid (**A**) and ferulic acid (**B**) pendant groups in herbaceous feedstocks compared to switchgrass RCF oil (black bottom spectra).

117
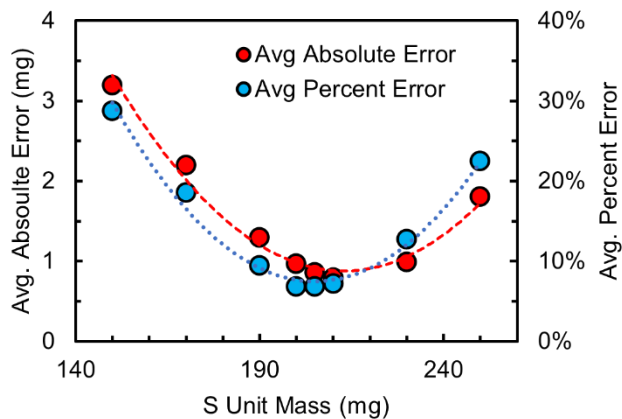
Figure C4. Example of oil yield calibration factor calculation for poplar. The percent error between the measured gravimetric mass and mass measured by NMR was minimized with an S unit value of 200 g/mol (note this is not the molecular weight but rather the average S unit plus side chain mass). G unit mass is obtained by subtracted one formyl (CH_2O) group from the S unit mass to give 170 g/mol.
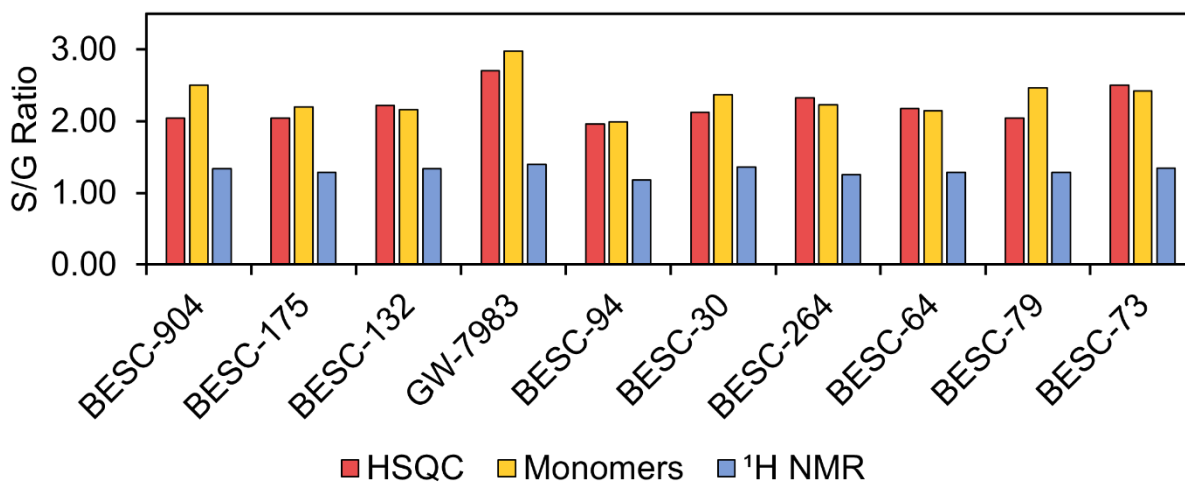
Figure C5. Comparison of S/G ratio measurements from HSQC NMR, monomer yields via GC-FID, and from the ^{1}H NMR oil yield method.
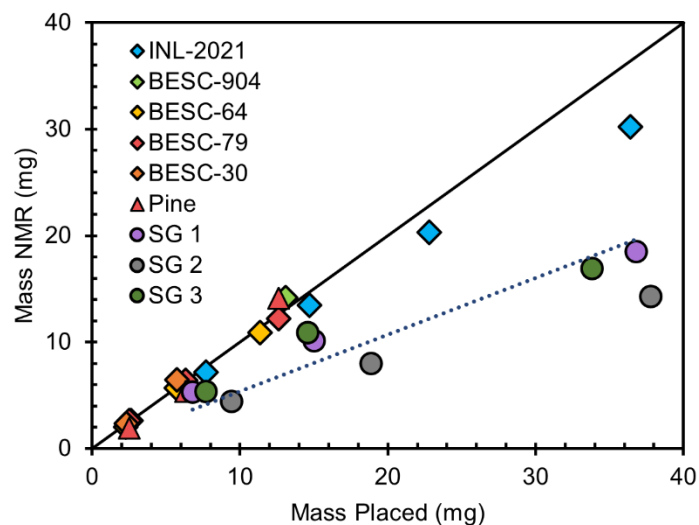
Figure C6: Comparison of oil yield determined gravimetrically and by the ^{1}H NMR method. Gravimetric mass is calculated from the concentration of a stock solution of oil from a particular variant. This total oil was obtained after evaporation of methanol from an aliquot of the reaction liquor (approximately 5 mL), liquid-liquid extraction in ethyl acetate and water, and then massing this larger quantity of oil. Finally the oil was redissolved in a known amount of methanol.

Figure C7. Images of **A**) a single hopper loaded with biomass **B**) The solids-loading robot with 70 biomass hoppers loaded.
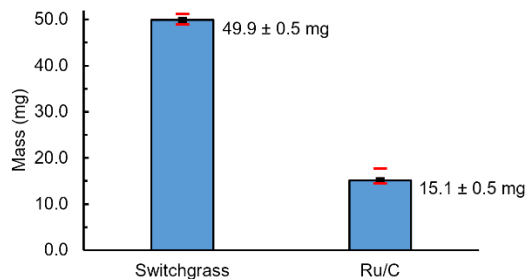
Figure C8. Dispensing accuracy of the Symex Powdernium solids loading robot. Instrument was set to dispense 50 mg of biomass with 1 mg tolerance, and 15 mg of Ru/C with 1 mg tolerance. This data corresponds to the average of 150 dispensing events for switchgrass and Ru/C. Error bars are the standard deviation of all measurements. The red bars indicate the maximum and minimum measurements. Reaction results are shown in **Figure 21**.
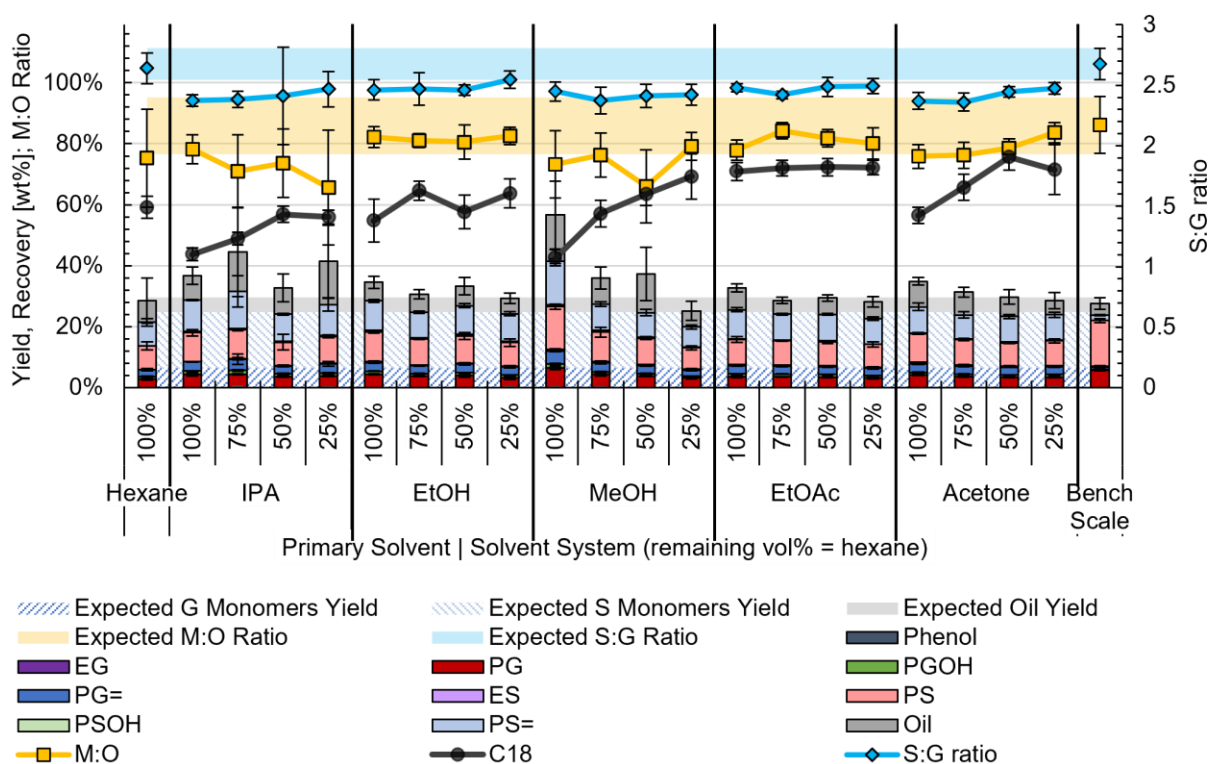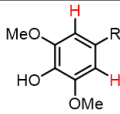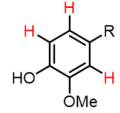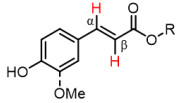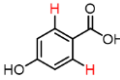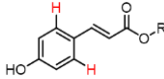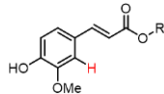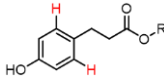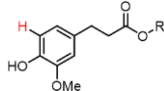

Figure C9: Influence of workup solvent on monomer yield and oil yield. Higher polarity solvents such as methanol decreased octadecane recovery, leading to inflated monomer and oil yields. The 75% ethyl acetate in hexane system showed good agreement with bench scale results shown as expected yields in the graph below.
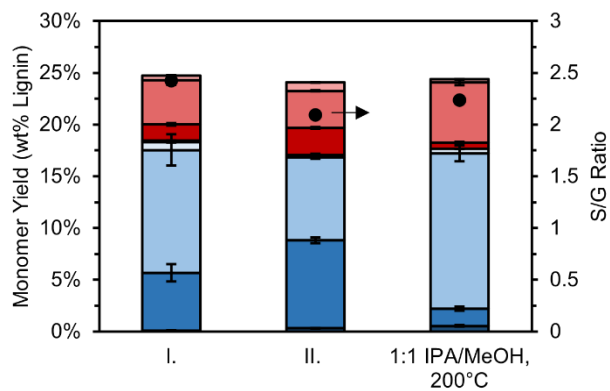
Figure C10. Comparison of monomer yields obtained with different workup methods (Method I versus Method II) compared to the 75 mL batch reaction. HTP conditions: 50 mg poplar, 15 mg 5 wt% Ru/C, 0.5 mL 1:1 IPA/MeOH, 6 hours, 200 °C. 75 mL batch conditions: 2 grams poplar, 600 mg 5 wt% Ru/C, 20 mL 1:1 IPA/MeOH, 6 hours, 200 °C. Error bars represent the standard deviation of triplicate measurements for HTP Method I and the 75 mL batch, and twelve measurements for HTP Method II.

Supplemental Tables

Table C1. Integral ranges for ferulate and coumarate derived RCF products. All chemical shifts are referenced to the acetone residual solvent peak at $\delta = 2.05$ ppm.

	Chemical shift (ppm)	Structure
Total S lignin	6.2-6.6	R= propyl, propanol, propenyl, or ethyl
Total G lignin	6.6-7.2	R= propyl, propanol, propenyl, or ethyl
Unsaturated hydroxycinnamate α $(I_{HC_\alpha} = I_{HC_\beta})$	$\alpha = 7.57\text{-}7.63$ $\beta = 6.31\text{-}6.41$	
para-Hydroxybenzoic acid	7.91	
Coumaric acid/methyl coumarate	7.54	
Ferulic acid/methylferulate	7.33	
Dihydrocoumaric acid 3-(4-hydroxyphenyl)propionic acid	7.04	
Methylhydrocoumarate methyl 3-(4-hydroxyphenyl)propanoate	7.07	
Hydroferulic acid 3-(4-hydroxy-3-methoxyphenyl)propionic acid	6.87	

Methylhydroferulate		
methyl 3-(4-hydroxy-3-	6.84	
methoxyphenyl)propanoate		